Chapter 2

Acid Catalysis……

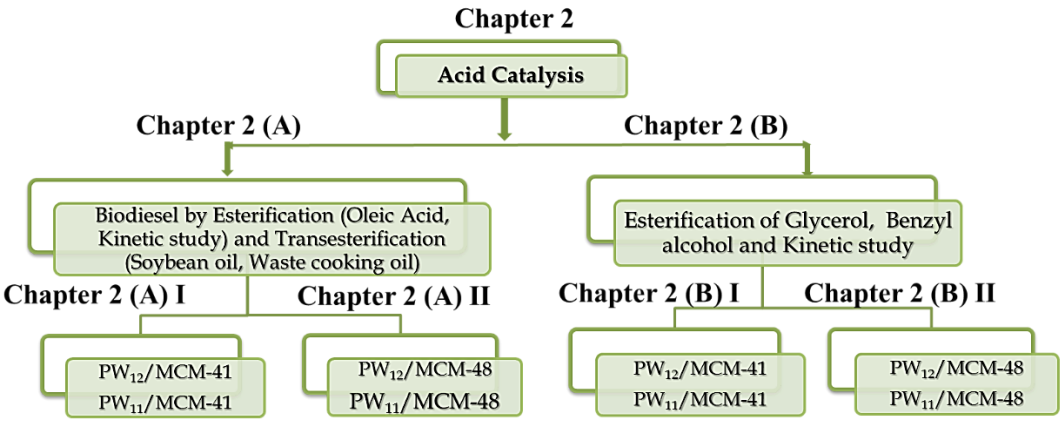

CHAPTER 2A

Biodiesel Synthesis……

1) Esterification of Oleic Acid

&

2) Transesterification of Soybean Oil and Waste Cooking Oil

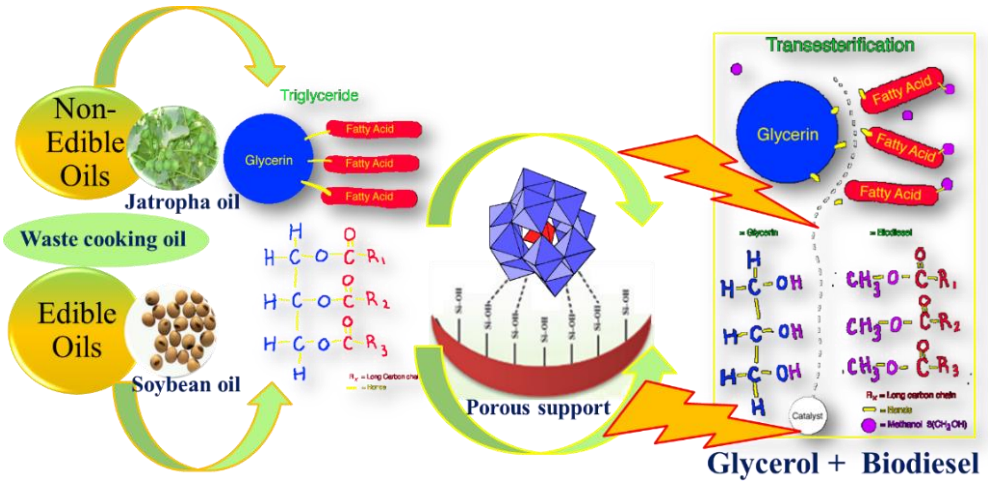

Journal of Cleaner Production 72 (2014) 46–56

Contents lists available at ScienceDirect

Journal of Cleaner Production

journal homepage: www.elsevier.com/locate/jclepro

12-Tungstophosphoric acid supported on mesoporous molecular material: synthesis, characterization and performance in biodiesel production

Sukriti Singh, Anjali Patel*

Polyoxometalate and Catalysis Laboratory, Department of Chemistry, Faculty of Science, The M. S. University of Baroda, Vadodara 390002, India

ARTICLE INFO

Article history:
Received 28 August 2013
Received in revised form
25 February 2014
Accepted 25 February 2014
Available online 6 March 2014

Keywords:
12-Tungstophosphoric acid
Mesoporous molecular material
Waste cooking oil
Biodiesel
Kinetic study

ABSTRACT

12-Tungstophosphoric acid (TPA) supported on mesoporous molecular material (Mobile Composition of Matter – MCM-48) was synthesized, characterized and its use as a heterogeneous catalyst was explored for biodiesel production via oleic acid esterification with methanol. The effect of various reaction parameters such as molar ratio, mass of catalyst, reaction time and reaction temperature was evaluated. The catalyst shows excellent activity (95% conversion) towards biodiesel production. The kinetic study revealed that the esterification of oleic acid follows the first order rate law with activation energy of 40.3 kJ mol^{-1}. The catalyst was recyclable after simple regeneration without significant loss in conversion. The excellent catalytic activity over the present catalyst was extended to transesterification reaction for biodiesel production from waste cooking oil and jatropha oil, as low cost feedstock. The physicochemical properties of the produced biodiesel were further studied and the results show that the obtained properties are comparable with the ASTM specifications. Scale up procedure shows excellent conversions. A single step production procedure was also suggested for biodiesel production.

Green Chemistry

CRITICAL REVIEW

View Article Online
View Journal | View Issue

Cite this: *Green Chem.*, 2015, **17**, 89

Recent progress on supported polyoxometalates for biodiesel synthesis *via* esterification and transesterification

Nilesh Narkhede, Sukriti Singh and Anjali Patel*

Received 8th September 2014,
Accepted 29th September 2014

DOI: 10.1039/c4gc01743a

www.rsc.org/greenchem

Biodiesel is now recognized as a "green fuel" that has several advantages over conventional diesel. In the present review we discuss the catalytic esterification and transesterification reactions to the clean synthesis of biodiesel, over most readily investigated supported polyoxometalates to meet future societal demands. Here for the first time, we are reviewing biodiesel synthesis using supported lacunary polyoxometalates; also how the prevailing reaction conditions like reaction time, alcohol content, temperature, and catalyst amount affect the catalytic activity of the catalyst is discussed in detail. The new results for supported lacunary polyoxometalates are included where the effect of catalysts and supports was correlated with the catalytic activity.

Fuel 159 (2015) 720–727

Contents lists available at ScienceDirect

Fuel

journal homepage: www.elsevier.com/locate/fuel

Mono lacunary phosphotungstate anchored to MCM-41 as recyclable catalyst for biodiesel production via transesterification of waste cooking oil

Sukriti Singh, Anjali Patel *

Polyoxometalates and Catalysis Laboratory, Department of Chemistry, Faculty of Science, The M. S. University of Baroda, Vadodara 390002, Gujarat, India

HIGHLIGHTS

- Mono lacunary phosphotungstate anchored MCM-41 was synthesized and characterized.
- Biodiesel production by esterification of oleic acid with methanol.
- Detail catalytic study for transesterification of waste cooking oil with methanol.
- Potential of being used as recyclable catalysts after simple regeneration.
- Kinetics of esterification and transesterification, scope extended to other oils.

GRAPHICAL ABSTRACT

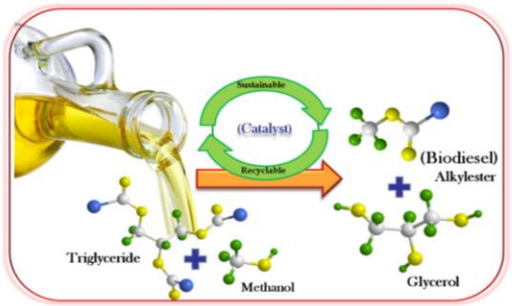

ARTICLE INFO

Article history:
Received 18 December 2014
Received in revised form 20 March 2015
Accepted 1 July 2015
Available online 9 July 2015

Keywords:
Mono lacunary phosphotungstate
MCM-41
Biodiesel
Waste cooking oil
Kinetics

ABSTRACT

Mono lacunary phosphotungstate (PW_{11}) anchored to MCM-41 was synthesized and characterized by various physicochemical techniques. Preliminary studies for biodiesel production by esterification of oleic acid was carried out and study was further extended to transesterification of waste cooking oil. The Kinetic study reveals that the reactions follow first order kinetics and activation energy for transesterification was 64.1 kJ/mol. The present catalyst can be recycled without any significant change in % conversion. The high activity of this new catalyst for transesterification reactions suggests an alternative path as well as reduction in cost for the production of biodiesel under mild reaction conditions.

The technology of deriving biofuels from sustainable bio-resources has been receiving much attention globally due to its potential impact in terms of environment friendliness, low energy intensive operations and optimal utilization of bio-resources. Bio-diesel is considered an equal replacement of diesel which can be made from esterification of free fatty acids (FFAs) with low molecular weight alcohols or transesterification of triglycerides (TGs) of virgin or used vegetable oils (either edible or non-edible) [1-3] (Chart 1). It is meant to be produced in India mainly from *Jatropha curcas* and, to an extent, from other non-edible virgin oils (in particular *Karanj* or *Pongamia pinnata*). It requires little or no engine modification up to 20% blend (known as B20) in petroleum diesel [3].

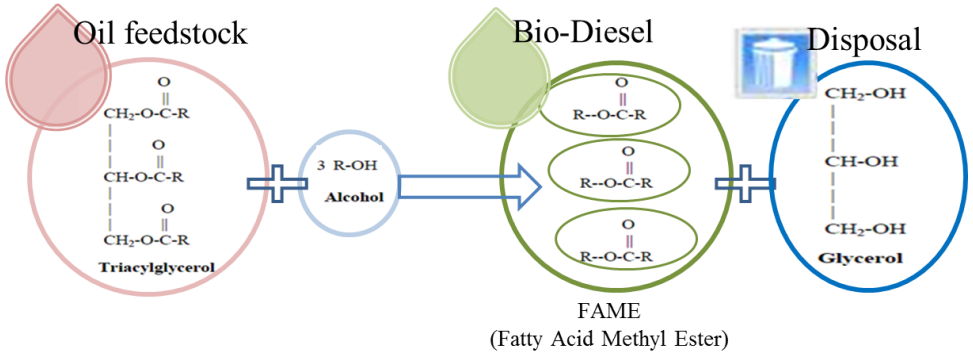

Chart 1. Schematic of biodiesel production and glycerol generation as waste.

Compared to diesel, using bio-diesel fulfil following benefits [4-7]:

- Substantially reduces emissions of unburned hydrocarbons (HC), carbon monoxide (CO), sulfates, polycyclic aromatic hydrocarbons, nitrated polycyclic aromatic hydrocarbons, and particulate matter (PM).
- Bio-diesel also reduces greenhouse gas emissions because carbon dioxide released from bio-diesel combustion is offset by the carbon dioxide sequestered while growing the different edible, non-edible oil or other feedstock.
- Use of 100% blend (B100) reduces carbon dioxide emissions by more than 75% compared to petroleum diesel. Its higher cetane number improves the combustion quality.

- Due to the existence of low volatility nature of biodiesel, it is easier and safe to handle it than petroleum.
- Biodiesel is cost effective because it is produced locally.

Biodiesel status today

On a world scale, biodiesel finds applications as fuel for domestic vehicular use, railways as well as in aircrafts in many countries. Most of the countries have been focusing on the development of biofuels to negate the effects of rising crude oil prices apart from addressing vehicular pollution and global warming. In 2007, McDonalds of UK announced it would start producing biodiesel from the waste oil, by-product of its restaurants. This fuel would be used to run its fleet [8]. British train operating company Virgin Trains claimed to have run the UK's first "biodiesel train", which was converted to run on 80% petroleum based diesel and 20% biodiesel [9]. Also in 2007, Disneyland began running the park trains on B98 (98% biodiesel). The program was discontinued in 2008 due to storage issues, but in January 2009, it was announced that the park would then be running all trains on biodiesel manufactured from its own used cooking oils. On November 7, 2011 United Airlines flew the world's first commercial aviation flight on a microbially derived biofuel using Solajet, Solazyme's algae-derived renewable jet fuel. Neste's NEXBTL renewable diesel is now being used by the city and county of San Francisco, California since December 11, 2015. This switch from petroleum diesel to renewable diesel will achieve a significant 50 percent greenhouse gas emissions reduction to the city's diesel fleet [10]. India, being one of the developing countries with huge energy demand is increasingly focusing on an alternative source of fuel. In biodiesel production process, raw materials account for almost 75% of total biodiesel cost. As a by-product of biodiesel synthesis, glycerol can be sold to match the diesel prices (Chart 1).

Basically all vegetable oils and animal fat can be used as feedstock for biodiesel production (Chart 2).

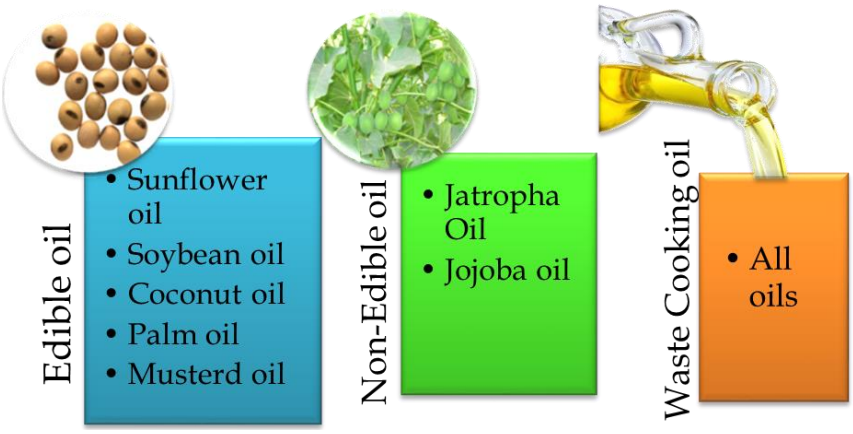

Chart 2. Different feedstocks for biodiesel production.

Most of these oils and fats have a similar chemical composition having chain length of 16 and 18 carbons as well as saturation or unsaturation, however they contain different amounts of individual fatty acids. Methyl esters from these fatty acids have similar combustion characteristics as in diesel engine, because the major components are straight chain hydrocarbons with a chain length of about 16 carbons (hexadecane/cetane). In the recent times, major source of feedstocks for biodiesel production are soybean oil, coconut oil, sunflower oil and palm oil [11-15].

Several methodologies are available, which utilize homogeneous, heterogeneous as well as bio-catalysts for the synthesis of biodiesel. Although enzymatic catalysts are very selective and present high conversions using low oil to alcohol molar ratios [16], they are very expensive and show unstable activities [17]. Supercritical conditions require high temperature and hence increasing the overall cost of biodiesel production processes.

The conventional biodiesel production technology involves the use of alkaline homogeneous catalysts such as NaOH and KOH but sometimes CH_3ONa or CH_3OK are also employed [18-20] mainly in large-scale production plants. These are not compatible for feedstocks with large amounts of FFAs and

moisture due to soaps formation that strongly affect the feasibility of glycerol separation. The traditional liquid acids such as HCl and H_2SO_4 were found to be more efficient [21] but they suffers from the traditional problems and higher costs. Hence alternative methods have been developed for biodiesel synthesis.

Heterogeneous acid catalyzed transesterification reactions have the strong potential to replace homogeneous catalyst because of its obvious advantages such as their insensitiveness to FFA content, simultaneously occurrence of esterification and transesterification, avoiding washing step, low product contamination and easy separation as well as recycling of the catalyst [22-24].

Number of reports are available for esterification of FFAs using different heterogeneous acid catalysts such as, clays [25], zeolite [26-28], ion exchange resin [28-30], carbon based material [28, 31], metal oxides as well as sulfated metal oxides [28, 32-33], WO_3/ZrO_2 [34-35] and propylsulfonic acid functionalized mesoporous silica [36-37].

Recently, anchored $H_3PW_{12}O_{40}$ have received tremendous interest in biodiesel production due to their known advantages. As there are number of reports available for the same, for the sake of simplicity, we have categorized them on basis of following class of supports: Metal oxides (Silica, Alumina, Zirconia, Niobia), Clays, Carbons, Zeolites and Mesoporous silicas/Metal organic frameworks (MOFs).

- **$H_3PW_{12}O_{40}$ supported to metal oxides supports (SiO_2, ZrO_2, Nb_2O_5, Al_2O_3 and Ta_2O_5)**

Dalai and co-workers have reported the use of $H_3PW_{12}O_{40}$ impregnated on to four different supports such as hydrous zirconia, silica, alumina and activated carbon [38]. Synthesized catalysts were used for the biodiesel production from low quality canola oil. The $H_3PW_{12}O_{40}$ anchored to ZrO_2 showed best activity.

Castanheiro and co-workers synthesized series of $H_3PW_{12}O_{40}$, supported on silica [39] and catalysts were used for esterification of palmitic acid with

methanol. It was observed that the catalytic activity decreases in the series: PW-silica > SiW-silica > PMo-silica.

Essayem and group have reported $H_3PW_{12}O_{40}/SiO_2$ and $Cs_2HPW_{12}O_{40}$ for transesterification of rapeseed oil [40]. These catalysts possessed Brønsted acidity of high strength and catalytic activity, better than H_2SO_4 and H_3PO_4, however the acid strength didn't necessarily correlate with catalytic activity. Zirconia is another metal oxide which has attracted much attention because of its known advantages. Halligudi and group have carried out the comparative study of zirconia anchored $H_3PW_{12}O_{40}$ in transesterification of sunflower oil with methanol [41].

Guo et al. reported synthesis of mesostructured Ta_2O_5 -based hybrid catalysts functionalized by both alkyl-bridged organosilica moieties and $H_3PW_{12}O_{40}$. Different loadings from 3.6 to 20.1 %, were obtained by a one-step sol-gel hydrothermal route in the presence of a triblock copolymer surfactant. The catalyst showed a promising activity in the esterification of lauric acid and myristic acid, in the transesterification of tripalmitin, as well as soybean oil [42-44].

Dias and co-workers have reported the synthesis, characterization and application of $H_3PW_{12}O_{40}/ZrO_2$ catalyst for esterification of oleic acid with ethanol as a model reaction to produce long chain ester [45].

Sai Prasad and co-workers reported $H_3PW_{12}O_{40}$ anchored to hydrous zirconia for the esterification of palmitic acid with methanol [46]. The catalyst with 20 wt% $H_3PW_{12}O_{40}$ calcined at 300 ^oC exhibited the highest activity. Different kinetic models were applied to correlate the experimental kinetic data and kinetic parameters were evaluated. The same group have reported $H_3PW_{12}O_{40}$ anchored to SnO_2 for the esterification of palmitic acid with methanol [47]. The catalyst with 15 wt% $H_3PW_{12}O_{40}$ was reported as the best composition of the catalyst, calcined at the temperature of 400 ^oC.

Niobium is an interesting and noteworthy catalyst as well as a support for different catalytic reactions. The catalytic applications of niobium compounds have increased in recent years [48-50]. Niobia can also be used as a promoter and also as a solid acid catalyst. Since it is reducible over a wide temperature range, niobia is also known as a typical strong metal support interacting with oxide. Sai Prasad and group have reported the catalytic activity of $H_3PW_{12}O_{40}$ impregnated on niobium oxide for esterification of palmitic acid and transesterification of used cooking oil [48-50]. The esterification activity was correlated with acidity of the catalysts, which is dependent on the presence of intact Keggin ions on the support. Effect of calcination temperature was studied and it was observed that the new phase WO_3 was observed for catalyst calcined above 500 ^oC.

Biodiesel synthesis from crude jatropha oil was carried out by Badday et al. using an ultrasound-assisted process [51]. Several γ-alumina anchored $H_3PW_{12}O_{40}$ catalysts were synthesized and characterized to elucidate their catalytic behaviours. Different design models such as full factorial design, Taguchi's algorithm and response surface methodology have been established for optimizing the data.

Sheikh and co-workers synthesised catalysts: $H_3PW_{12}O_{40}$ and Cs exchanged $H_3PW_{12}O_{40}$ anchored to supports, ZrO_2 and SiO_2 [52]. Leaching of the active species during 1 h reaction, based upon final conversion at specified reaction conditions, fell in the following order: 20% $H_3PW_{12}O_{40}/Al_2O_3$ = 20% $H_3PW_{12}O_{40}/ZrO_2$ > 20%WO_3/ZrO_2 > 20% $H_3PW_{12}O_{40}/SiO_2$ > CsHPW.

- **$H_3PW_{12}O_{40}$ supported to clays**

Yadav and co-workers reported the use of different lower and higher alcohols *viz.*; methanol, ethanol, n-propanol and n-octanol, for the synthesis of respective fatty acid esters by transesterification of vegetable oil (triglycerides) [53]. The superacid $H_3PW_{12}O_{40}$ was used to increase the acidity and so the activity by loading on to K-10. The best catalyst (10% $H_3PW_{12}O_{40}$/Clay) was

further investigated for the different refined, crude, cooked vegetable oil. The same group has also reported the use of $H_3PW_{12}O_{40}$ anchored to K-10 montmorillonite clay for transesterification of edible and non-edible oil at very high temperatures and pressure [54]. The activity decreases significantly during the fourth recycle and any post treatment cannot be given to regenerate the catalysts due to the alteration in clay pore structure, because of a collapse resulting in a severe reduction in surface area.

The esterification of FFA, oleic acid was carried out over $H_3PW_{12}O_{40}$ immobilized on the 3-aminopropyltriethoxysilane ($H_2N(CH_2)_3Si(OC_2H_5)_3$) functionalized Palygorskite by Wang and group. 15% (w/w) $H_3PW_{12}O_{40}$ catalyst, $H_3PW_{12}O_{40}$/APTES-Pa showed excellent activity and steady reusability up to four cycles [55].

Amazon kaolin flint was also successfully utilized by Barros and co-workers as a support for incorporation of $H_3PW_{12}O_{40}$ in different proportions, 20, 40 and 60 wt% via. impregnation in aqueous solution (HCl 0.1 and 0.5 mol L^{-1}) and acetonitrile [56]. The catalytic results showed that $H_3PW_{12}O_{40}$ anchored on metakaolins with acid treatment promoted good conversion of oleic acid esterification, followed by a gradual increase with added support in $H_3PW_{12}O_{40}$.

Bokade et al. [57] have reported the synthesis of methyl oleate biodiesel over $H_3PW_{12}O_{40}$ anchored montmorillonite K10 by response surface methodology and kinetic modelling. The 20% (w/w) $H_3PW_{12}O_{40}$/K10 follows green principles with potential advantages of complete oleic acid conversion, at milder operating conditions.

Pires and co-workers compared kaolin waste, MK700, and SBA-15 impregnated with $H_3PW_{12}O_{40}$ [58]. The obtained solid acid catalysts were characterized by various techniques. The surface acidities were measured by acid-base titrations with KOH. The catalytic activity of the catalysts were

evaluated for the esterification of deodorized palm oil (DDPO) and 25% $H_3PW_{12}O_{40}$/MK700 was found to be best. From the results, it was concluded that the studied solids (MK700) are promising supports and appear to be attractive heterogeneous catalysts for preparation of esters from low quality oils and fats.

- **$H_3PW_{12}O_{40}$ supported on Carbon**

Activated carbon fibre (ACF) has also been used as a support for heterogenizing $H_3PW_{12}O_{40}$ by Monge et al. [59]. They further demonstrated that washing with ethanol and H_2SO_4 provides an acidic medium which reduces $H_3PW_{12}O_{40}$ leaching and H^+ coming from the H_2SO_4 regenerate the active sites and thereby maintains the catalytic activity for a higher number of cycles.

Badday et al. have reported optimization of biodiesel production process from jatropha oil catalyzed by activated carbon-anchored $H_3PW_{12}O_{40}$ catalyst under application of ultrasonic energy [60]. Influence of ultrasonic energy on different process was elucidated. Also they have not observed any leaching which revealed that the reaction was predominately heterogeneous in nature. Very recently the same group reported ultrasound-assisted transesterification of crude Jatropha oil by activated carbon-anchored $H_3PW_{12}O_{40}$ catalyst [61]. They have elucidated the effect of water and FFA contents in the jatropha oil on the reaction. The catalysts showed moderate water tolerance to a limit of 1% w/w water content.

- **$H_3PW_{12}O_{40}$ anchored to Zeolites**

Patel and group demonstrated the use of $H_3PW_{12}O_{40}$ anchored to Hβ [62] for biodiesel production by esterification of oleic acid. The catalyst showed high activity and high turnover number- 1048. The kinetic study as well as Koros-Nowak test were carried out, and it was found that esterification of oleic acid follows first order kinetics with the calculated activation energy Ea = 45.2 kJ

mol^{-1}. Preliminary studies for transesterification of Jatropha oil and waste cooking oil were also carried out.

Dalai and co-worker have demonstrated the use of H-Y, H-β and H-ZSM-5 zeolites as supports for $H_3PW_{12}O_{40}$ [63]. Their catalytic activity was tested for esterification of FFA present in the green seed canola (GSC) oil, and transesterification of GSC oil using a stirred tank reactor for biodiesel production. In this study, $H_3PW_{12}O_{40}$ impregnated HY zeolite showed higher catalytic activity for esterification, and $H_3PW_{12}O_{40}$ impregnated Hβ zeolite showed higher catalytic activity for the transesterification reaction compared to other catalysts. A catalyst, 55% $H_3PW_{12}O_{40}$/H-β showed optimum catalytic activity for both esterification and transesterification. Also, the catalyst was also used for etherification of by-product glycerol. Further, the same group reported application of $H_3PW_{12}O_{40}$ impregnated HY zeolite for esterification of FFA of GSC oil [64]. A 10.2% $H_3PW_{12}O_{40}$ loaded HY zeolite showed optimum catalytic activity in esterification of oleic acid.

- **$H_3PW_{12}O_{40}$ anchored to Mesoporous silica/MOFs**

The discovery of the M-41S family of mesoporous materials (especially MCM-41 and MCM-48) [65-66] has greatly increased the range of supports for preparing heterogeneous catalysts as discussed in *General Introduction*.

Castanheiro et al. reported a detailed study on esterification of palmitic acid for biodiesel production over $H_3PW_{12}O_{40}$ immobilized on SBA-15 [67]. They observed small leaching of the $H_3PW_{12}O_{40}$ from SBA-15 to liquid phase during the reaction.

Patel et al. reported synthesis and characterization of $H_3PW_{12}O_{40}$ anchored to MCM-41 [68] and SBA-15 [69] for esterification of palmitic acid and oleic acid, respectively with methanol. The transesterification reaction of waste cooking oil was also carried out for biodiesel production. Both the catalysts showed good recyclability up to four cycles without any loss in activity. The excellent

catalytic performance was attributed to the large surface area and pore diameter of the mesoporous supports as well as the acidic strength of $H_3PW_{12}O_{40}$.

Dalai and coworkers reported synthesis of $H_3PW_{12}O_{40}$ anchored using organic functional group and was incorporated into the SBA-15 [70]. Catalytic activity was tested for esterification and transesterification of canola oil. They observed that organically functionalized $H_3PW_{12}O_{40}$ anchored to SBA-15 shows higher catalytic activity for esterification of FFA, whereas $H_3PW_{12}O_{40}$ incorporated into SBA-15 shows higher catalytic activity for transesterification of waste green seed canola oil.

Fazaeli et al. synthesized $H_3PW_{12}O_{40}$ anchored to Al–functionalized SBA-15 mesoporous molecular sieve featuring a well-defined three-dimensional (3D) mesoporosity [71]. The prepared catalyst ($H_3PW_{12}O_{40}$/Al–SBA-15) was tested for the esterification process of palmitic acid to produce methyl palmitate. The effects of the methanol/oil ratio, catalyst amounts, reaction time, and reaction temperature on the conversion are also reported in this paper. By using a 35 wt% of $H_3PW_{12}O_{40}$/Al–SBA-15 with methanol/oil molar ratio of 20:1 at reflux of methanol, the oil maximum conversion was achieved over the solid catalyst under mild conditions.

An inherent challenge in using metal-organic frameworks (MOFs) for catalysis is how to access the catalytic sites generally confined inside the porous structure, in particular for substrates larger than the pores. In this regard Jiu and group [72] demonstrated the synthesis of cubic and octahedral crystal forms of NENU type MOFs and used them to encapsulate $H_3PW_{12}O_{40}$. The cubic crystals were then applied for biodiesel production, reaching maximum conversion of fatty acids (C_{12}-C_{22}) in comparison to <22% using octahedral crystals.

The present chapter comprises of biodiesel synthesis via. esterification of oleic acid and transesterification of soybean oil over the synthesized catalysts. Influence of various reaction parameters (catalyst amount, acid/alcohol molar ratio, reaction time and temperature) on catalytic performance was studied to optimize the conditions for obtaining maximum conversions. All the catalysts were regenerated and reused up to four cycles and regenerated catalysts were characterized for acidic strength, FT-IR, Raman and XRD analysis. The quality of biodiesel synthesized by transesterification of soybean oil was tested by ^{1}H-NMR, FT-IR, acid value, flash point, pour point and viscosity.

EXPERIMENTAL

Materials

All used chemicals were of A. R. grade. Oleic acid and methanol were purchased from Merck. All the oil samples were procured from local market and used without any pre-treatment. Waste cooking oil was obtained from household activities.

Catalytic reactions

Esterification of oleic acid

The esterification of oleic acid (0.01 mol) with methanol (0.4 mol) and 100 mg catalyst, was carried out in a 50 mL batch reactor fitted with a double walled air condenser, Dean-Stark apparatus, magnetic stirrer and guard tube. The reaction mixture was heated at 60 ^{o}C for 8 h. The obtained products were evaluated on a gas chromatograph (Nucon-5700) using a BP1 capillary column (30 m length, 0.25 mm internal diameter). GC programming parameters: Injector temperature= 240 ^{o}C, Detector temperature= 260 ^{o}C, Column temperature= 80-250 ^{o}C with rate 10 ^{o}C/min. Product identification was done by comparison with standard authentic sample, methyl oleate.

Transesterification of soybean oil

Reaction was carried out in a 100 mL glass reactor, provided with mechanical stirring, thermometer and condenser. In a typical run, 5 g oil was added to reactor vessel followed by methanol (40 g) and catalyst addition (250 mg). The reaction mixture was refluxed at 65 °C for 8 h with constant stirring (600 rpm) in order to keep the system uniform in temperature and suspension. After completion of reaction, mixture was rotary evaporated at 50 °C to separate excess methanol. The conversion of FFA to biodiesel was calculated by means of acid value (AV) of oil layer with following equation,

$$\text{Conversion}(\%) = \left(1 - \frac{\text{AV}_{\text{BD}}}{\text{AV}_{\text{SO}}}\right) \times 100$$

Where, AV_{BD} is acid value of biodiesel (oil layer) and AV_{SO} refers to acid value of soybean oil [68, 73-74].

RESULTS AND DISCUSSION

2A (I) Esterification of oleic acid and transesterification of oils over PW_{12}/MCM-41 and PW_{11}/MCM-41.

The esterification of oleic acid (OA) with methanol over the present catalyst is shown in Scheme 1. The esterification reaction is an equilibrium-limited reaction. In order to overcome the equilibrium limitation of the esterification of oleic acid, the reaction was carried out by taking methanol in excess.

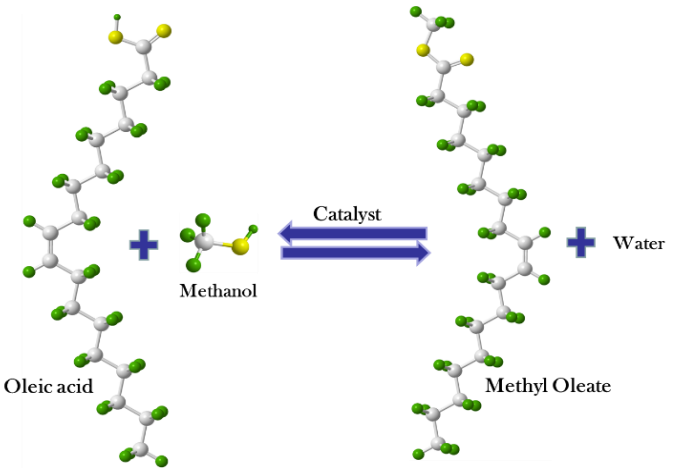

Scheme 1. Esterification of oleic acid with methanol.

Esterification of OA over PW_{12}/MCM-41 [68]

The optimized conditions for esterification of OA over $(PW_{12})_3$/MCM-41 (conversion 99%) are as follows,

Mole ratio of OA to methanol: 1:40

Amount of catalyst : 100 mg

Reaction temperature : 60 ^oC

Reaction time : 10 h

- ***Esterification of OA over PW_{11}/MCM-41.***

Effect of % loading of PW_{11}

To study the effect of % loading (Figure 1) esterification reaction was carried out with $(PW_{11})_1$/MCM-41, $(PW_{11})_2$/MCM-41, $(PW_{11})_3$/MCM-41 and $(PW_{11})_4$/MCM-41. It was observed that with an increase in the % loading of PW_{11}, % conversion also increases. For 30% PW_{11} loading, maximum conversion was obtained. The enhanced catalytic activity for 30% PW_{11} is due to the higher acidity, surface area and good dispersion of active species inside the mesopores of MCM-41. On increasing the % loading to 40%, no significant increase in conversion was observed, which might be due to the blocking of the active sites due to formation of multilayer on the support. This multilayer formation can hinder the reactant molecules to reach out to the active sites and intern there is no significant increase in the conversion. Hence, $(PW_{11})_3$/MCM-41 was considered for further studies.

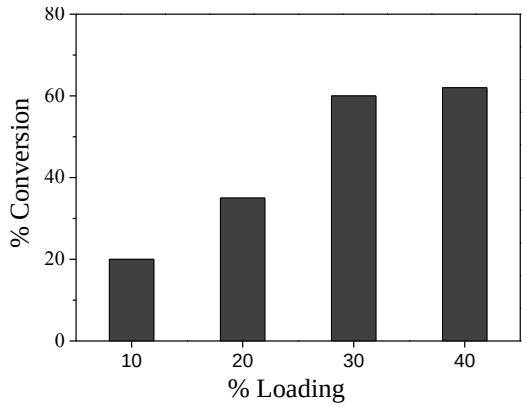

Figure 1. Effect of % loading of PW_{11}: mole ratio OA: methanol- 1:40, catalyst amount- 100 mg, temperature- 60 ^oC, time- 8 h.

Effect of mole ratio of OA to methanol

Variation of OA/methanol mole ratio was carried out to see its effect on esterification reaction. The reaction was carried out with 100 mg catalyst for 8 h at 60 ^{o}C (Figure 2). In order to improve the rate of esterification, higher molar ratio of OA to alcohol was employed. It can be observed from Figure 2 that the OA conversion increases with an increase in OA/methanol mole ratio and reaches an optimum of 60 % conversion at 1:40 mole ratio. With an added increase in the molar ratio there was only a small increase in conversion. Hence, 1:40 molar ratio was selected for obtaining high conversion.

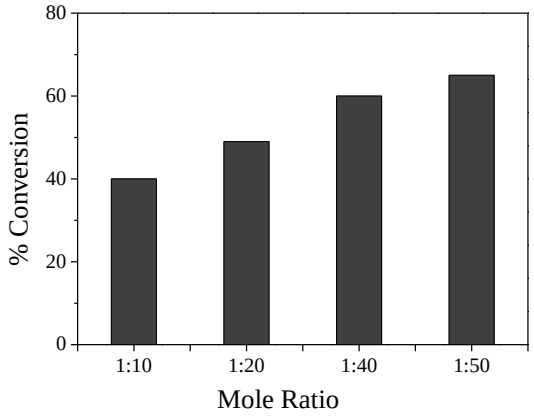

Figure 2. Effect of mole ratio OA: methanol: catalyst amount- 100 mg, temperature- 60 °C, time- 8 h.

Effect of catalyst amount

The effect of catalyst amount on OA conversion was investigated. The catalyst amount was varied in the range from 50-150 mg (Figure 3).

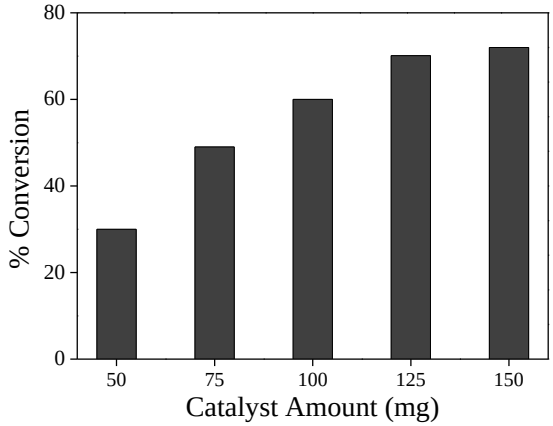

Figure 3. Effect of catalyst amount: mole ratio- 1:40, temperature- 60 °C, time- 8 h.

It was observed from Figure 3, that the OA conversion increases with the increase in amount of $(PW_{11})_3$/MCM-41 and reaches a maximum of 72% conversion with 125 mg catalyst. An increase in conversion with an increase in the catalyst amount can be attributed to an increase in the availability, number of catalytically active sites and acidity of the catalyst. However, with a further increase in the amount of catalyst, the OA conversion remains constant.

Effect of reaction time

The effect of reaction time on OA conversion was investigated (Figure 4). It was observed that OA conversion increases with an increase in reaction time. The maximum OA conversion was 89 % in 14 h. With further increase in the reaction time there is no significant increase in the conversion, which might be due to blocking of the active sites with the product molecules and attainment of equilibrium. After 14 h, no significant increase in conversion was observed.

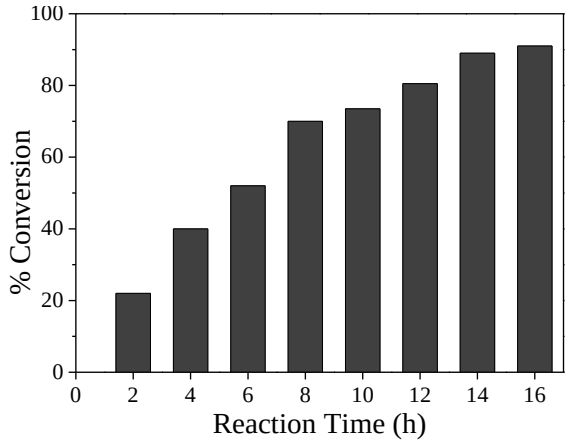

Figure 4. Effect of reaction time: mole ratio- 1:40, catalyst amount- 125 mg, temperature- 60 °C.

Effect of reaction temperature

The esterification of OA is typically an endothermic reaction. Effect of reaction temperature on OA conversion was studied (Figure 5) and it was found that as the reaction temperature increases conversion of OA also increases from 45-60 ^{o}C. At 60 ^{o}C, 89% OA conversion was achieved in 14 h.

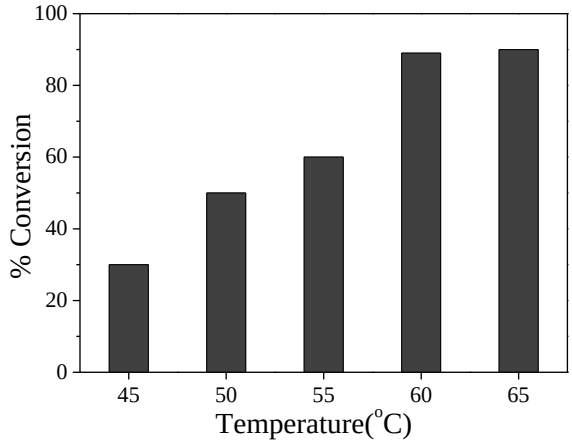

Figure 5. Effect of reaction temperature: catalyst amount- 125 mg, mole ratio- 1:40, time- 14 h.

Optimized conditions: (89% conversion) mole ratio OA to alcohol- 1:40; amount of catalyst- 125 mg, temperature- 60 °C and time- 14 h.

Kinetic study

A detailed kinetic study was carried out for esterification of OA over $(PW_{11})_3$/MCM-41. In all the experiments, reaction mixtures were analyzed at fixed interval of time using GC. The esterification of OA with methanol was carried in 1:40 molar ratio, since methanol was taken in large excess, the rate law is expected to follow first order dependence.

The plot of log C_o/C *versus* time (Figure 6) shows a linear relationship of OA consumption with respect to time. With an increase in reaction time there is a gradual and linear decrease in the OA concentration over $(PW_{11})_3$/MCM-41. These observations indicate that the esterification of OA follows first order dependence with respect to time.

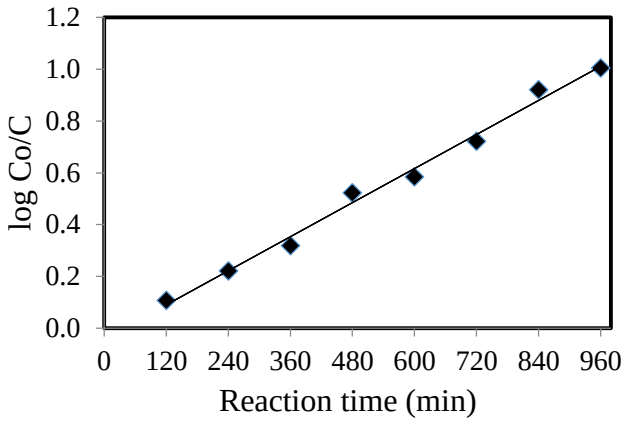

Figure 6. First-order plot for esterification of OA over $(PW_{11})_3$/MCM-41.

This was further supported by the study of the effect of catalyst concentration on the rate of esterification of OA. Catalyst concentration was calculated based on active amount of PW_{11} (mmol) taken for the heterogeneous catalyst. The catalyst concentration was varied from 3×10^{-3} to 12×10^{-3} mmol at a fixed substrate concentration of 10 mmol and at a temperature of 60 °C. It can be observed from Figure 7, that rate of reaction increases linearly with an increase in catalyst concentration.

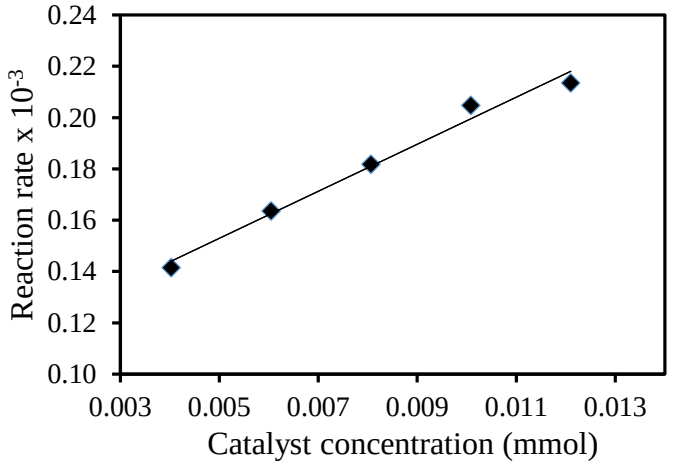

Figure 7. Plot of reaction rate versus catalyst concentrations.

The graph of ln k versus 1/T was plotted (Figure 8) and value of activation energy (Ea) was determined from plot using the Arrhenius equation.

$$k = Ae^{-Ea/RT} \qquad \text{Eq. (1)}$$

The calculation of activation energy refers to apparent term, without considering the adsorption process.

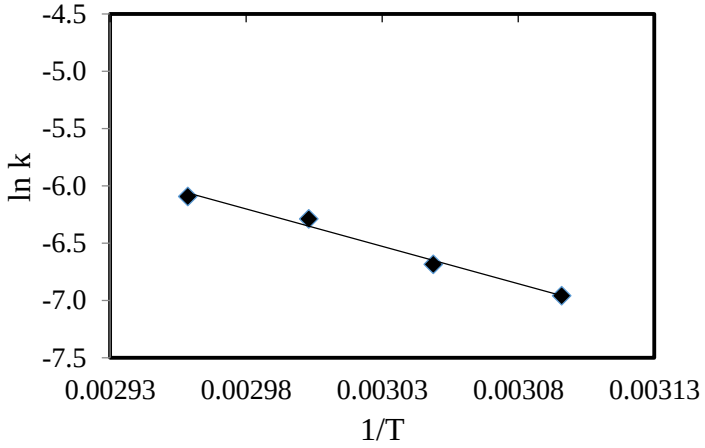

Figure 8. Arrhenius plot for determination of activation energy.

It was important to recognize that whether the reaction rate is diffusion/mass transfer limited or truly governed by the chemical step, where the catalyst is being used to its maximum capacity. It is reported that the activation energy for diffusion limited reactions is as low as 10-15 kJ/mol. The reactions whose rates are truly governed by a chemical step usually show activation energy excess of 25 kJ/mol [75]. The observed activation energy was 54.3 kJ mol^{-1} for $(PW_{11})_3$/MCM-41 and hence, the rate was truly governed by chemical step and there was no diffusion/mass transport limitation.

- ***Transesterification of Soybean oil***

Soybean oil (SO) is a vegetable oil and is one of the most widely consumed cooking oil. The main FFA constituents of SO are Palmitic acid (11%), Stearic acid (4%), Oleic acid (23%), Linoleic acid (54%) and Linolenic acid (8%) [76]. Thus, SO possesses triglyceride esters of both saturated and unsaturated FFA and is perfect feedstock to study the catalytic behaviour. In addition to this, waste cooking oil (WCO) is also an interesting alternative for low cost biodiesel feedstock which can be obtained from canteens, restaurants and houses. General scheme for biodiesel production via. transesterification of triglyceride is shown in Scheme 2.

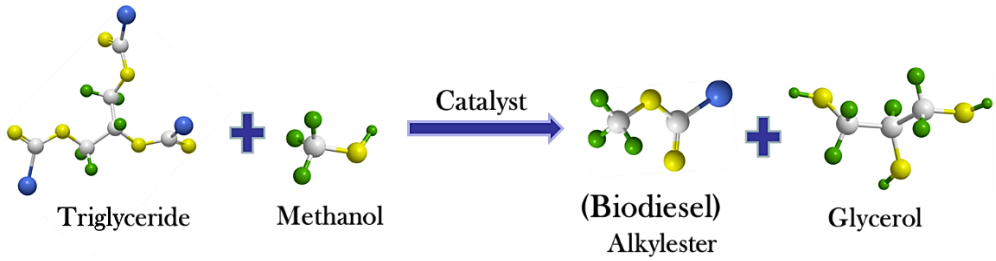

Scheme 2. Biodiesel production from transesterification of triglyceride.

Various properties of SO and WCO are given in Table 1.

Table 1. Properties of SO and WCO investigated in the present work.

Properties	SO	WCO
Colour	Pale yellow	Pale yellow
Acid value, mg KOH/g	0.467	4.19
Saponification value, mg KOH/g	178.3	190.4
Iodine value, g I_2/100g oil	121.4	99.3
Average Molecular weight, g/mol	946.5	904

Acid values and saponification values were determined by acid-base titration and from these values average molecular weight was determined using following equation,

$$M = \left(\frac{56.1 \times 1000 \times 3}{SV - AV}\right)$$

Where, SV denotes saponification value and AV denotes to acid value.

Effect of reaction parameters such as loading, oil/alcohol ratio, catalyst amount, time and temperature were studied to optimize conditions.

Effect of % loading of PW_{12}/PW_{11}

To study the effect of % loading of PW_{12}/PW_{11} transesterification reaction was carried out with 10-40% loaded catalysts (Figure 9). It was observed that with increase in % loading of PW_{12}/PW_{11}, % conversion was also increased up to 30% loading. The enhanced activity could be assigned to the increase in active sites. For 30 and 40% loadings, difference in the conversion was not significant. Hence, 30% loaded catalysts were selected for carrying out detailed study.

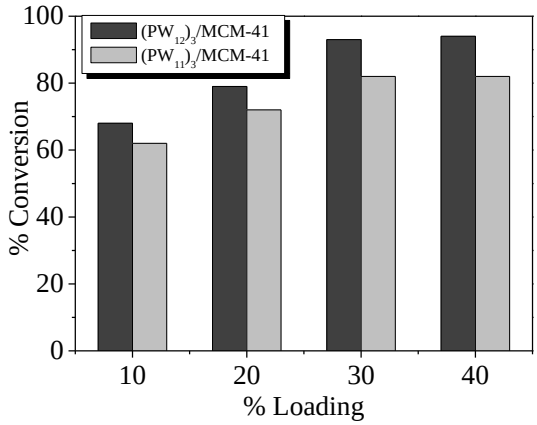

Figure 9. Effect of % loading of PW_{12}/PW_{11}: w/w ratio SO to alcohol- 1:4, catalyst amount- 250 mg, temperature- 65 °C and time- 8 h.

Effect of catalyst amount

Effect of catalyst amount on SO conversion was investigated by varying the catalyst amount in the range 75 mg- 300 mg (Figure 10). The SO conversion increased with the increase in catalyst amount and reaches a maximum of 93% conversion for $(PW_{12})_3$/MCM-41 and 85% conversion for $(PW_{11})_3$/MCM-41 with 250 mg catalyst. The increase in conversion could be attributed to an increase in the number of available catalytically active sites. However, with further increase in catalyst amount to 300 mg, the conversion remains constant due to attainment of saturation/equilibrium conversion.

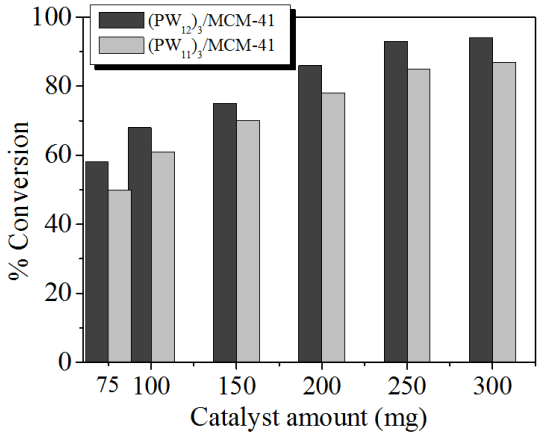

Figure 10. Effect of catalyst amount: w/w ratio of oil to alcohol- 1:4, temperature- 65 °C and time- 8 h.

Effect of ratio (W/W) SO to methanol

Transesterification reaction to produce biodiesel consists of a series of consecutive reversible reactions to produce 3 moles of ester and glycerol. Effect of molar ratios of oil to methanol (Figure 11) was studied and it was seen that on increasing the methanol ratio, viscosity of reaction mixture decreases. This promotes better mixing between reactants and catalyst, which enhances the rate of mass transfer. Eventually resulting to higher conversion within a fixed reaction time. The % conversion accordingly increases with the increase in mole ratio. In the present reaction conditions i.e. 1:4 molar ratio, 93% and 85% conversion was achieved respectively for $(PW_{12})_3$/MCM-41 and $(PW_{11})_3$/MCM-41.

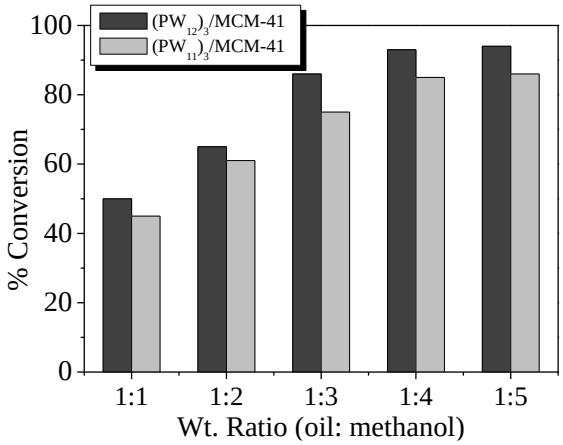

Figure 11. Effect of weight ratio of oil/methanol: catalyst amount- 250 mg, temperature- 65 °C and time- 8 h.

Effect of reaction time

The conversion of SO increases with increase in reaction time from 2-7 h (Figure 12). On increasing the reaction time to 8 h maximum conversion is achieved for both the catalysts, but on further increasing time to 8 h, no significant increase in the % conversion was observed. These results indicated that for maximum conversion 8 h reaction time was optimum.

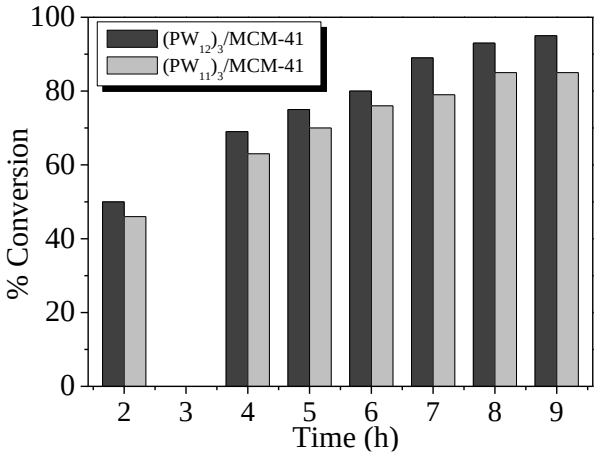

Figure 12. Effect of reaction time: wt. ratio of oil/alcohol- 1:4, catalyst amount- 250 mg, temperature- 65 °C.

Effect of reaction temperature

The effect of temperature on reaction was studied and it was seen that the temperature evidently affects both reaction rate and conversion of SO into biodiesel (Figure 13).

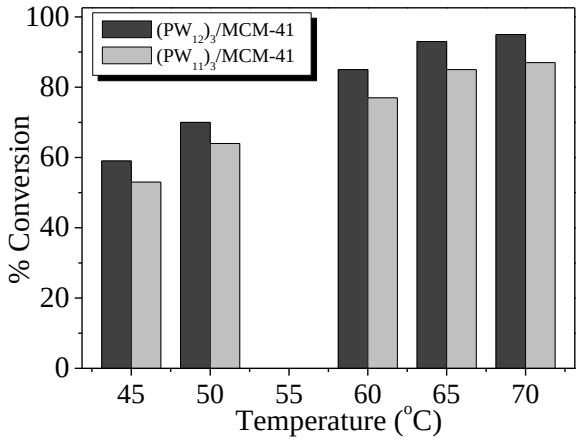

Figure 13. Effect of reaction temperature: w/w ratio of oil to alcohol- 1:4, catalyst amount- 250 mg and time- 8 h.

With increase in temperature from 45 to 60 ^{o}C, conversion increases linearly. It was seen that a maximum conversion was obtained at 65 ^{o}C for both the catalysts. On the other hand, conversion levels off for temperatures beyond 65 ^{o}C, which can be ascribed to attainment of boiling point of methanol. Birla et al. [77] demonstrated that for temperatures higher than methanol boiling point of 65 ^{o}C, it vaporizes, thus, methanol remains in vapor phase in reactor and was less available in reaction environment. Hence, maximum conversion, 93% for $(PW_{12})_3$/MCM-41 and 85% for $(PW_{11})_3$/MCM-41, was obtained at 65 ^{o}C.

***Optimized conditions*:** [93% conversion for $(PW_{12})_3$/MCM-41 and 85% conversion for $(PW_{11})_3$/MCM-41] wt. ratio of SO/methanol (W/W)- 1:4, catalyst amount- 250 mg, time- 8 h, temperature- 65 ^{o}C, stirring speed- 600 rpm.

- ***Transesterification of WCO***

The optimised conditions for transesterification of WCO over $(PW_{12})_3$/MCM-41 [68] (85% conversion) are as follows:

Mole ratio oil to alcohol : 1:8,
Amount of catalyst : 300 mg
Temperature : 65 ^{o}C
Time : 16 h

Detailed optimization studies for transesterification of WCO over $(PW_{11})_3$/MCM-41 (Figure 14) were also carried out.

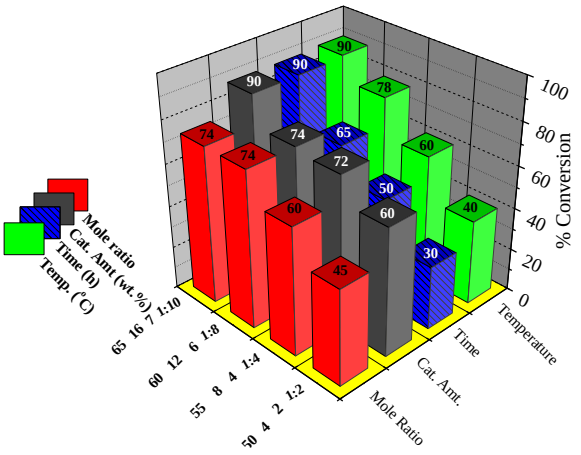

Figure 14. Optimization of reaction parameters for transesterification of WCO over $(PW_{11})_3$/MCM-41.

***Optimized conditions**:* [90% conversion- $(PW_{11})_3$/MCM-41] w/w ratio oil to methanol- 1:8, catalyst wt.%- 7 (350 mg), time- 16 h and temperature- 65 °C.

Under optimized conditions different oil feedstocks were also studied and % conversion as well as their properties are given in Table 2.

Table 2. Transesterification of different triglycerides with methanol.

Properties	JO	SfO	CO	MO
Acid value (mg KOH g^{-1})	37.11	0.18	0.37	1.85
Saponification value (mg KOH g^{-1})	230.4	196.3	193.6	203.6
Iodine value (g I_2/100g oil)	108	115.2	110.4	125.0
Average Molecular weight (g mol^{-1})	871	858	871	834
Conversion (%)[a]	86	80	85	87

Reaction conditions: [a] *$(PW_{11})_3$/MCM-41: catalyst amount- 350 mg, oil/methanol w/w ratio- 1: 8, temperature- 65 °C, time- 16 h. JO- Jatropha oil, SfO- Sunflower oil, CO- Cottonseed oil, MO- Mustard oil.*

Control experiments and Heterogeneity tests

The control experiment using PW_{12}/PW_{11} and MCM-41 was carried out under optimized conditions of both the reactions (Table 3).

Table 3. Control experiments for esterification [a] and transesterification [b].

Catalyst	% Conv. OA [a]	TON	% Conv. SO [b]	TON
MCM-41	8	-	6	-
PW_{12}	92	902	88	234
$(PW_{12})_3$/MCM-41*	99	1015	93	247
PW_{11}	80	854	75	210
$(PW_{11})_3$/MCM-41**	89	950	85	239

Catalyst amount- [a] *PW_{12}- 23 mg and PW_{11}- 28.8 mg,* [a] *$(PW_{12})_3$/MCM-41- 100 mg,* [a] *$(PW_{11})_3$/MCM-41- 125 mg, mole ratio* [a] *OA/alcohol- 1:40,* [a] *time- $(PW_{12})_3$/MCM-41- 8 h, $(PW_{11})_3$/MCM-41- 14 h, temp.- 60 °C;* [b] *57.6 mg (PW_{12}/PW_{11}),* [b] *$(PW_{12})_3$/MCM-41 and $(PW_{11})_3$/MCM-41- 250 mg,* [b] *SO/Alcohol- 1:4,* [b] *time- 8 h, temperature- 65 °C. Turnover number (TON)= moles of product obtained/moles of catalyst (active species).*

Heterogeneity test was carried out by filtering the catalyst from the reaction mixture at 60 ^{o}C after 8 h and the filtrate was allowed to react up to 14 h (OA esterification) (Table 4). The reaction mixture of 8 h and filtrates were analyzed by gas chromatogram. No change in % conversion of filtrate indicates that the present catalyst falls into category C [78]. Category C means, that there is no leaching of the active species (PW_{12}/PW_{11}) from the support. Heterogeneity test for transesterification of SO (Table 4) was also carried out as described above and it was found that catalysts are truly heterogeneous in nature.

Table 4. Heterogeneity tests for $(PW_{12})_3$/MCM-41 and $(PW_{11})_3$/MCM-41.

Reaction	Catalyst	% Conversion	TON
OA	$(PW_{12})_3$/MCM-41 (4 h) [a]	68	697
	Filtrate (8 h) [a]	68	697
	$(PW_{11})_3$/MCM-41 (8 h) [b]	70	747
	Filtrate (14 h) [b]	70	747
SO	$(PW_{12})_3$/MCM-41 (4 h)	65	173
	Filtrate (8 h)	65	173
	$(PW_{11})_3$/MCM-41 (4 h)	63	337
	Filtrate (8 h)	63	337

Esterification of OA: catalyst amount- [a] 100 mg, [b] 125 mg, mole ratio OA/methanol- 1:40, temperature- 60 °C. Transesterification of SO: W/W ratio- 1:4, catalyst amount- 250 mg, temperature- 65 °C.

Recycling and regeneration of catalysts

Catalytic activity of regenerated catalysts

The catalyst recycling is a key parameter to consider the feasibility of a solid catalyst for biodiesel production; since it can reduce the overall process costs. After the reactions, the catalysts were separated from the reaction mixture by simple centrifugation; first washing was done with methanol to remove the products, then the subsequent washings were done by distilled water. The

catalysts were then dried at 100 °C, and recovered catalysts were charged for the further run. (Figure 15). There was no appreciable change in the % conversion for both reactions even after using regenerated catalyst up to four cycles.

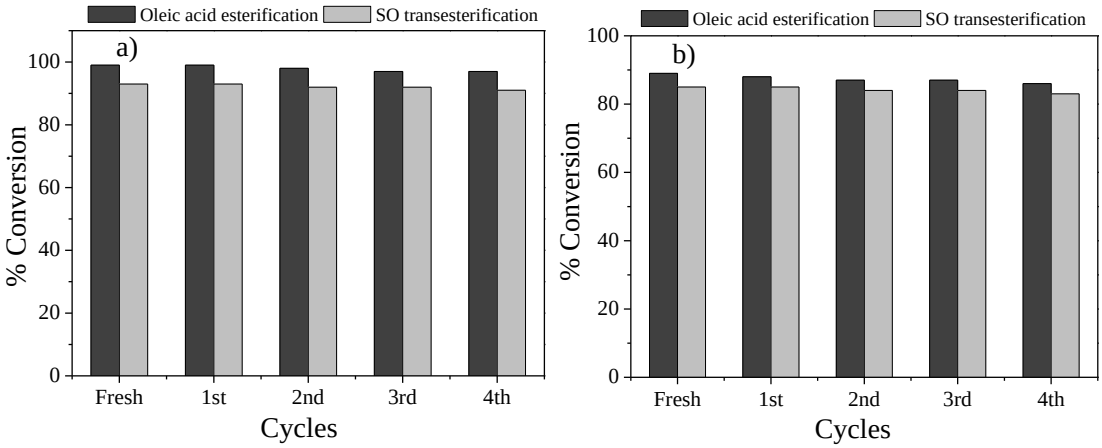

Figure 15. Recycling of catalysts under optimized conditions of OA esterification, SO transesterification, (a) $(PW_{12})_3$/MCM-41 and (b) $(PW_{11})_3$/MCM-41.

Characterization of Regenerated catalysts

The regenerated catalysts were characterized by EDS, FT-IR, FT-Raman, XRD and n-butyl amine acidity value in order to confirm the retention of the catalyst structure, after the completion of the reaction. Absence of any leaching of W and P from catalyst was confirmed by carrying out an analysis of the used catalyst (EDS) as well as the product mixtures after the reaction (AAS). The EDS analysis (in wt%) of the reused catalyst R-$(PW_{12})_3$/MCM-41 did not show any appreciable loss in the tungsten content as compared to the fresh catalyst (fresh catalyst, W-18.0; P-0.3; used catalyst, W-17.8; P-0.3). The EDS analysis (in wt%) of the reused catalyst R-$(PW_{11})_3$/MCM-41 did not show any appreciable loss in the tungsten content as compared to the fresh catalyst (fresh catalyst, W-16.2; P-0.18; used catalyst, W-16.0; P-0.17). Analysis of the product mixtures shows that if any W was present it was below the detection limit, which corresponds to less than 1 ppm (by AAS). These observations strongly suggest that there is no leaching of any active species from the support.

No appreciable shift in FT-IR band position of the recycled catalyst compared to fresh catalyst indicates retention of Keggin structure on MCM-41 (Figure 16). FT-IR spectra of recycled catalyst (Figure 16a, b) shows retention of W=O and W-O-W bands, respectively at 962 and 896 cm^{-1}. No appreciable shift in the FT-IR band position of regenerated catalyst compared to fresh one indicates retention of PW_{12}/PW_{11} structure into MCM-41.

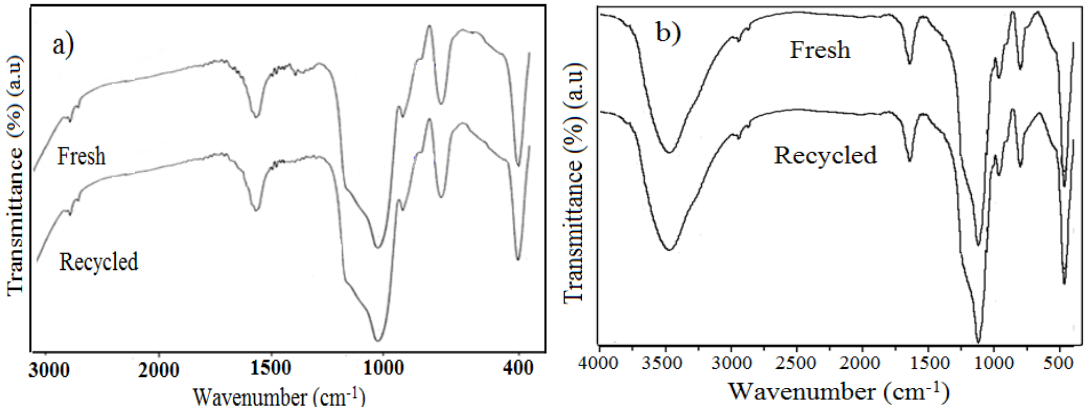

Figure 16. FT-IR spectra of fresh and recycled catalysts, (a) $(PW_{12})_3$/MCM-41 and (b) $(PW_{11})_3$/MCM-41.

Raman spectra of recycled catalysts (Figure 17) shows retention of typical bands of PW_{12}/PW_{11} even after recycling. The spectrum is slightly different from the fresh one in terms of intensity. However, no appreciable shift suggests retention of structure after recycling.

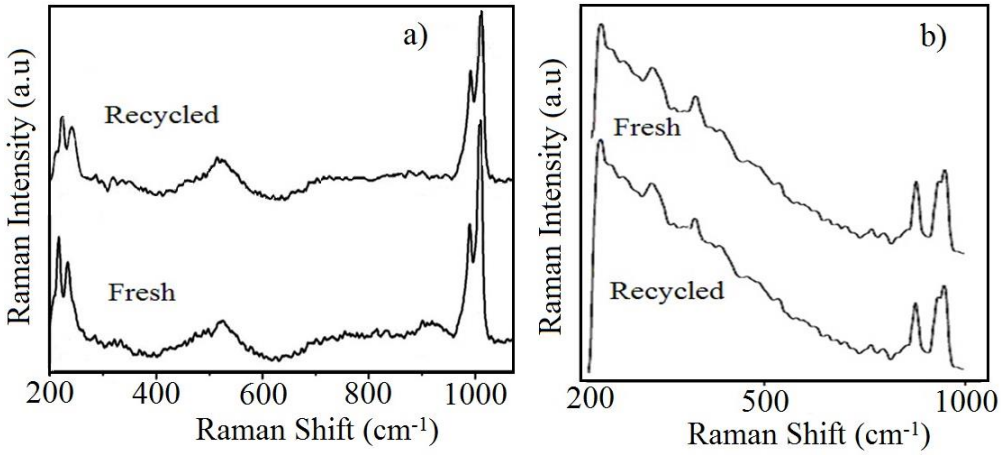

Figure 17. FT-Raman spectra of fresh and recycled catalysts, (a) $(PW_{12})_3$/MCM-41 and (b) $(PW_{11})_3$/MCM-41.

XRD patterns (Figure 18) of the recycled catalysts were identical with the fresh one suggesting the retention of MCM-41 framework as well as Keggin unit (PW_{12}/PW_{11}) in the recycled catalysts.

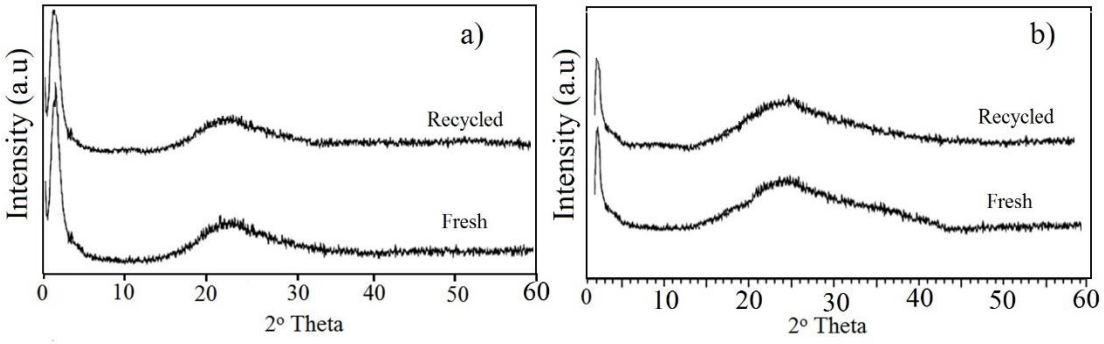

Figure 18. XRD patterns of fresh and recycled catalysts, a) $(PW_{12})_3$/MCM-41 and b) $(PW_{11})_3$/MCM-41.

Further, the acidity value for fresh [$(PW_{12})_3$/MCM-41- 3.6 mequiv. g^{-1}, $(PW_{11})_3$/MCM-41- 3.0 mequiv. g^{-1}] and reused catalysts [$(PW_{12})_3$/MCM-41- 3.2 mequiv. g^{-1}, $(PW_{11})_3$/MCM-41- 2.9 mequiv. g^{-1}] also did not show any appreciable change in acidity. Hence there was no deactivation of the catalysts and the catalysts were truly heterogeneous nature.

2A (II) Esterification of OA and transesterification of oils over PW_{12}/MCM-48 and PW_{11}/MCM-48.

- ***Esterification of OA***

Optimization studies for maximum conversion was carried out similar to the *previous section (I).*

Effect of % loading of PW_{12}/PW_{11}

To study the effect of % loading of PW_{12}/PW_{11}, reaction was carried out with 10-40% PW_{12}/PW_{11} loadings (Figure 19). It was observed that with an increase in the % loading of PW_{12}/PW_{11}, % conversion also increases. This may be due to the increase in value of total acidity (acidity of PW_{12} based catalyst is more than PW_{11} based catalyst). For 30% PW_{12}/PW_{11} loading, maximum conversion was obtained. For 30% and 40% loading there is no significant increase in total acidity and conversion. Hence, the catalyst containing 30% loading of PW_{12}/PW_{11}, were used for detailed study.

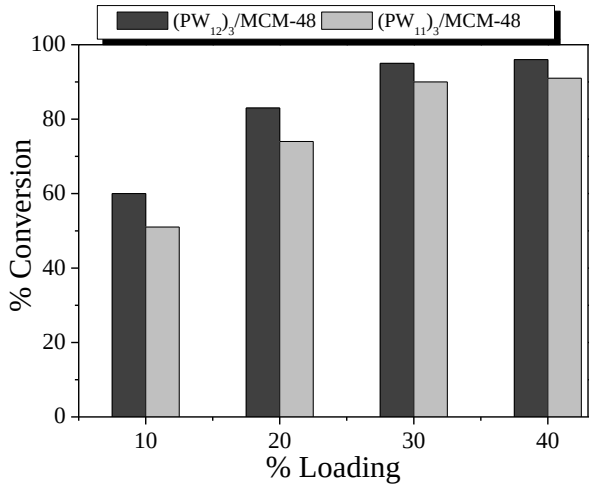

Figure 19. Effect of % loading of PW_{12}/PW_{11}: molar ratio of OA/alcohol- 1:20, catalyst amount- 100 mg, temperature- 60 ^{o}C, time- 8 h for $(PW_{12})_3$/MCM-48 and 14 h for $(PW_{11})_3$/MCM-48.

Effect of mole ratio of OA to methanol

OA conversion can be increased by introducing an excess amount of methanol to shift the equilibrium in the forward direction i.e. towards the product side. In order to test the effect of molar ratio, esterification reaction was carried out by varying mole ratio of oleic acid to methanol, with 100 mg of the catalyst for 8 h at 60 ^{o}C. It can observed from Figure 20, that OA conversion increases with increase in acid to methanol ratio and reaches a maximum at 1:20 mole ratio. With further increase in mole ratio, no significant increase in conversion was observed. Hence 1:20 molar ratio of oleic acid to methanol was optimized for further studies.

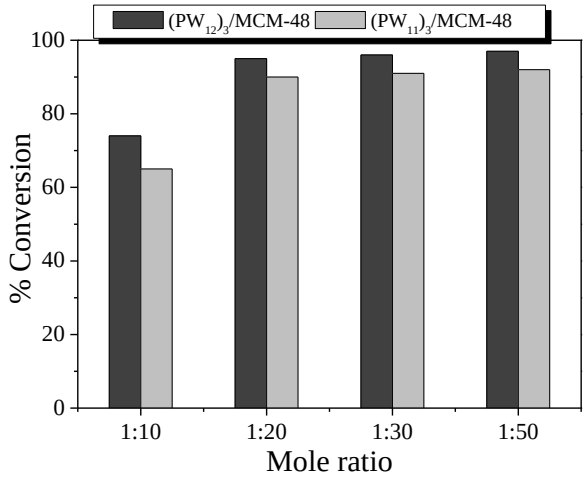

Figure 20. Effect of molar ratio OA/methanol: catalyst amount- 100 mg, temperature- 60 ^{o}C, time- 8 h for $(PW_{12})_3$/MCM-48 and 14 h for $(PW_{11})_3$/MCM-48.

Effect of catalyst amount

In this study, catalyst mass was varied within a range of 50-150 mg (Figure 21). The OA conversion increased with increase in amount of both the catalysts and reaches an optimum at 100 mg. The increase in conversion with an increase in the catalyst amount can be attributed to an increase in the availability and number of catalytically active sites. 100 mg catalyst gives 95% conversion for $(PW_{12})_3$/MCM-48 and 89% conversion for $(PW_{11})_3$/MCM-48.

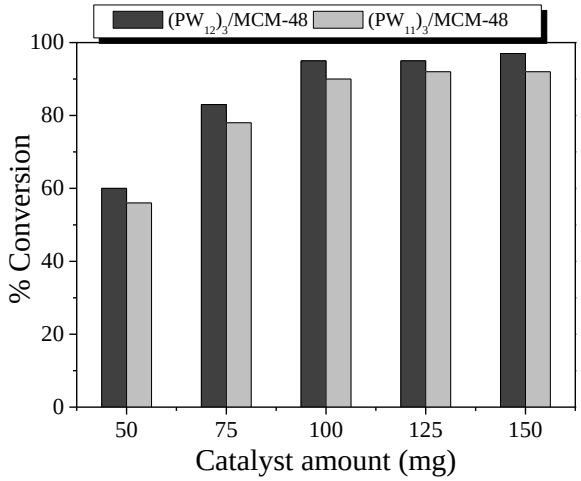

Figure 21. Effect of catalyst amount: molar ratio OA/methanol- 1:20, temperature- 60 ^{o}C, time- 8 h for $(PW_{12})_3$/MCM-48 and 14 h for $(PW_{11})_3$/MCM-48.

Effect of reaction time

In order to determine the effect of reaction time on the conversion, reactions were carried out at the different reaction times, by keeping other reaction parameters constant, namely catalyst amount (100 mg), OA/methanol molar ratio (1:20) and temperature constant (60 ^{o}C). It was observed from Figure 22, that conversion increases with increase in the reaction time. The maximum conversion of OA was obtained in 8 h for $(PW_{12})_3$/MCM-48 and 14 h for $(PW_{11})_3$/MCM-48.

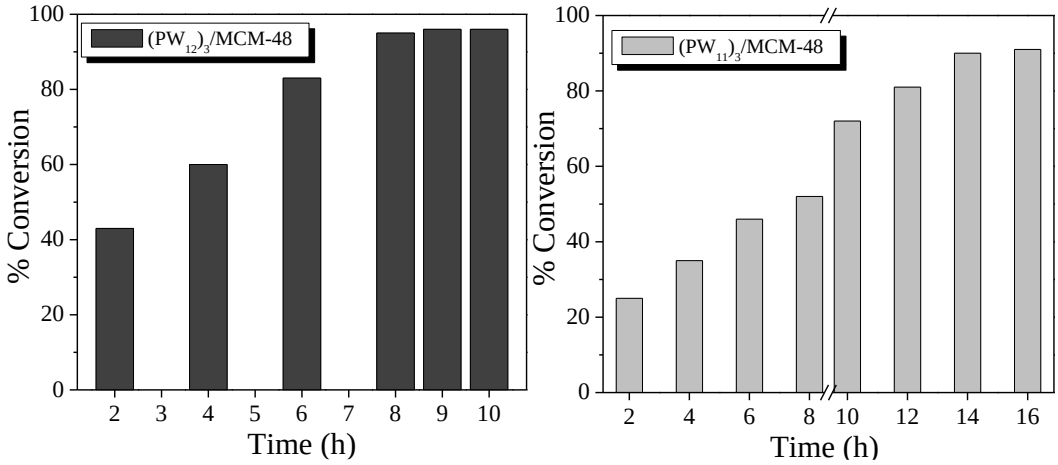

Figure 22. Effect of reaction time: molar ratio OA/methanol- 1:20, catalyst amount- 100 mg, temperature- 60 ^{o}C, time- 8 h for $(PW_{12})_3$/MCM-48 and 14 h for $(PW_{11})_3$/MCM-48.

Effect of reaction temperature

To study the effect of reaction temperature, temperature was varied between 40-70 °C while keeping the other parameters constant. The primary advantage of a higher temperature is to obtain a shorter reaction time, hence in the present conditions it was found that with increase in reaction temperature % conversion also increases (Figure 23). The results in figure, reveal that 45%, 66% conversion was found corresponding to 40 ^{o}C and 50 ^{o}C, respectively. Highest conversion was achieved at 60 ^{o}C and further increase in temperature did not improve the conversion. This may be due to the fact that temperatures higher than the methanol boiling point (65 ^{o}C) causes methanol to vaporize. Thus, methanol remained in the vapor phase in the reactor and was less available in the reaction environment. Hence, 60 ^{o}C was optimum for obtaining maximum conversion.

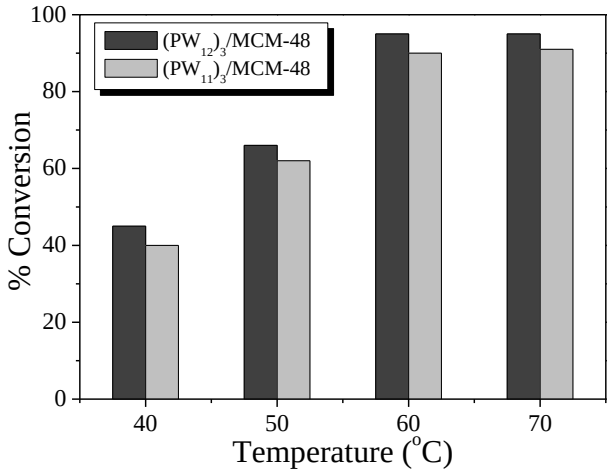

Figure 23. Effect of reaction temperature: molar ratio OA/methanol- 1:20, catalyst amount- 100 g, time- 8 h for $(PW_{12})_3$/MCM-48 and 14 h for $(PW_{11})_3$/MCM-48.

Optimized conditions: **[**95% Conversion $(PW_{12})_3$/MCM-4 and 89% Conversion $(PW_{11})_3$/MCM-48]: mole ratio OA/methanol- 1:20, catalyst amount- 100 mg, temperature- 60 ^{o}C and time- 8 h for $(PW_{12})_3$/MCM-48 and 14 h for $(PW_{11})_3$/MCM-48.

Kinetic study

A detailed kinetic study was carried out on esterification of OA over $(PW_{12})_3$/MCM-48 and $(PW_{11})_3$/MCM-48. The plot of log Co/C versus time shows linear relation with respect to time (Figure 24). With an increase in reaction time there is a linear decrease in the OA concentration. This observation indicates that the esterification of OA follows first order dependence with respect to time.

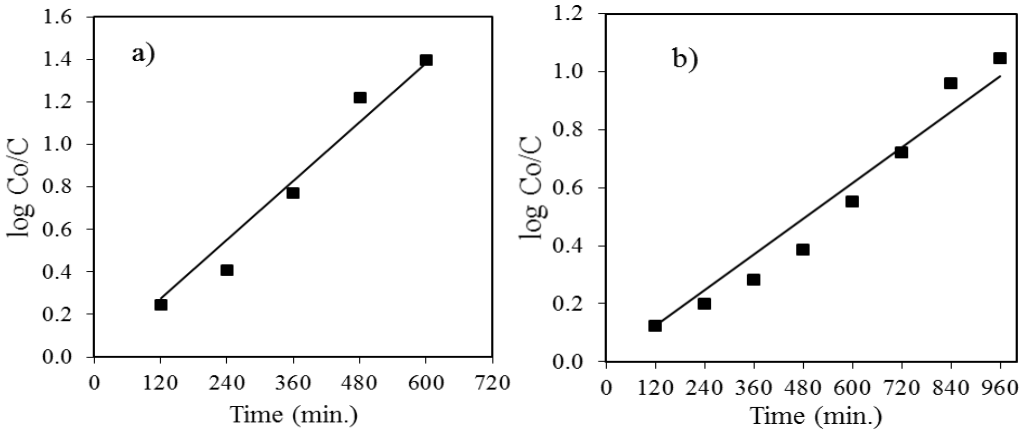

Figure 24. First order plot for esterification of OA over (a) $(PW_{12})_3$/MCM-48 and (b) $(PW_{11})_3$/MCM-48.

The catalyst concentration was varied from 4×10^{-3} to 12×10^{-3} mmol at a fixed substrate concentration of 10 mmol at 60 °C. It was observed from plot of reaction rate versus catalyst concentration (Figure 25) that rate of reaction increases with an increase in the catalyst concentration.

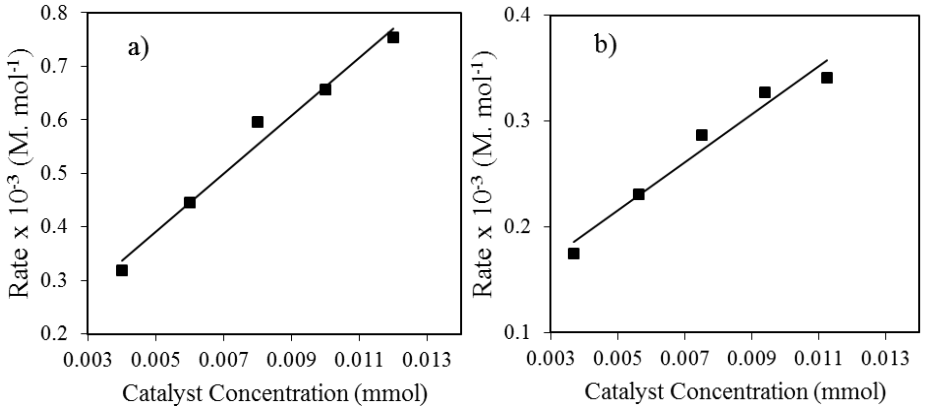

Figure 25. Plot of reaction rate versus catalyst concentrations over (a) $(PW_{12})_3$/MCM-48 and (b) $(PW_{11})_3$/MCM-48.

The graph of ln k versus 1/T was plotted (Figure 26) and the values Ea were determined from the plot using Arrhenius Equation. In the present case the observed value of Ea was 40.3 kJ mol^{-1} for $(PW_{12})_3$/MCM-48 and 52.3 kJ mol^{-1} for $(PW_{11})_3$/MCM-48. These results suggest that the rate is truly governed by a chemical step and the reaction was not surface type diffusion limited catalysis.

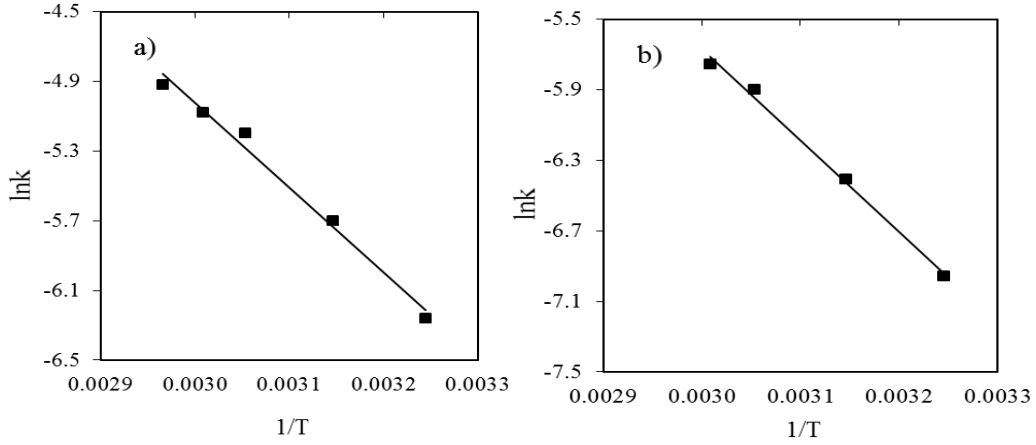

Figure 26. Arrhenius plots for determination of activation energy, a) $(PW_{12})_3$/MCM-48 and b) $(PW_{11})_3$/MCM-48.

The value of Ea for $(PW_{12})_3$/MCM-48 was found to be low as compared to $(PW_{11})_3$/MCM-48, which suggests the order of catalyst, $(PW_{12})_3$/MCM-48 > $(PW_{11})_3$/MCM-48.

- ***Transesterification of SO***

Effect of % loading of PW_{12}/PW_{11}

To study the effect of % loading of PW_{12}/PW_{11} on MCM-48, reaction was carried out with 10-40% loaded catalysts (Figure 27). It was observed that with increase in % loading of PW_{12}/PW_{11}, conversion was also increases up to 30% loading. The enhanced activity could be assigned to increase in the active sites PW_{12}/PW_{11}. Further, 40% loaded catalysts showed no significant increase in the conversion. Hence, 30% loaded catalysts were selected for detailed study.

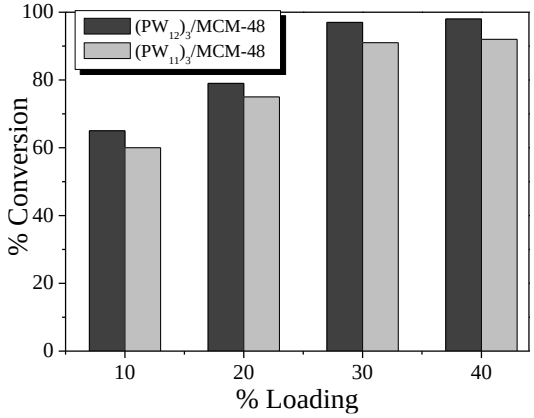

Figure 27. Effect of % loading of PW_{12}/PW_{11}: molar ratio SO/methanol- 1:4, catalyst amount- 250 mg, temperature- 65 ^{o}C, time- 8 h.

Effect of catalyst amount

Effect of catalyst amount on oil conversion was investigated by varying the amount in range 100-300 mg (Figure 28).

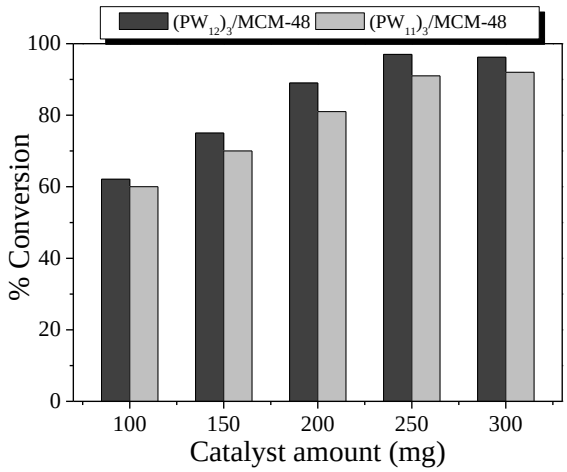

Figure 28. Effect of catalyst amount: molar ratio SO/methanol- 1:4, temperature- 65 ^{o}C, time- 8 h.

The conversion increased with the increase in amount of both catalysts and reached a maximum of 97% for $(PW_{12})_3$/MCM-48 and 91% for $(PW_{11})_3$/MCM-48 with 250 mg catalyst. The increase in the conversion can be attributed to an increase in the number of available catalytically active sites. However, with a further increase in the amount of catalyst to 300 mg, the conversion remains constant due to attainment of saturation/equilibrium conversion. Hence, 250 mg catalyst amount was optimised for further reactions.

Effect of ratio (W/W) oil to methanol

Transesterification reaction consists of a series of consecutive reversible reactions to produce three moles of esters and one mole of glycerol. The effect of w/w ratio of SO to methanol was studied in the range of 1: 1 to 1: 5 (Figure 29) and it was seen that on increasing the methanol ratio the viscosity of reaction mixture decreases. This promotes better mixing between reactants and catalyst, which enhances the rate of mass transfer. This eventually results in a higher conversion within a fixed reaction time. The conversion accordingly increases with increase in methanol ratio up to 1: 4. On further increasing the molar ratio no significant increase in conversion was observed, which might be due to saturation of active sites with methanol molecules rather than oil. At optimum 1: 4 w/w ratio, maximum conversion was achieved for both the catalysts.

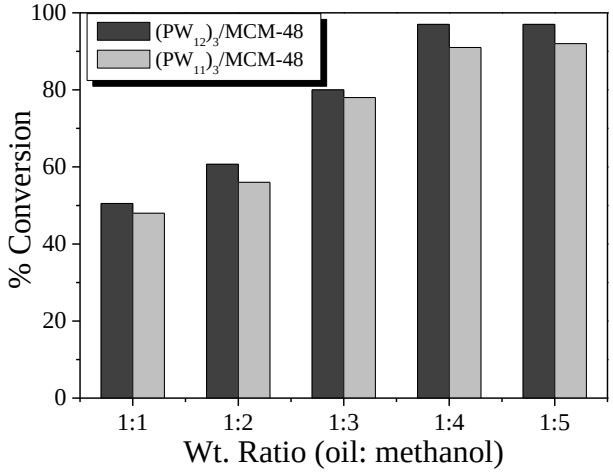

Figure 29. Effect of ratio of SO/methanol (W/W): catalyst amount- 250 mg, temperature- 65 ^{o}C, time- 8 h.

Effect of reaction time

The conversion of SO over both the catalysts increases with increase in the time from 2 to 8 h (Figure 30). At 8 h, the conversion was maximum for both the catalysts, but on further increasing the reaction time there was no significant increase in the percentage conversion. On further increasing the reaction time there was no significant increase in conversion, due to the blocking of active sites by glycerol molecules formed during the reaction.

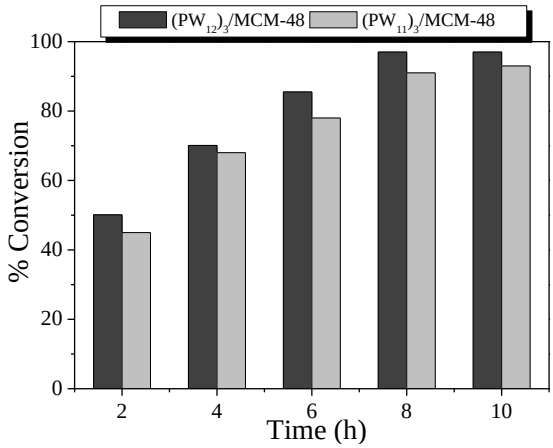

Figure 30. Effect of reaction time: wt. ratio of SO/methanol- 1:4, catalyst amount- 250 mg, temperature- 65 °C.

Effect of reaction temperature

The effect of temperature on the reaction was studied and it was observed that temperature evidently affects both the reaction rate and conversion of SO (Figure 31).

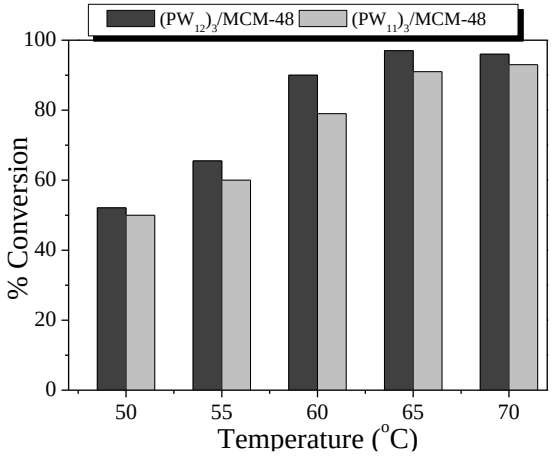

Figure 31. Effect of reaction temperature: W/W ratio of SO/methanol- 1:4, catalyst amount- 250 mg, time- 8 h.

At 50 °C, 52% conversion for $(PW_{12})_3$/MCM-48 and 50% conversion for $(PW_{11})_3$/MCM-48 was observed. But with a subsequent increase in temperature, percentage conversion was also increased. It was observed that a maximum conversion was obtained at 65 °C for both the catalysts. On the other hand, the conversion decreased for temperatures beyond 65 °C which can be ascribed to attainment of boiling point of methanol. Thus, methanol remained in the vapour phase in the reactor and was less available for the reaction.

***Optimized conditions*:** [97% conversion- $(PW_{12})_3$/MCM-48 and 91% conversion- $(PW_{12})_3$/MCM-48], wt. ratio SO/methanol (W/W)- 1: 4, catalyst amount- 250 mg, time- 8 h, temperature- 65 ^oC, stirring speed- 600 rpm.

- ***Transesterification of WCO***

Application of the present catalysts was extended to transesterification of WCO with methanol (Figure 32) and detailed optimisation, similar to SO was carried out.

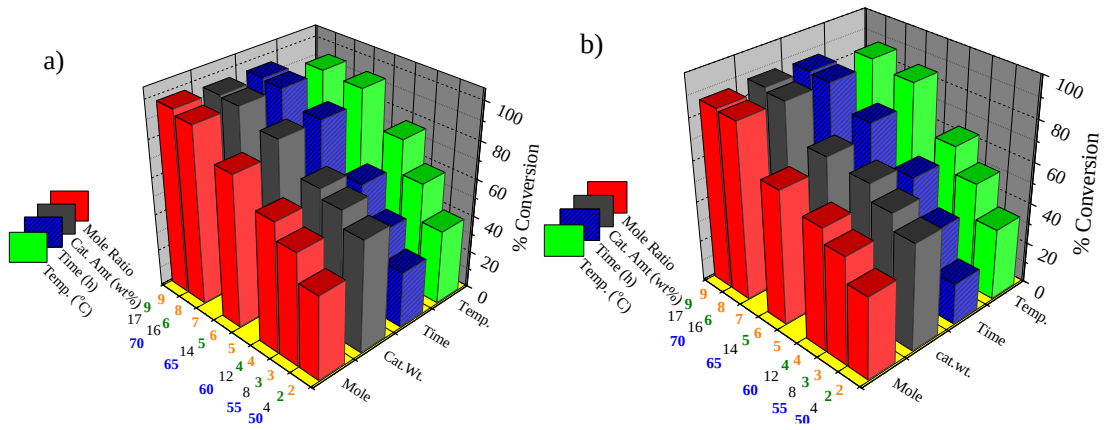

Figure 32. Optimization reaction parameters for transesterification of WCO over (a) $(PW_{12})_3$/MCM-48, and (b) $(PW_{11})_3$/MCM-48.

Optimized conditions: [95% conversion for $(PW_{12})_3$/MCM-48, and 86% conversion for $(PW_{11})_3$/MCM-48)], w/w ratio oil to alcohol 1:8; catalyst wt.%-6 (300 mg); time 16 h and temperature 65 °C.

Under optimized conditions, different oil feedstocks were also studied and % conversion as well as their properties are given in (Table 5).

Table 5. Transesterification of different triglycerides with methanol.

Properties	JO	SfO	CO	MO
Acid value (mg KOH g^{-1})	37.11	0.18	0.37	1.85
Saponification value (mg KOH g^{-1})	230.4	196.3	193.6	203.6
Iodine value (g I_2/100g oil)	108	115.2	110.4	125.0
Average Molecular weight (g mol^{-1})	871	858	871	834
Conversion (%)[a/b]	93/85	88/82	90/81	90/83

Reaction conditions: amount of catalyst- 300 mg, oil/methanol w/w ratio- 1:8, temperature- 65 °C, time- 16 h. [a] $(PW_{12})_3$/MCM-48, [b] $(PW_{11})_3$/MCM-48.

Control experiments and Heterogeneity tests

The control experiments with MCM-48 and PW_{12}/PW_{11} were also carried out under optimized conditions for both the reactions (Table 6). It was observed from table that MCM-48 was not much active towards both the reactions, indicating that the catalytic activity was mainly due to PW_{12}/PW_{11}.

Table 6. Control experiments for esterification [a] and transesterification [b].

Catalyst	% Conv. OA [a]	TON [a]	% Conv. SO [b]	TON [b]
MCM-48	10	-	8	-
PW_{12}	92	902	88	234
$(PW_{12})_3$/MCM-48	95	1189	97	266
PW_{11}	80	854	75	210
$(PW_{11})_3$/MCM-48	90	960	91	267

Catalyst amount- [a] PW_{12}/PW_{11}- 23 mg, [a] supported catalyst- 100 mg, mole ratio [a] OA/alcohol- 1:40, [a] time- $(PW_{12})_3$/MCM-41- 8 h, $(PW_{11})_3$/MCM-41- 14 h, temp.- 60 °C; [b] 57.6 mg (PW_{12}/PW_{11}), [b] supported catalyst- 250 mg, [b] SO/alcohol- 1:4, [b] time- 8 h, temperature- 65 °C.

The same reaction was carried out by taking the active amount of PW_{12}/PW_{11} and it was observed that catalytic activities of PW_{12}/PW_{11} have been retained in the respective catalysts indicating that PW_{12}/PW_{11} behaves as real active species. Thus, we were successful in anchoring PW_{12}/PW_{11} to MCM-48 without any significant loss in activity and hence in overcoming the traditional problems of homogeneous catalysis.

Heterogeneity test (Table 7) was carried out by filtering the catalyst from the reaction mixture at 60 ^oC after 4 h and subsequently the filtrate was allowed to react up to 8 h. The reaction mixture of 4 h and filtrates were analysed by GC. Similar heterogeneity test was also carried out for reaction of SO. No change in the % conversion of OA and SO indicates that the catalysts falls into category C [78] and the catalysts are truly heterogeneous in nature.

Table 7. Heterogeneity tests for different reactions.

Reaction	Catalyst	% Conversion	TON
OA	$(PW_{12})_3$/MCM-48 (4 h)	68	697
	Filtrate (8 h)	68	697
	$(PW_{11})_3$/MCM-48 (8 h)	70	747
	Filtrate (14 h)	70	747
SO	$(PW_{12})_3$/MCM-48 (4 h)	65	173
	Filtrate (8 h)	65	173
	$(PW_{11})_3$/MCM-48 (4 h)	63	337
	Filtrate (8 h)	63	337

Esterification of OA: catalyst amount- 100 mg, mole ratio OA/methanol- 1:20, temperature- 60 °C. Transesterification of SO: W/W ratio of SO/methanol- 1:4, catalyst amount- 250 mg, temperature- 65 °C.

Recycling and regeneration of catalysts

Catalytic activity of regenerated catalysts

The catalyst was recycled to test its activity as well as stability (Figure 33). Catalysts from different reactions were recovered following the procedure discussed in *section 2A (I).* The recovered catalyst was charged for the subsequent run. Recycling study by transesterification of SO was also carried out using similar procedure. There was no appreciable change in conversion for both reactions even after using regenerated catalyst up to four cycles.

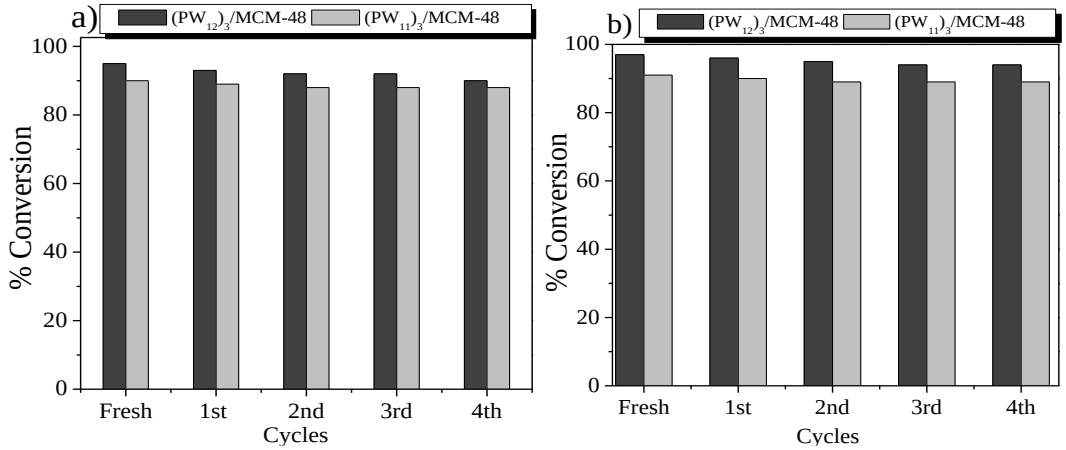

Figure 33. Recycling of the catalysts under optimized conditions, (a) OA esterification and (b) Transesterification of SO.

Characterization of regenerated catalysts

The regenerated catalysts were characterized by EDS, FT-IR, Raman, XRD and acidity measurement. The EDS analysis (in wt%) of the reused catalyst R-$(PW_{12})_3$/MCM-48 was carried out and values are close to the fresh catalyst (Fresh: W- 17.7, P- 0.30; Recycled: W- 17.4, P- 0.30). EDS analyses of R-$(PW_{11})_3$/MCM-48 shows that the values are close to fresh catalyst (Fresh: W-15.9, P-0.18; Recycled: W-15.0, P-0.164). The leaching of tungsten (W) from catalysts was confirmed by carrying out an analysis of the product mixtures (by AAS). Analysis of the product mixtures show that if any W was present it was below the detection limit, which corresponds to less than 1 ppm. On the basis of these results, it can be concluded that there was no leaching of PW_{12}/PW_{11} species from the support. The FT-IR data for the fresh as well as

the regenerated catalysts are presented in Figure 34. No appreciable shift in the FT-IR band position of the regenerated catalysts compared to fresh catalyst indicates the retention of Keggin structure of PW_{12}/PW_{11} on MCM-48.

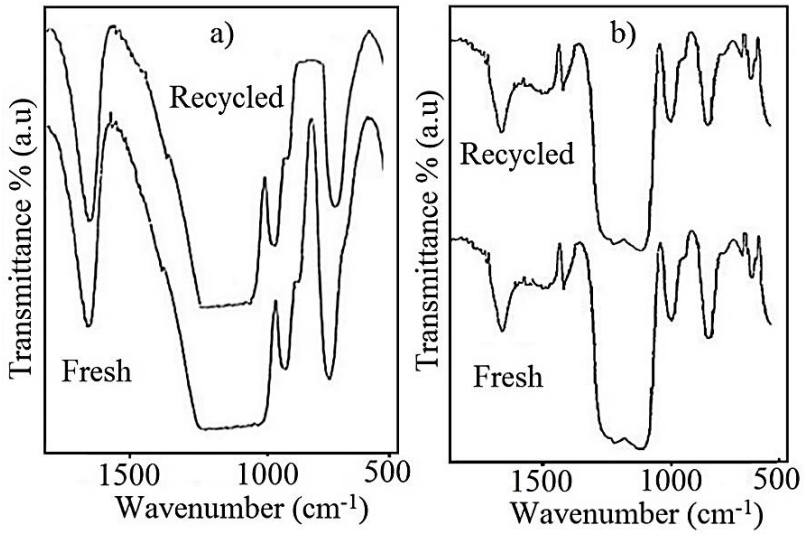

Figure 34. FT-IR spectra of fresh and recycled catalysts, (a) $(PW_{12})_3$/MCM-48 and (b) $(PW_{11})_3$/MCM-48.

This was further confirmed by Raman spectra of reused catalysts, showing retention of the typical bands of PW_{12}/PW_{11} (Figure 35). However, the spectrum is slightly different from the fresh one in terms of intensity, although this might not be significant in the reutilization of the catalysts.

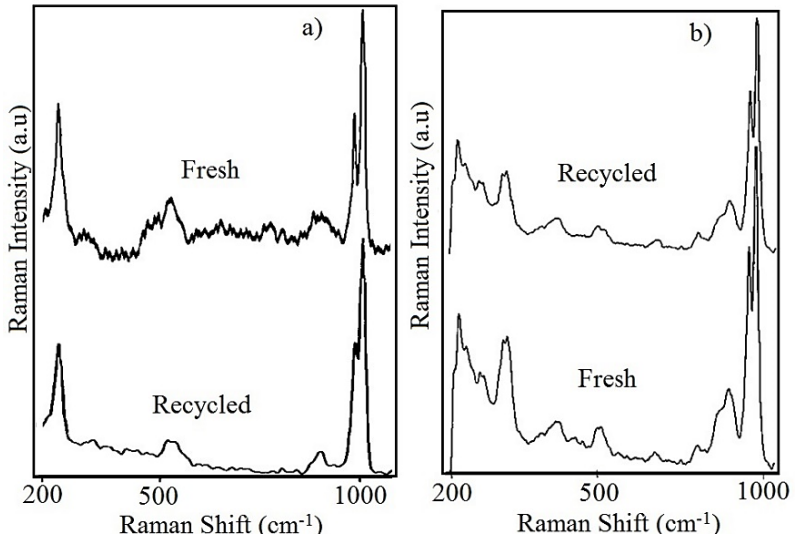

Figure 35. Raman spectra of fresh and recycled catalysts, (a) $(PW_{12})_3$/MCM-48 and (b) $(PW_{11})_3$/MCM-48.

XRD also shows no change in the property of recycled catalysts (Figure 36) indicating retention of pore structure of MCM-48 as well as the Keggin structure. Further, the acidity value of fresh [$(PW_{12})_3$/MCM-48- 3.9 mequiv. g^{-1}, $(PW_{11})_3$/MCM-48- 3.4 mequiv. g^{-1}] and reused catalyst [$(PW_{12})_3$/MCM-48- 3.5 mequiv. g^{-1}, $(PW_{11})_3$/MCM-48- 3.2 mequiv. g^{-1}] also did not show any appreciable change in acidity. Hence there was no deactivation of the catalyst.

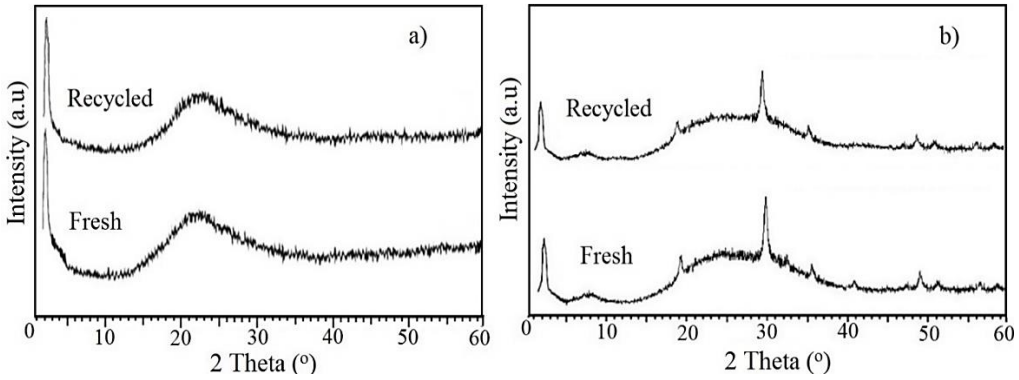

Figure 36. XRD patterns of fresh and recycled catalysts, (a) $(PW_{12})_3$/MCM-48 and (b) $(PW_{11})_3$/MCM-48.

Characterization of biodiesel derived from transesterification of SO and WCO

The biodiesel sample from transesterification of SO as well as WCO was characterized by FT-IR and ^{1}H-NMR analysis. The biodiesel i. e. fatty acid ester obtained by transesterification reaction was designated by BDSO and BDWCO.

FT-IR analysis for fatty acid methyl esters

The FT-IR spectra have been used to identify functional groups and the bands corresponding to various stretching and bending vibrations in the sample of biodiesel derived from soybean oil (Figure 37). The position of carbonyl group in FT-IR is sensitive to substituent effects and to the structure of the molecule. The methoxy ester carbonyl group in BDSO appears at 1744 cm^{-1}. The band at 3465 cm^{-1} corresponds to the overtone of ester functional group. The C-O stretching vibration in BDSO shows two asymmetric coupled vibrations at 1162 cm^{-1} and 1098 cm^{-1} due to C-C(=O)-O and 1031 cm^{-1} due to O-C-C.

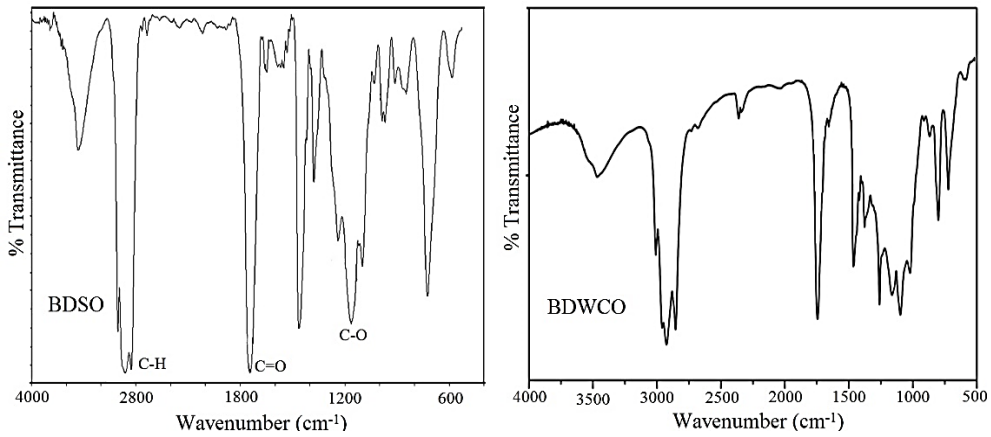

Figure 37. FT-IR spectrum of biodiesel samples, BDSO and BDWCO.

The FT-IR spectrum (Figure 37) of BDWCO exhibited bands at 1743 cm^{-1} and 1741 cm^{-1} characteristic for methoxy ester carbonyl group. The overtone of ester functional group was observed at 3465 cm^{-1}. The C-O stretching vibration revealed two coupled vibrations at 1119 cm^{-1} and 1171 cm^{-1} due to (C-C(=O)-O) and at 1017 cm^{-1} as a result of (O-C-C).

^{1}H NMR of biodiesel samples

Biodiesel samples were characterized by ^{1}H-NMR spectroscopy (Figure 38). The characteristic peak of methoxy protons was observed as a singlet- 3.678 ppm and a triplet of CH_2 protons at 2.296 ppm for BDSO and 2.8 ppm for BDWCO. These two peaks are the distinct for the confirmation of methyl esters present in biodiesel. These data confirm the formation of high quality of biodiesel.

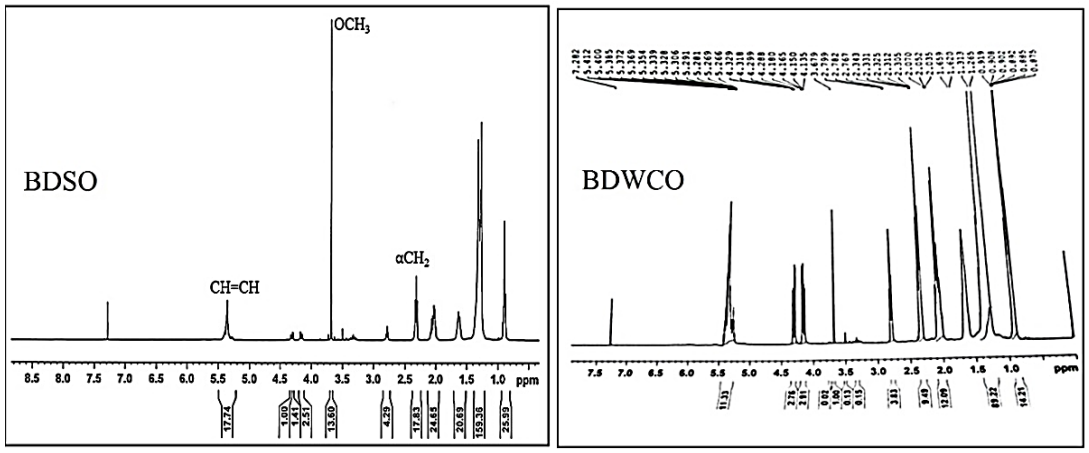

Figure 38. ^{1}H-NMR of biodiesel sample, BDSO and BDWCO.

Properties of biodiesel produced

The physical and chemical properties of biodiesel were studied. The biodiesel was prepared in the laboratory scale. The biodiesel sample BDSO, BDWCO were analysed for various properties. The properties measured were compared with the ASTM specifications and the results are presented in Table 8. Acid value is a measure of the FFA content of the biodiesel. Free fatty acids in the oil indicate incomplete transesterification or oxidative degradation where fatty acid methyl ester molecules are regenerated during shelving. Acid numbers higher than 0.8 mg KOH/g have been associated with fuel system deposits and reduced life of fuel pumps and filters [79-80]. The acid value of BDSO and BDWCO were found to be quite below the required limit. The kinematic viscosity indicates the flow capability of any fuel and it was found that it was within the limits of ASTM standards for BDSO and BDWCO. Flash point is the lowest temperature at which vapours from a fuel will ignite on application of a small flame under standard test conditions. The flash point of BDSO, BDWCO sample falls within the limits of ASTM standard.

Table 8. Properties of synthesised biodiesel with different feedstocks.

Property	Testing procedure	ASTM D6751 Standard, Biodiesel	ASTM D 975 Standard, diesel fuel	BDSO	BDWCO
Acid Value, mg KOH/g	ASTM D1980-87	0.5	-	<0.05	<0.8
Viscosity at 40 ^{o}C	ASTM D446	1.9 to 6	1.3 to 4.1	5.1	4.8
Flash point (^{o}C)	-	100 to 170	60 to 80	164	110
Pour point (^{o}C)	ASTM D97	-15 to 10	(-35) to 15	4	-2

Biodiesel is safer than petro-diesel to handle and store because it has a little bit higher flash point than petro-diesel. The pour point of BDSO was 4, which may be due to the higher content of unsaturated fatty acid in raw soybean oil. The results were found to be within the specified limits and BDSO, BDWCO was suitable not only for the tropical region but also for moderate temperate region.

However, further research and development on additional fuel properties and the effects of biodiesel on the engine are necessary.

Probable reaction mechanism over the present catalysts (PW_{12}/PW_{11} anchored to MCM-41/MCM-48) can be explained as below. Hexagonal pore dimension and high surface area of the present catalyst facilitates the diffusion of large triglyceride molecules inside the catalyst surface leading to high conversion. The carbocation is formed by acid sites of the catalyst with the carbonyl oxygen [81]. A tetrahedral intermediate is formed by nucleophilic attack of methanol to the carbocation. The tetrahedral intermediate eliminates H_2O to form biodiesel. This mechanism can be extended to di-glycerides or tri-glycerides.

Scale up experiments and possible industrial scheme for biodiesel production

In the present work, an attempt was also made to scale up the experiment for transesterification of SO, WCO and JO for biodiesel synthesis using up to 300 g feedstock over $(PW_{12})_3$/MCM-48 under optimized conditions for comparison with the batch scale. The sample was further separated using centrifuge. Experimental setup and separation of biodiesel has been shown in Figure 39.

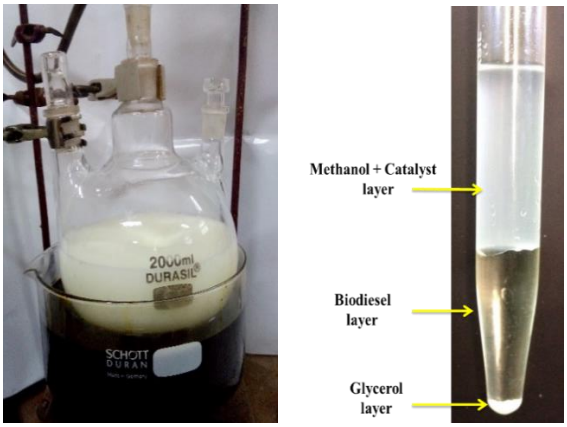

Figure 39. Scale up experiment (left), biodiesel and glycerol separation (right).

Similar results can be expected with other oil feedstocks for scale up experiments, without changing any mechanistic requirement of the system. Hence, depending on the requirements, the size of the unit can be scaled up to

get higher production capacity. A possible scheme of this integrated process using heterogeneous acid catalysts is shown in Figure 40.

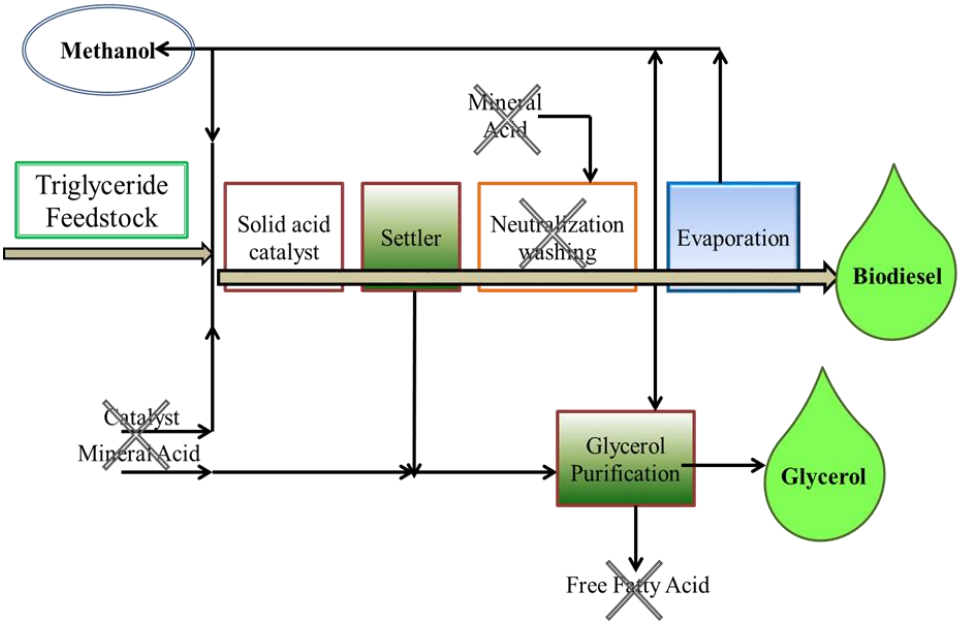

Figure 40. Process for biodiesel production over heterogeneous acid catalysts.

After completion of transesterification reaction settling can be used to separate the two products, i.e. crude glycerol and biodiesel. After settling, crude glycerol is washed with water to remove impurities and the traces of the catalyst. In heterogeneous catalysis, the reaction mainly takes place on the surface of active sites. Hence, after completion of reaction, the unreacted as well as by-product molecules must be removed from the surface in order to activate the catalyst for next run.

Conclusions

- The present catalysts showed excellent activities for biodiesel synthesis via *esterification of FFA, oleic acid*.
- Kinetic studies show that esterification of oleic acid *follows first* order rate law without any diffusion or mass transfer limitation.
- The present catalysts also exhibits *outstanding activities* for *transesterification of triglyceride* feedstock, *soybean oil* and *waste cooking oil* with methanol under mild conditions.
- The *recycling studies* showed that both the catalysts can be reused several times without any significant loss in the activity.
- The EDS, FT-IR, FT-Raman, XRD as well as acidity measurements of *reused catalysts* shows *no structural changes or loss in acidity* indicating catalytic systems are stable.
- The higher activities enables the catalysts to be used for different *feedstocks that are rich in FFAs*.
- We have successfully developed scale up experiments for *environmentaly benign* biodiesel production from soybean oil and waste cooking oil.
- From the catalytic activity as well as kinetic studies the order of catalysts was found to be *$(PW_{12})_3$/MCM-48 > $(PW_{12})_3$/MCM-41> $(PW_{11})_3$/MCM-48> $(PW_{11})_3$/MCM-41.*

References

1. Z. Helwani, M. R. Othman, N. Aziz, W. J. N. Fernando, J. Kim, Fuel Process. Technol., 90, 1502, (2009).
2. A. Demirbas, Energy Convers. Manage., 50, 14, (2009).
3. B. Buczek, L. Czepirski, Inform AOCS, 15,186, (2004).
4. A. Demirbas, Energy Convers. Manage., 44, 2093, (2003).
5. C. Stavarache, M. Vinatoru, R. Nishimura, Y. Maeda, Ultrason. Sonochem., 12, 367, (2005).
6. A. Sarin, *Biodiesel Production and Properties*, Royal Society of Chemistry, Cambridge, UK, (2012).
7. R. Luque, J. A. Melero (Eds.), *Advances in biodiesel production Processes and technologies*, Woodhead Publishing Limited, Cambridge, UK, (2012).
8. P. V. Tekade, O. A. Mahodaya, G. R. Khandeshwar, B. D. Joshi, Sci. Revs. Chem. Commun., 2(3), 208, (2012).
9. G. Pahl, *Biodiesel: Growing a New Energy Economy*. Chelsea Green Publication Company, US, (2004).
10. Taken from- www.biodieselmagazine.com/articles/645306.
11. S. Peter, E. Weidner, Eur. J. Lipid Sci. Technol., 109, 11, (2007).
12. Z. Tang, L. Wang, J. Yang, Eur. J. Lipid Sci. Technol., 110, 747, (2008).
13. N. Dizge, C. Aydiner, D. Y. Imer, M. Bayramoglu, A. Tanriseven, B. Keskinler, Bioresour. Technol., 100, 1983, (2009).
14. V. B. Veljkovic, O. S. Stamenkovic, Z. B. Todorovic, M. L. Lazic, D. U. Skala, Fuel., 88, 1554, (2009).
15. C. C. M. Silva, N. F. P. Ribeiro, M. V. M. Souz, D. A. G. Aranda, Fuel Process. Technol., 91, 205, (2010).
16. M. A. Jackson, J. W. King, J. Am. Oil Chem. Soc., 73, 353, (1996).
17. Y. Zhang, M. A. Dube, D. D. McLean, M. Kates, Bioresour. Technol., 89, 1, (2003).
18. D. Y. C. Leung, Y. Guo, Fuel Process. Technol., 87, 883, (2006).
19. M. Y. Koh, T. I. M. Ghazi, Renew. Sustain. Energy Rev., 15, 2240, (2011).

20. G. Mendow, N. S. Veizaga, C. A. Querini, Bioresour. Technol., 102, 6385, (2011).
21. S. V. Ghadge, H. Raheman, Biomass Bioenerg., 28, 601, (2005).
22. V. P. Amish, N. Subrahmanyam, P. A. Payal, Fuel, 88, 625, (2009).
23. G. C. Martins, T. Sergio, M. L. Ledo, U. Schuchardt, Bioresour. Technol., 99, 6608, (2008).
24. S. H. Shuit, Y. T. Ong, K. T. Lee, B. Subhash, S. H. Tan, Biotechnol. Adv., 30, 1364, (2012).
25. L. S. do Nascimento, L. M.Z. Titoa, R. S. Angélica, C. E. F. da Costa, J. R. Zamian, G. N. da Rocha Filho, Appl. Catal. B: Env., 101, 495, (2011).
26. S. R. Kirumakki, N. Nagaraju, S. Narayanan, Appl. Catal. A: Gen., 273, 1, (2004).
27. A. A. Kiss, A. C. Dimian, G. Rothenberg, Adv. Synth. Catal., 348, 75, (2006).
28. K. H. Chung, B.G. Park, J. Ind. Eng. Chem., 15, 388, (2009).
29. M. A. Harmer, W. E. Farneth, Q. Sun, J. Am. Chem. Soc., 118, 7708, (1996).
30. M. A. Harmer, Q. Sun, A. J. Vega, W. E. Farneth, A. Heidekum, W. F. Hoelderich, Green Chem., 2, 7, (2000).
31. T. Okuhara, Catal. Today, 73, 167 (2002).
32. Y. Wang, Y. Liu, C. Liu, Energy Fuel, 22, 2203, (2008).
33. A. A. Kiss, A. C. Dimian, G. Rothenberg, Energy Fuel, 22, 598, (2008).
34. Y.M. Park, D.W. Lee, D. K. Kim, J.S. Lee, K. Y. Lee, Catal. Today, 131, 238, (2008).
35. Y. M. Park, J. Y. Lee, S. H. Chung, I. S. Park, S. Y. Lee, D. K. Kim, J. S. Lee, K. Y. Lee, Bioresource Technol., 101, S59, (2010).
36. I. K. Mbaraka, K. J. McGuire, B.H. Shanks, Ind. Eng. Chem. Res., 45, 3022 (2006).
37. J. A. Melero, L. F. Bautista, G. Morales, J. Iglesias, D. Briones, Energy Fuel, 23, 539, (2009).
38. M. G. Kulkarni, R. Gopinath, L. C. Meher, A. K. Dalai, Green Chem., 8, 1056, (2006).

39. C. S. Caetano, I. M. Fonseca, A. M. Ramos, J. Vital, J. E. Castanheiro, Catal. Comm., 9, 1996, (2008).
40. B. Hamad, R. O. L. Souza de, G. Sapaly, M. G. C. Rocha, P. G. P. Oliveira de, W. A. Gonzalez, E. A. Sales, N. Essayem, Catal. Commun., 10, 92, (2008).
41. G. Sunita, B. M. Devassy, A. Vinu, D. P. Sawant, V. V. Balasubramanian, S. B. Halligudi, Catal. Commun., 9, 696, (2008).
42. L. Xu, W. Li, J. Hu, X. Yang, Y. Guo, Appl. Catal. B: Env., 90, 587, (2009).
43. L.Xu,Y.Wang, X. Yang, J. Hu, W. Li and Y. Guo, Green Chem., 11, 314, (2009).
44. L. Xu, W. Li, J. Hu, K. Li, X. Yang, F. Ma, Y. Guo, X. Yu, Y. Guo, J. Mater. Chem., 19, 8571, (2009).
45. C. F. Oliveira, L. M. Dezaneti, F. A. C. Garcia, J. L. de Macedo, J. A. Dias, S. C. L. Dias, K. S. P. Alvim, Appl. Catal. A: Gen., 372, 153, (2010).
46. K. Srilatha, N. Lingaiah , P. S. Sai Prasad, B. L. A. Prabhavathi Devi, R. B. N. Prasad, Reac. Kinet. Mech. Cat., 104, 211, (2011).
47. K. Srilatha, Ch. Ramesh Kumar, B. L. A. Prabhavathi Devi, R. B. N. Prasad, P. S. Sai Prasada, N. Lingaiah, Catal. Sci. Technol., 1, 662, (2011).
48. K. Srilatha, N. Lingaiah, B. L. A. P. Devi, R. B. N. Prasad, S. Venkateswar, P. S. S. Prasad, Appl. Catal. A: Gen., 365, 28, (2009).
49. K. Srilatha, T. Issariyakul, N. Lingaiah, P. S. Sai Prasad, J. Kozinski, A. K. Dalai, Energy Fuel, 24, 4748, (2010).
50. K. Srilatha, B. L. A. Prabhavathi Devi, N. Lingaiah, R. B. N. Prasad, P. S. Sai Prasad, Bioresour. Technol., 119, 306, (2012).
51. A. S. Badday, A. Z. Abdullah, K. T. Lee, Appl. Energy, 105, 380, (2013).
52. R. Sheikh, M. S. Choi, J. S. Im, Y. H. Park, J. Ind. Eng. Chem., 19, 1413, (2013).
53. V. V. Bokade, G. D. Yadav, Process Saf. Environ. Prot., 85 (B5), 372, (2007).
54. V. V. Bokade, G. D. Yadav, Ind. Eng. Chem. Res., 48, 9408, (2009).
55. L. X. Zhang, Q. Z. Jin, J. H. Huang, Y. F. Liu, L. Shan, X. G. Wang, Energ. Source. Part A, 34, 1037, (2012).
56. O. da Silva Lacerda, J. R. M. Cavalcanti, T. M. de Matos, R. S. Angélica, G. N. da Rocha Filho, I. de C. Lopes Barros, Fuel, 108, 604, (2013).

57. K. Y. Nandiwale, V. V. Bokade, Ind. Eng. Chem. Res., 53 (49), 18690, (2014).
58. L. H. O. Pires, A. N. de Oliveira, O. V. Monteiro Jr., R. S. Angélica, C. E. F. da Costa, J. R. Zamian, L. A. S. do Nascimento, G. N. R. Filho, Appl. Catal. B: Env., 160-161, 122, (2014).
59. J. A.Monge, G. Trautwein, J. P. Marco-Lozar, Appl. Catal. A, 468, 432, (2013).
60. A. S. Badday, A. Z. Abdullah, K. T. Lee, Renew. Energy, 50, 427, (2013).
61. A. S. Badday, A. Z. Abdullah, K. T. Lee, Renew. Energy, 62, 10, (2014).
62. A. Patel, N. Narkhede, Energy Fuels, 26, 6025, (2012).
63. C. Baroi, S. Mahto, C. Niu, A.K. Dalai, Appl. Catal. A, 469, 18, (2014).
64. C. Baroi, A. K. Dalai, Appl. Catal. A: Gen., 485, 99, (2014).
65. C. T. Kresge, M. E. Leonowicz, W. J. Roth, J. C. Vartuli, J. S. Beck, Nature, 359, 710, (1992).
66. J. S. Beck, J. C. Vartuli, W. J. Roth, M. E. Leonowicz, C. T. Kresge, K. D. Schmitt, C. T. W. Chu, D. H. Olson, E. W. Sheppard, S. B. McCullen, J. B. Higgins, J. L. Schlenker, J. Am. Chem. Soc., 114, 10834, (1992).
67. I. Tropecelo, M. H. Casimiro, I. M. Fonseca, A. M. Ramos, J. Vital, J. E. Castanheiro, Appl. Catal. A: Gen., 390, 183, (2010).
68. V. Brahmkhatri, A. Patel, Ind. Eng. Chem. Res., 50, 6620, (2011).
69. V. Brahmkhatri, A. Patel, Appl. Catal. A: Gen., 403, 161, (2011).
70. C. Baroi, A. K. Dalai, Catal. Today, 207, 74, (2013).
71. R. Fazaeli , H. Aliyan, Rus. J. Appl. Chem., 88, 676, (2015).
72. Y. Liu, S. Liu, D. He, N. Li, Y. Ji, Z. Zheng, F. Luo, S. Liu, Z. Shi, C. Hu, J. Am. Chem. Soc., 137, 12697, (2015).
73. A.T. Kiakalaieh, N.A.S. Amin, A. Zarei, I. Noshadi, Appl. Energy, 102, 283, (2013).
74. G. Corro, U. Pal, N. Tellez, Appl. Catal. B., 129, 39, (2013).
75. G. C. Bond, *Heterogeneous Catalysis: Principles and Applications*, Oxford Chemistry Series; Clarendon Press: Oxford, Ch.- 3, p 49, (1974).
76. A. K. Endalew, Y. Kiros, R. Zanzi, Biomass Bioenergy, 35, 3787, (2011).

77. A. Birla, B. Singh, S. N. Upadhyay, Y.C. Sharma, Bioresour. Technol. 106, 95, (2012).
78. R. A. Sheldon, M. Walau, I. W. C. E. Arends, U. Schuchurdt, Acc. Chem. Res., 31, 485, (1998).
79. US Department of Energy, Energy efficiency and renewable energy. Biodiesel handling and use guidelines. 3. Edition. DOE/GO-102006-2358, (2006).
80. D. Y. C. Leung, B. C. P. Koo, Y. Guo, Bioresour. Technol., 97, 250, (2006).
81. A. Patel, N. Narkhede, Catal. Sci. Technol., 3, 3317, (2013).

CHAPTER 2B

Esterification of Alcohols…….

1) Glycerol

2) Benzyl Alcohol

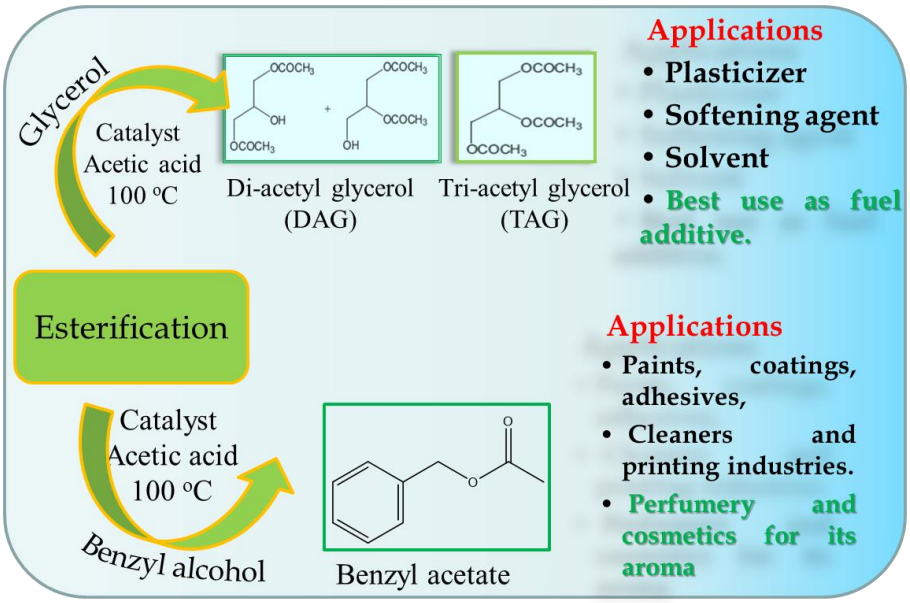

I&EC research
Industrial & Engineering Chemistry Research

Article

pubs.acs.org/IECR

Bifunctional Catalytic Activity of 12-Tungstophosphoric Acid Impregnated to Different Supports for Esterification and Oxidation of Benzyl Alcohol: A Comparative Study on Catalytic Activity and Kinetics

Anjali Patel* and Sukriti Singh

Polyoxometalates and Catalysis Laboratory, Department of Chemistry, Faculty of Science, The M.S. University of Baroda, Vadodara 390002, India

Supporting Information

ABSTRACT: The bifunctional catalytic activity of 30% 12-tungstophosphoric acid impregnated to MCM-41 (TPA_3/MCM-41) and zirconia (TPA_3/ZrO_2) was explored for acid catalysis as well as oxidation reactions. The effect of various reaction parameters such as molar ratio, amount of catalyst, time, and temperature was studied to optimize the conditions for maximum conversion. The catalysts show the potential of being used as recyclable catalytic materials after simple regeneration without significant loss in conversion. TPA_3/MCM-41 shows high activity in terms of % conversion toward esterification as well as oxidation reaction as compared to that of TPA_3/ZrO_2. High catalytic activity of TPA_3/MCM-41 may be due to its porosity and higher surface area as well as high total acidity.

Ind. Eng. Chem. Res. 2013, 52, 10896−10904

I&EC research
Industrial & Engineering Chemistry Research

Article

pubs.acs.org/IECR

Selective Green Esterification and Oxidation of Glycerol over 12-Tungstophosphoric Acid Anchored to MCM-48

Sukriti Singh and Anjali Patel*

Polyoxometalates and Catalysis Laboratory, Department of Chemistry, Faculty of Science, The M. S. University of Baroda, Vadodara 390002, India

Supporting Information

ABSTRACT: 12-Tungstophosphoric acid anchored to mesoporous material (MCM-48) was synthesized and characterized by thermogravimetric−differential thermal analysis, Brunauer−Emmett−Teller analysis, Fourier transform infrared spectroscopy, ^{29}Si nuclear magnetic resonance, X-ray diffraction, and transmission electron microscopy. The efficacy for the esterification of glycerol with acetic acid was investigated and 50% selectivity toward diacetyl and 30% for triacetyl glycerol was obtained under mild reaction conditions. The kinetic study was carried out, and it was found that esterification of glycerol follows first-order kinetics, and the rates are not mass transfer limited. As a cleaner alternative to traditional procedures, environmentally benign oxidation of glycerol was investigated with H_2O_2, and 40.5 and 33.6% selectivity for dihydroxyacetone and glyceraldehyde was obtained, respectively. The catalyst can be used up to four cycles without significant loss in conversion.

Ind. Eng. Chem. Res. 2014, 53, 14592−14600

Fuel 118 (2014) 358–364

Contents lists available at ScienceDirect

Fuel

journal homepage: www.elsevier.com/locate/fuel

A green and sustainable approach for esterification of glycerol using 12-tungstophosphoric acid anchored to different supports: Kinetics and effect of support

Anjali Patel *, Sukriti Singh

Polyoxometalates and Catalysis Laboratory, Department of Chemistry, Faculty of Science, The M.S. University of Baroda, Vadodara 390002, Gujarat, India

HIGHLIGHTS

- Synthesis of 12-tungstophosphoric acid anchored to MCM-41 and zirconia.
- Thermal and textural characterization.
- Glycerol esterification to yield useful glycerol ester products.
- Kinetic and thermodynamic parameters optimized.
- Potential of being used as recyclable catalysts after simple regeneration.

GRAPHICAL ABSTRACT

ARTICLE INFO

Article history:
Received 1 May 2013
Received in revised form 5 September 2013
Accepted 5 November 2013
Available online 18 November 2013

Keywords:
12-Tungstophosphoric acid
Heterogeneous
Esterification
Glycerol
Kinetic

ABSTRACT

Environmentally benign solid acid catalysts consisting of 12-tungstophosphoric anchored to MCM-41 and zirconia were synthesized and characterized. The efficacy for the esterification of glycerol, a value added byproduct from biodiesel production was investigated. Conditions for maximum conversion was optimized by varying different reaction parameters, such as, glycerol/acetic acid mole ratio, amount of the catalyst, reaction time and reaction temperature. The kinetic study was carried out, and it was found that esterification of glycerol follows first order kinetics and the rates are not mass transfer limited. Also activation energy and ΔG was determined. The difference in % conversion as well as selectivity was correlated with the nature of supports, value of activation energy as well as ΔG. The catalysts showed potential of being used as recyclable material after simple regeneration without significant loss in conversion.

Microporous and Mesoporous Materials 195 (2014) 240–249

Contents lists available at ScienceDirect

Microporous and Mesoporous Materials

journal homepage: www.elsevier.com/locate/micromeso

Undecatungstophosphate anchored to MCM-41: An ecofriendly and efficient bifunctional solid catalyst for non-solvent liquid-phase oxidation as well as esterification of benzyl alcohol

Anjali Patel *, Sukriti Singh

Polyoxometalates and Catalysis Laboratory, Department of Chemistry, Faculty of Science, The M.S. University of Baroda, Vadodara 390002, India

ARTICLE INFO

Article history:
Received 12 July 2013
Received in revised form 14 April 2014
Accepted 19 April 2014
Available online 26 April 2014

Keywords:
Undecatungstophosphate
Bifuctional catalyst
MCM-41
Oxidation
Esterification

ABSTRACT

Undecatungstophosphate anchored to MCM-41 was synthesized and characterized by various physico-chemical techniques. The bifunctional catalytic activity was evaluated for esterification as well oxidation reactions of benzyl alcohol. The influence of different parameters such as molar ratio, amount of catalyst, reaction time and reaction temperature on oxidation as well as esterification of benzyl alcohol was investigated for maximum conversion. Detailed kinetic studies reveal that the reactions follow first order kinetics and the low values of activation energy for esterification and oxidation indicates that the reaction rate is truly governed by the chemical step. The present bifunctional catalyst can be recycled without any significant difference in % conversion for both reactions. Further, oxidation and esterification of various alcohols were also carried out under optimized conditions to see the effect of chain length and type of alcohols.

Valorisation of Glycerol

Glycerol is one of the most versatile and valuable chemical substances known, with more than a thousand uses and applications [1-3]. It is the main coproduct of biodiesel and rapid development in biodiesel production is leading to a dramatic increase in its production. Due to its versatile physical and chemical properties use of glycerol in advanced organic syntheses is now emerging as a fascinating challenge for chemists (Chart 1).

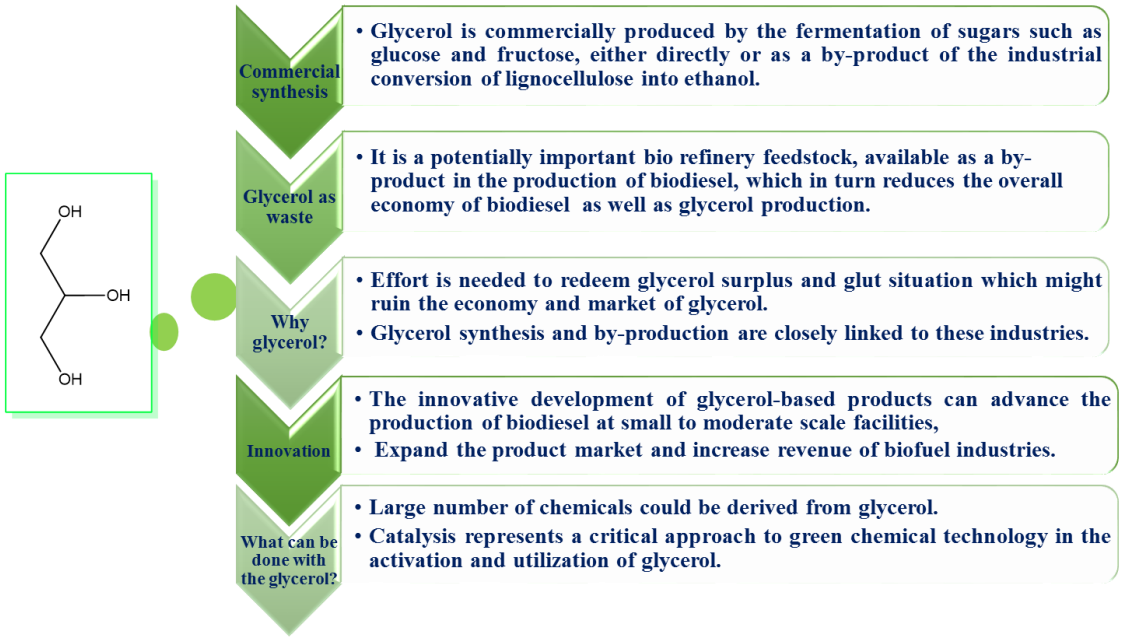

Chart 1. Outlook for glycerol valorisation

The wide realm of glycerol applications are presented in Chart 2 [4-6].

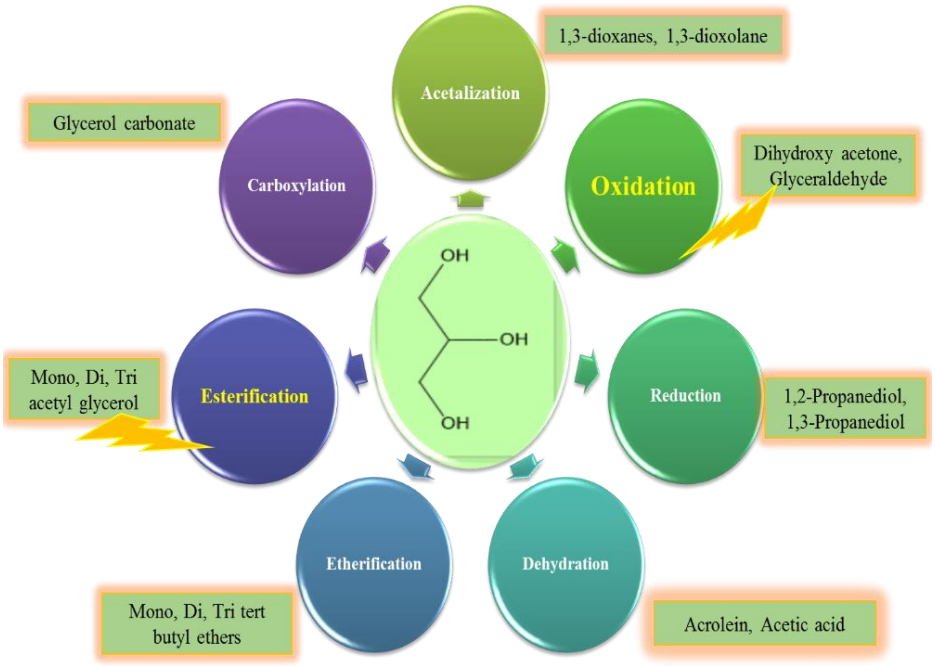

Chart 2. Various glycerol transformations.

The transformations of glycerol into fuel oxygenates by esterification reaction [7-9] are among chemical reactions that draw interest of many researchers. One of its potential and promising values has been envisioned for the automotive and bio-refinery industries to transform it into fuel additive. Acetyl glycerol's [10–12] have been identified as valuable replacement of fuel additive which depends on depleting sources, price uncertainty and growing environmental concern of petroleum feedstock. Various application of these products can be summarised in Table 1.

Table 1. Applications of products derived from glycerol esterification.

Products	Applications	References
Monoacetyl glycerol (MAG)	Manufacture of explosives, tanning agent, and solvent for dyes.	[10]
Diactyl glycerol (DAG)	Plasticizer, softening agent and solvent. **Best use as fuel additive.**	[7, 13]
Triacetyl glycerol (TAG)	Solvent for dissolving or diluting drugs and organic compounds. **Best use as fuel additive** for improving the anti-knocking, cold and viscosity properties of biodiesel.	[12, 14, 15]

The reaction of glycerol with acetic acid affords a mixture of acetyl glycerol (MAG, DAG, TAG). To increase the selectivity for TAG especially, a large excess of acetic acid should be used. The production of TAG in high selectivity by the direct reaction with acetic acid is difficult, because the reaction is consecutive and the water formed may shift the equilibrium.

Number of heterogeneous catalysts are reported for glycerol esterification reaction such as Zeolite [16], Amberlyst-15 [16-18], niobic acid [16], Starbon acid, ion exchange resins [19], sulfated activated carbon [11], sulfated zirconia [20-22] and sulphated alumina [23], functionalized mesoporous silica-type SBA-15 [12], mesoporous silica MCM-41 sulphonated and functionalized with different alkyl chains (methyl, ethyl, propyl and phenyl) [12], Niobium [24], Zirconia [25, 26], hydroxylated magnesium fluorides [26], reaction under supercritical carbon dioxide ($scCO_2$) [27], sulfonic acid (SO_3H) carbonized sucrose [28] as well as sulfonic acid functionalized cellulose [29] and graphene oxide [30] have been reported. Some of the above reactions comprising of sulfated activated carbon, ion exchange resins, Amberlyst etc. are marked by the limitation of high reaction pressure, temperature (120 ^oC) and activation of the catalysts, which poses a question on sustainability.

The literature survey shows that there are number of reports on glycerol esterification using anchored $H_3PW_{12}O_{40}$. Ferreira et al. [31] reported $H_3PW_{12}O_{40}$ immobilized into a silica matrix was used in the esterification of glycerol with acetic acid. High molar ratio of glycerol to acetic acid leads in lower selectivity values to MAG, which can be explained due to the high glycerol conversion promote the DAG and TAG formation. Same group [32] carried out glycerol esterification with $H_3PMo_{12}O_{40}$ acid encaged in USY zeolite. After 3 h of reaction time the glycerol conversion was 68%, with a selectivity of 59% to DAG, 37% to MAG and 2% to TAG. Ferreira and co-worker [33] later supported $H_3PW_{12}O_{40}$ on activated carbon. After 3 h of reaction, the glycerol conversion was 86%, with a selectivity of 63% to DAG, 25% to MAG

and 11% to TAG. The amount of active species in the catalyst, after the reactions, was measured by ICP. The catalyst only lost 10% of the $H_3PW_{12}O_{40}$ from the activated carbon support.

Lingaiah and group reported niobic acid supported $H_3PW_{12}O_{40}$ [34]. The catalysts exhibited excellent acetylation activity within short reaction time. The catalyst showed 90% conversion within 30 min of reaction time. They found that acidity of the catalysts depends upon the amount of $H_3PW_{12}O_{40}$ on niobic acid. The glycerol conversion was well correlated with the acidity of the catalysts. The selectivity during glycerol acetylation not only depends on the nature of catalyst but also on reaction time. Same group [35] carried out synthesis of $H_3PW_{12}O_{40}$ supported on Cs-containing ZrO_2 catalyst. They suggested that Cs-containing catalysts possess stronger acidic sites compared to the catalyst without Cs. The esterification activity and selectivity not only depended on the nature of the catalyst but also on reaction parameters such as temperature, time and mole ratio of glycerol to acetic acid.

Khayoon and Hameed [36] developed hybrid SBA-15 functionalized with $H_3PMo_{12}O_{40}$. 15% loaded catalyst showed corresponding selectivity of 86% for both DAG and TAG at the best reaction conditions of 110 ^oC. Temperature was found to be a dominant parameter controlling the endothermic esterification of glycerol with acetic acid and enhances the formation of DAG and TAG.

Zhu and co-workers [37] reported synthesis of bio-additives over zirconia supported catalysts using $H_4SiW_{12}O_{40}$, $H_3PW_{12}O_{40}$ and $H_3PMo_{12}O_{40}$ as active compounds. A 93.6% combined selectivity of DAG and TAG with complete glycerol conversion was obtained at 120 ^oC and 4 h of reaction time in the presence of $H_4SiW_{12}O_{40}/ZrO_2$.

Kim et al. [38] carried out comparative study of various types of solid acids, including silica-alumina (HUSY), $H_3PMo_{12}O_{40}$ supported on Nb_2O_5 and mesoporous SBA-15 etc. The acid strength affected the rates, showing an

increase in the intrinsic glycerol conversion turnover rate with an enhancement in the acid strength when the analogous type of solid acids were compared.

Recent literature reports show that, monoglyceride can be synthesized using direct esterification of glycerol with fatty acid in the presence of acidic catalyst and supported POMs have been used for the same. Hoo and Abdullah [39], showed synthesis of highly uniformed SBA-15 catalysts functionalized with $H_3PW_{12}O_{40}$. Characterization results showed that suitable $H_3PW_{12}O_{40}$ loading was beneficial for acid catalyzed glycerol esterification with lauric acid. High lauric acid conversion (70%) and monolaurin yield (50%) were shown in 6 h at 160 ^oC. Its ordered mesoporosity evidently resulted in shape selectivity effect to suppress by-products formation. Later the same group [40] showed kinetic evaluation for selective esterification of glycerol with lauric acid using post-impregnated $H_3PW_{12}O_{40}$ on SBA-15.

Very recently, Betiha and co-workers [41] carried out synthesis of micro-mesopores H_2N-PDVC polymer and reported the first successful immobilization of catalytically active acidic $H_3PW_{12}O_{40}$ material on the surface and pores of H_2N-PDVC framework material through ionic bonding interaction. The obtained catalyst exhibited high activity for glycerol acetylation under mild conditions (T- 100 ^oC, Gly: AA- 1:8 and time- 3 h) and also showed high selectivity towards TAG than previously described reports. Although the conversions and selectivity's towards the esters are good, new methods are needed to be explored wherein the reaction can proceed even at relatively lower molar ratios, catalyst amounts and temperatures. Thus, it is still a challenge to design a green and sustainable process for the same.

Esterification of Benzyl alcohol

Benzyl alcohol is a promising molecule in organic chemistry as number of organic transformations are possible. The huge amount of applications of alcohols has recently increased the interest in the synthesis of a variety of aromatic compounds by esterification via acid catalysis [42-43].

- Benzyl acetates are widely used in paints, coatings, adhesives, cleaners and printing industries.
- They have a very low solubility in water and used as extraction solvents for fine chemicals and pharmaceuticals, particularly for certain antibiotics.
- They are used as components of aroma with pleasant reminiscent of jasmine. Widely used in perfumery and cosmetics for its aroma.
- In synthetic flavorings to impart apple and pear flavors [44].

Due to the known disadvantages of homogeneous catalysts [45] the use of solid acids are convenient and also effective for acid-catalyzed reactions. A literature survey shows that many solid acid catalysts such as zeolites [46], ion exchange resins [47], Bronsted acidic ionic liquids [48, 49], $NbCl_5/Al_2O_3$ [50] and metal coated nanoparticals [51] have been found to be efficient catalysts in benzyl alcohol esterification.

Halligudi and group [52] carried out liquid phase esterification of benzyl alcohol to benzyl acetate with acetic acid over $H_4SiW_{12}O_{40}$ supported on zirconia embedded inside SBA-15 ($H_4SiW_{12}O_{40}/ZrO_2$/SBA-15). Catalytic activities have been correlated with acidity of the catalysts. The catalyst with 15 wt.% loading showed good catalytic activity with maximum 59% conversion and >96.1% selectivity to benzyl acetate as compared with other isomers at 373 K.

With a focus on recent developments in the conversion of glycerol and benzyl alcohol into value-added chemicals, we describe in this chapter the sustainable route towards solvent free valorisations of glycerol via esterification as well as

benzyl alcohol with acetic acid over phosphotungstates (PW_{12}/PW_{11}) anchored to MCM-41/MCM-48. The effects of different reaction variables such as catalyst concentration, mole ratio and reaction time were studied to optimize the conditions for maximum conversion. The catalysts were also recycled up to four times without any significant loss in the conversion.

EXPERIMENTAL

Materials

All chemicals used were of A.R. grade. 12-tungstophosphoric acid (PW_{12}), sodium tungstate, disodium hydrogen phosphate, glycerol (Gly), benzyl alcohol (BA) and acetic acid (AA) were used as received from Merck.

Catalytic reactions

Esterification of alcohols

The esterification of Gly (10 mmol) with AA (60 mmol); esterification of BA (10 mmol) with AA (20 mmol) was carried out in a 50 mL batch reactor provided with a double walled air condenser, Dean-Stark apparatus, magnetic stirrer, and a guard tube. The reaction mixture was refluxed at 100 ^{o}C for different time intervals. The obtained products were analysed on a GC (Shimatzu-2014) using a capillary column (RTX-5). GC analyses for Gly reactions were carried out according to following temperature program: initially, the oven temperature- 80 ^{o}C, then the temperature increased from 80 ^{o}C to 240 ^{o}C, with a rate- 5 ^{o}C/min and finally to 280 ^{o}C with a rate- 30 ^{o}C/min. Products were identified by comparison with the authentic samples and finally by gas chromatography mass spectroscopy (GC–MS).

RESULTS AND DISCUSSION

2B (I) Esterification of Gly and BA over PW_{12}/MCM-41 and PW_{11}/MCM-41.

- *Esterification of Gly*

The products obtained by esterification of Gly are shown in Scheme 1. Esterification is an equilibrium-limited reaction and in order to overcome the equilibrium limitation the reaction is carried out by taking AA in excess. The effect of various reaction parameters such as Gly/AA molar ratio, catalyst amount, time, and temperature was studied.

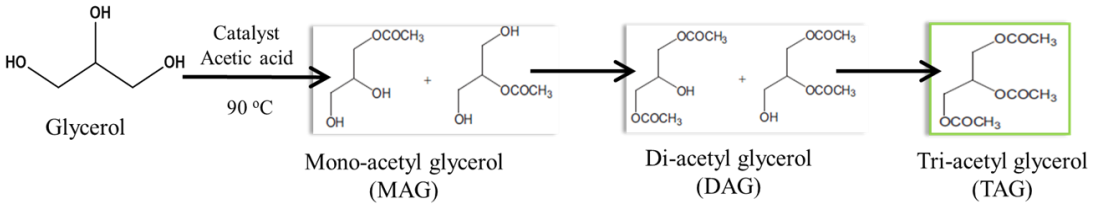

Scheme 1. Glycerol esterification reaction with acetic acid.

Effect of % loading of PW_{12}/PW_{11}

To study the effect of % loading reaction was carried out with 10-40% loading (Figure 1). It was observed that with an increase in the % loading of PW_{12}/PW_{11}, % conversion also increases. For 30% PW_{12}/PW_{11} loading, maximum conversion was obtained.

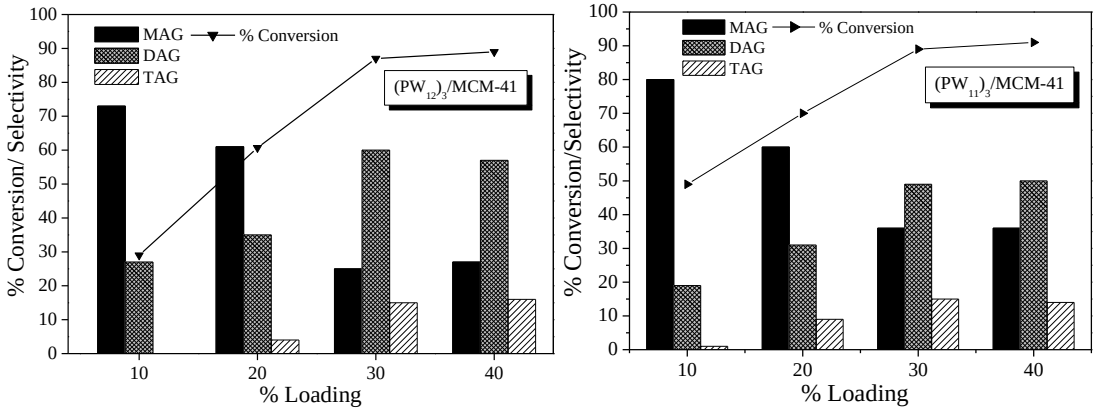

Figure 1. Effect of % loading of PW_{12}/PW_{11}: mole ratio of Gly: AA- 1:6, catalyst amount - 150 mg, temperature- 100 °C, time- 6 h.

On increasing the % loading to 40%, no significant increase in conversion was observed which might be due to blocking of the active sites due to formation

of multilayer on the support. This was also evident from value of surface area, which decreases for 40% loadings. This multilayer formation can hinder the reactant molecules to react with the active sites and intern there was significant increase in the conversion. Hence, 30% of PW_{12}/PW_{11} anchored to MCM-41 was considered for further studies.

Effect of mole ratio of Gly: AA

To see the effect of Gly: AA mole ratio, the reaction was carried out by varying the mole ratio. Reaction was studied with initial molar ratio of Gly: AA varying from 1:1 to 1:9. It was observed from Figure 2 that the conversion increases with an increase in Gly: AA mole ratio and reaches a maximum of 87% for $(PW_{12})_3$/MCM-41, at 1:6 molar ratio. With further increase in molar ratio there was only a small increase in conversion. Hence, the molar ratio of 1:6 was optimized.

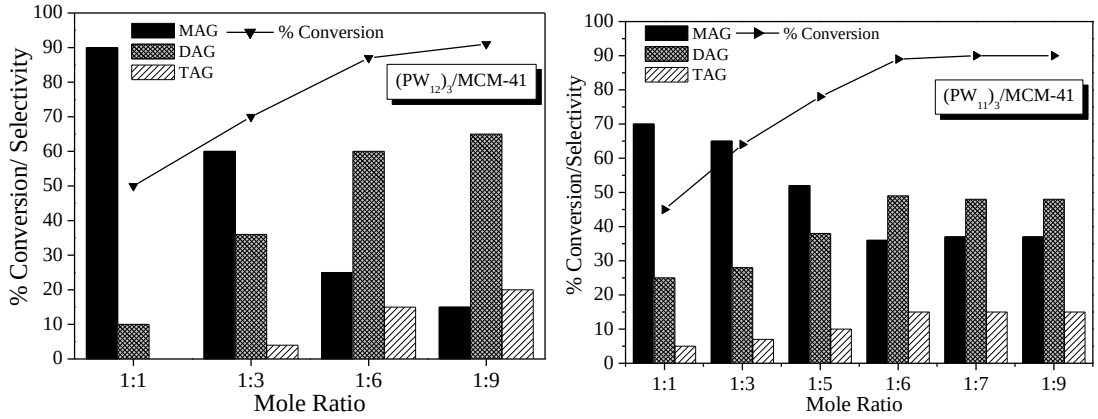

Figure 2. Effect of mole ratio Gly/AA: catalyst amount - 150 mg, temperature- 100 ^{o}C, time- 6 h.

Effect of catalyst amount

The catalyst amount was varied in the range 50 to 200 mg (Figure 3). It was observed from figure that initially the activity increases with an increase in catalyst amount. On further increasing catalyst amount from 100 to 150 mg, maximum conversion of Gly was obtained for both the catalysts. Under these conditions, after 150 mg there was no significant increase in the conversion with increase in catalyst amount. The distribution of DAG + TAG product was also optimum for both the catalysts with 150 mg amount.

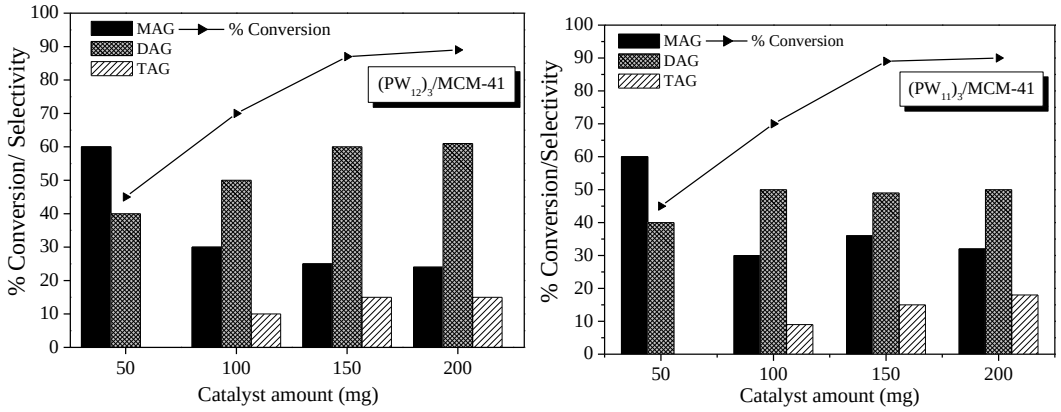

Figure 3. Effect of catalyst amount: mole ratio of Gly: AA- 1:6, temperature- 100 ^{o}C, time- 6 h.

Effect of reaction time

The effect of reaction time on conversion of Gly was studied (Figure 4). It was observed that Gly conversion increases with reaction time.

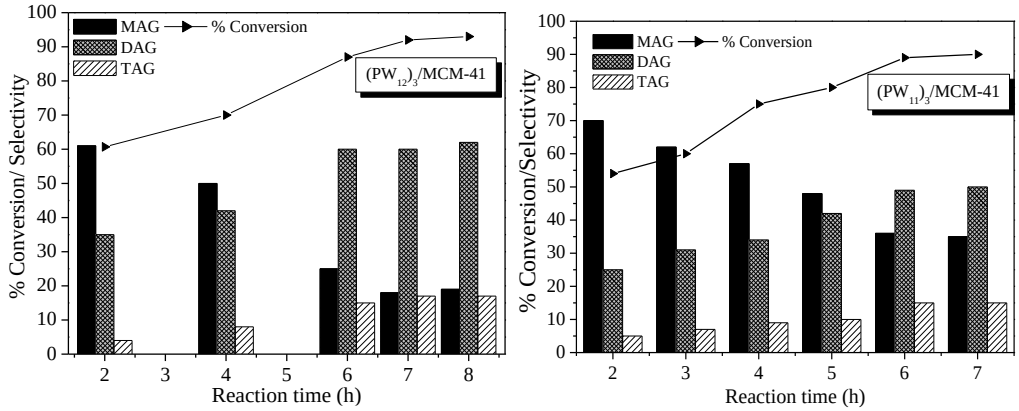

Figure 4. Effect of reaction time: mole ratio of Gly: AA- 1:6, catalyst amount- 150 mg, temperature- 100 ^{o}C.

Initially, at the start of reaction, selectivity towards MAG was high and as the reaction prolonged, selectivity towards DAG and TAG increased at the expense of MAG. The increase in selectivity for DAG and TAG with time is mainly due to the further esterification of MAG. Further, Gly conversion was nearly completed within 6 h time for $(PW_{12})_3$/MCM-41. The high catalytic activity of both the catalysts can be mainly co-related with the presence of intact Keggin ions on the supports. With further increase in the reaction time there was no significant increase in the conversion as well as distribution of the ester products. At 6 h, an optimum 88% conversion was achieved with 75% selectivity for DAG+TAG for $(PW_{12})_3$/MCM-41. Similar trend in activity was observed for $(PW_{11})_3$/MCM-41.

Effect of temperature

The effect of temperature on conversion was studied and it was found that with an increase in temperature from 70 to 100 ^oC the % conversion increases and product distribution of esters changes, which is as expected (Figure 5).

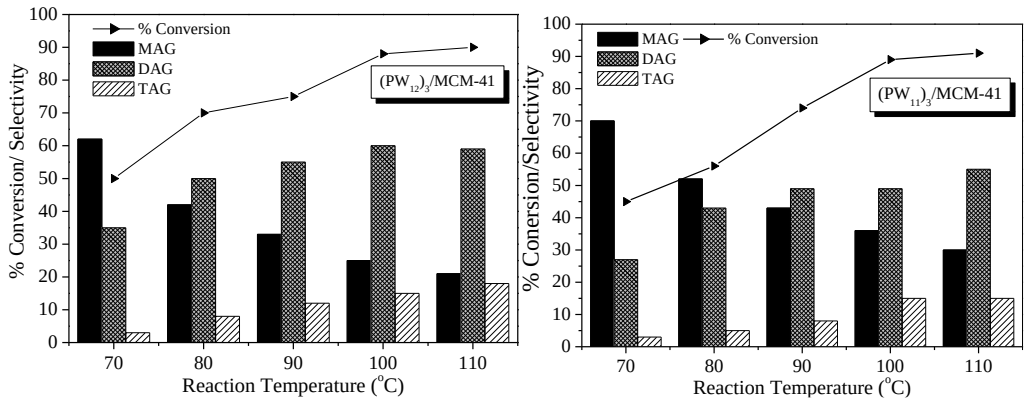

Figure 5. Effect of reaction temperature: mole ratio of Gly: AA- 1:6, catalyst amount- 150 mg, reaction time- 6 h.

At higher temperature, higher selectivity towards DAG and TAG was obtained. This can be explained due to the enhanced subsequent endothermic esterification of Gly with AA, at elevated temperature. At 100 ^oC, Gly maximum conversion (88%) was obtained for $(PW_{12})_3$/MCM-41. On further increasing the temperature, product distribution of higher esters remains

almost constant due to fast reaction rate and attainment of equilibrium for $(PW_{12})_3$/MCM-41. However, for $(PW_{11})_3$/MCM-41 there was saturation in conversion after 100 ^oC, but only slight enhancement in DAG selectivity. Hence, 100 ^oC temperature was found to be optimum.

Optimized conditions: [88% conversion for $(PW_{12})_3$/MCM-41, 89% Conversion for $(PW_{11})_3$/MCM-41] mole ratio Gly/AA- 1:6, catalyst amount- 150 mg, temperature- 100 °C and time- 6 h.

Kinetic study

A detailed study on the kinetic behaviour was carried out for esterification of Gly over $(PW_{12})_3$/MCM-41 and $(PW_{11})_3$/MCM-41. The esterification of Gly with AA was carried out with a 1:6 molar ratio and different reaction time.

The plot of log Co/C versus time (Figure 6) shows a linear relationship of Gly consumption with respect to time over both the catalysts. With increase in time, there was gradual increase in Gly conversion over both the catalysts. The rate law is expected to follow first order dependence. This was further supported by the study of the effect of catalyst concentration on the rate of reaction.

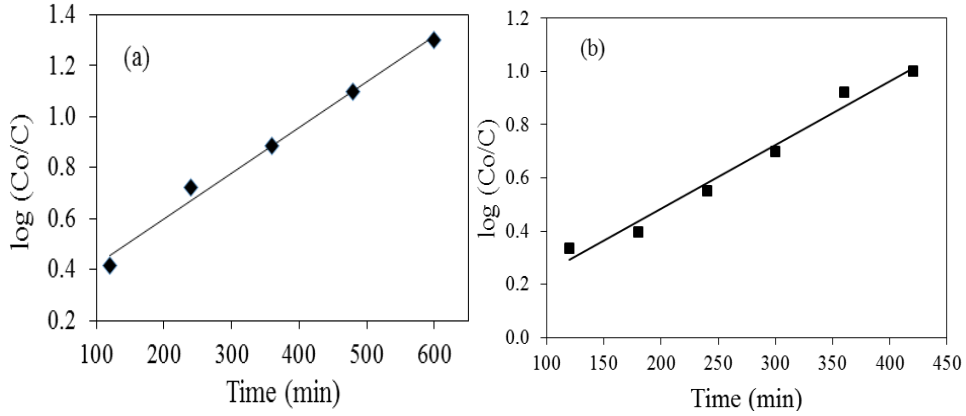

Figure 6. First-order plot for esterification of Gly over, (a) $(PW_{12})_3$/MCM-41 and (b) $(PW_{11})_3$/MCM-41.

The catalyst concentration was varied at a fixed substrate concentration of 10 mmol and at 100 ^{o}C temperature. It can be observed from Figure 7, that the rate of reaction increases with an increase in the catalyst concentration.

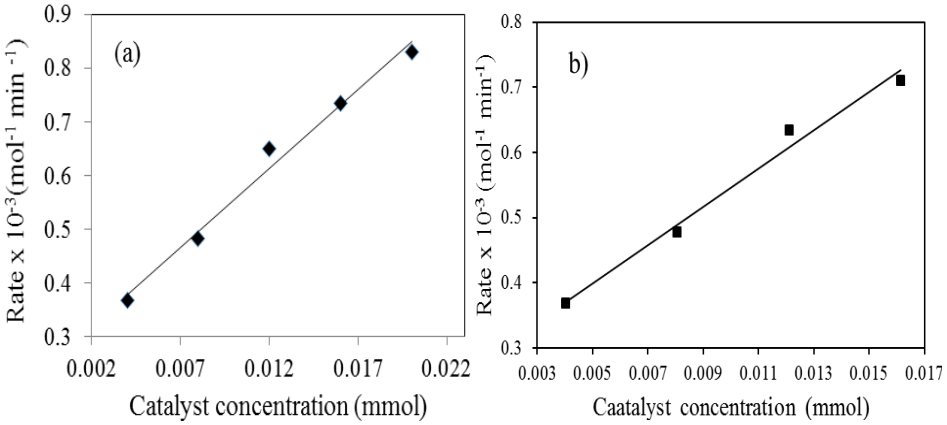

Figure 7. Plot of reaction rate versus catalyst concentrations for esterification of Gly over (a) $(PW_{12})_3$/MCM-41 and (b) $(PW_{11})_3$/MCM-41.

The graph of ln k versus 1/T was plotted (Figure 8) and the value Ea was determined. On increasing temperature from 333 K to 383 K there was linear increase in reaction rate due to activation of catalytic species. Ea for $(PW_{12})_3$/MCM-41 was found to be 42.3 kJ mol^{-1} and for $(PW_{11})_3$/MCM-41 it was 43 kJ mol^{-1} indicating that the rate is truly governed by the chemical step and there was no diffusion limitation/mass transfer limitation.

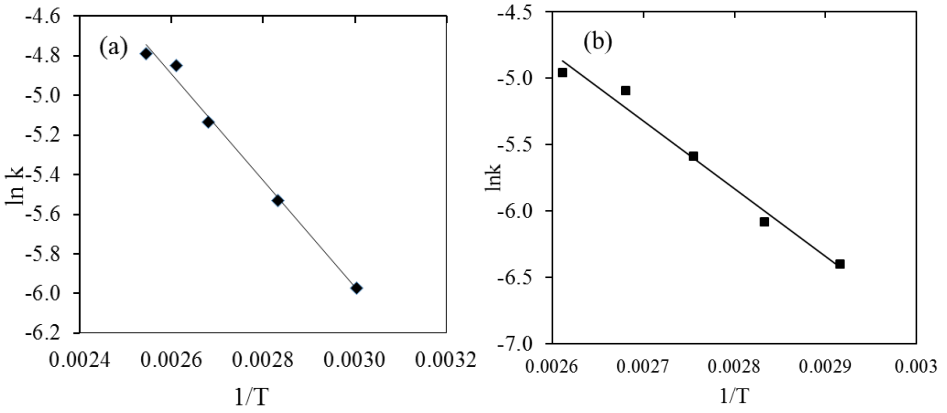

Figure 8. Arrhenius plots for determination of Ea, (a) $(PW_{12})_3$/MCM-41 and (b) $(PW_{11})_3$/MCM-41.

The Ea for $(PW_{12})_3$/MCM-41 was found to be low as compared to $(PW_{11})_3$/MCM-41 suggesting the following order,

- $(PW_{12})_3$/MCM-41 > $(PW_{11})_3$/MCM-41.

- ***Esterification of Benzyl alcohol (BA)***

Esterification of BA gives benzyl acetate (Scheme 2) and in order to overcome the equilibrium limitation, reaction was carried out by taking excess AA in order to favour the forward reaction.

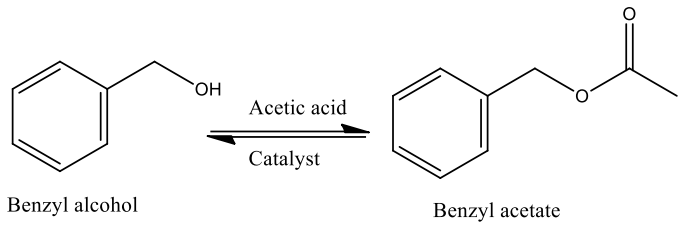

Scheme 2. Esterification of Benzyl alcohol.

Effect of % loading of PW_{12}/PW_{11}

To study the effect of % loading of PW_{12}/PW_{11} esterification reaction was carried out with 10-40% loaded catalysts (Figure 9). It was observed that with increase in the % loading of PW_{12}/PW_{11}, % conversion was also increases up to 30% loading. The enhanced activity could be due to increase in the active sites. For 30% and 40% loadings, the difference in conversion was not significant. Hence, 30% loaded catalysts were selected for carrying out detailed study.

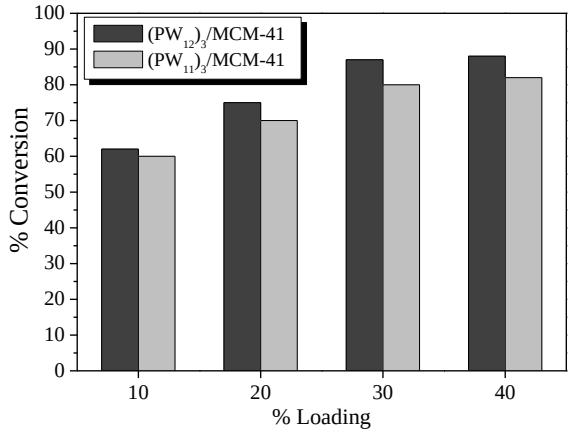

Figure 9. Effect of % loading: mole ratio of BA: AA- 1:2, catalyst amount - 150 mg, temperature- 100 °C, time- 1 h.

Effect of mole ratio of BA to AA

The effect of mole ratio of BA to AA was studied by taking 150 mg catalyst and subjecting to reaction for 1 h at 100 °C. It was observed from Figure 10 that upon increasing the concentration of acid 2 times, higher conversion was obtained. For both the catalysts conversion increased with an increase in BA: AA mole ratio and becomes almost constant after 1:2 mole ratio. Hence, 1:2 molar ratio was optimized for obtaining optimum conversion of 87% and 79% for $(PW_{12})_3$/MCM-41 and $(PW_{11})_3$/MCM-41 respectively.

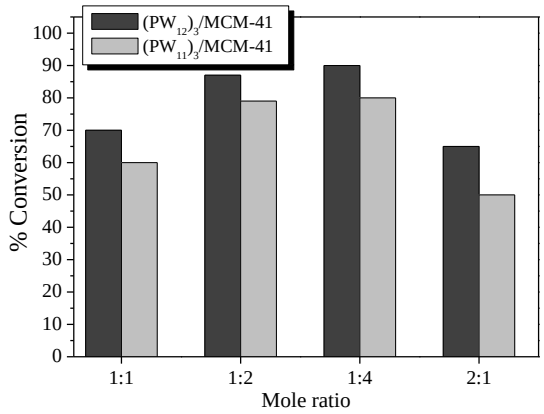

Figure 10. Effect of mole ratio of BA/AA: catalyst amount- 150 mg, temperature- 100 °C and time- 1 h.

Effect of catalyst amount

The effect of catalyst amount on BA conversion was investigated (Figure 11) by increasing the catalyst amount from 50 to 200 mg.

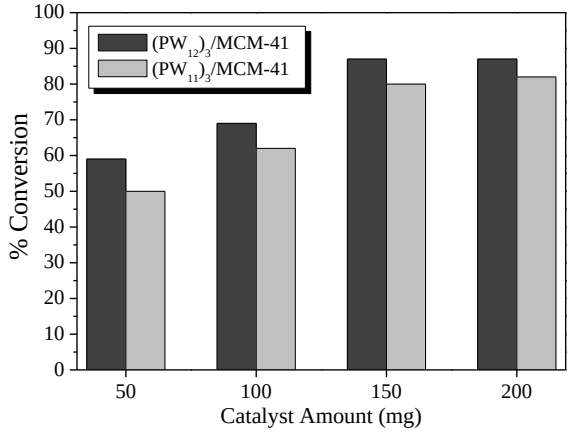

Figure 11. Effect of catalyst amount: mole ratio BA: AA- 1:2, temperature- 100 °C and time- 1 h.

It was observed from Figure 11, that the conversion increases with an increase in catalyst amount and reaches a maximum- 87% for $(PW_{12})_3$/MCM-41, respectively, with 150 mg catalyst. However, with a further increase in amount of catalyst, there was no considerable increase in conversion. Similar trend of reaction was observed for $(PW_{11})_3$/MCM-41.

Effect of reaction time

The effect of reaction time on conversion was studied and it was observed (Figure 12) that there was an increase in conversion with increase in reaction time. As the reaction time was prolonged, further esterification of BA was enhanced. Conversion reaches 96% in 2 h for $(PW_{12})_3$/ MCM-41, however, for $(PW_{11})_3$/MCM-41 higher reaction time (3 h) was needed for obtaining maximum (90%) conversion. Both catalysts give single selectivity (100%) towards benzyl acetate without formation of any side products.

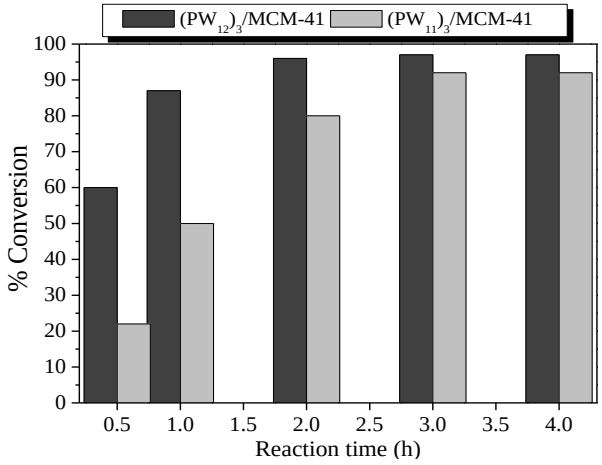

Figure 12. Effect of reaction time: mole ratio BA: AA- 1:2, catalyst amount- 150 mg, temperature- 100 °C.

Effect of reaction temperature

In order to determine the most favourable temperature, reaction was carried out at different temperatures 70-110 °C, keeping other parameters fixed (molar ratio- 1:2, catalyst amount- 150 mg) (Figure 13). The results show that conversion increases with an increase in temperature from 70 to 90 °C. Only a negligible improvement in conversion was observed on increasing temperature from 100 to 110 °C, so the temperature of 100 °C was found optimized for the maximum conversion of BA.

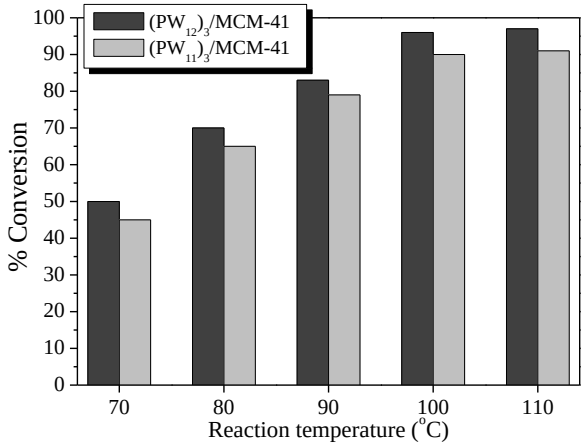

Figure 13. Effect of reaction temperature: mole ratio BA: AA- 1:2, catalyst amount- 150 mg, and time- 2 h for $(PW_{12})_3$/MCM-41 and 3 h for $(PW_{11})_3$/MCM-41.

Optimized conditions: [96% conversion for $(PW_{12})_3$/MCM-41 and 90% conversion for $(PW_{11})_3$/MCM-41] mole ratio of BA to AA- 1:2, catalyst amount- 150 mg, temperature- 100 °C, time- 2 h for $(PW_{12})_3$/MCM-41 and 3 h for $(PW_{11})_3$/MCM-41.

Kinetic study

A detailed kinetic study was carried out over $(PW_{12})_3$/MCM-41 and $(PW_{11})_3$/MCM-41. The plot of log Co/C versus time (Figure 14) shows a linear correlation of alcohol consumption with respect to time. With an increase in reaction time there was a gradual and linear decrease in alcohol concentration over both catalysts. These observations indicate that esterification of BA follows first order dependence with respect to time.

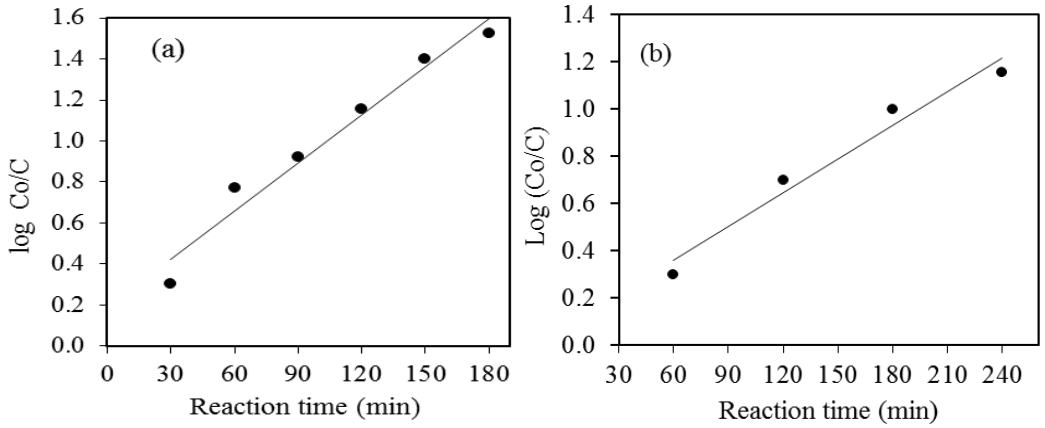

Figure 14. First-order plot for esterification of BA over, (a) $(PW_{12})_3$/MCM-41 and (b) $(PW_{11})_3$/MCM-41.

It was observed from Figure 15, that rate of reaction increases with an increase in the catalyst concentration. Plot of reaction rate versus catalyst concentration (Figure 15) also shows a linear relationship for $(PW_{12})_3$/MCM-41 and $(PW_{11})_3$/MCM-41.

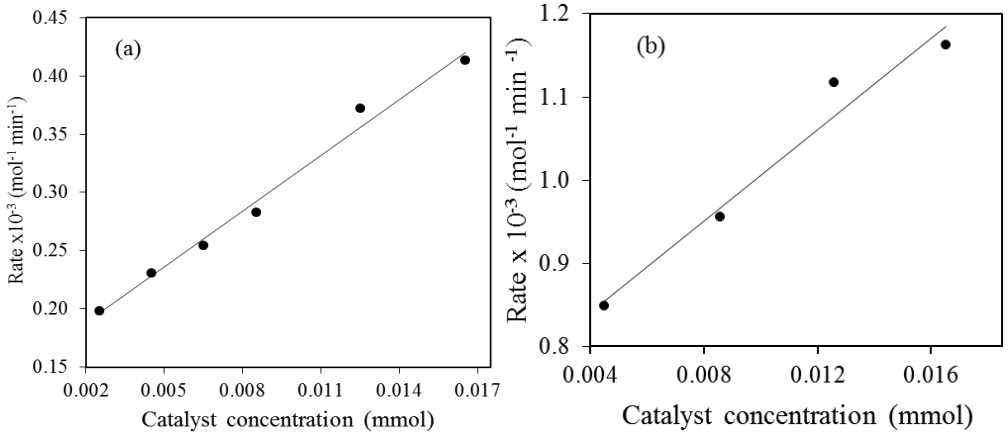

Figure 15. Plot of reaction rate versus catalyst concentrations for esterification of BA over, (a) $(PW_{12})_3$/MCM-41 and (b) $(PW_{11})_3$/MCM-41.

The graph of ln k versus 1/T was plotted (Figure 16), and value of Ea was determined from the plot. On increasing temperature from 343 to 373 K, the rate constant increases, due to activation of catalytic species. The Ea for $(PW_{12})_3$/MCM-41 was found to be 30.7 kJ mol^{-1}, and 32.5 $kJmol^{-1}$ for $(PW_{12})_3$/MCM-41, hence, in both cases the rate is truly governed by the chemical step and there was no diffusion limitation/mass transport limitation.

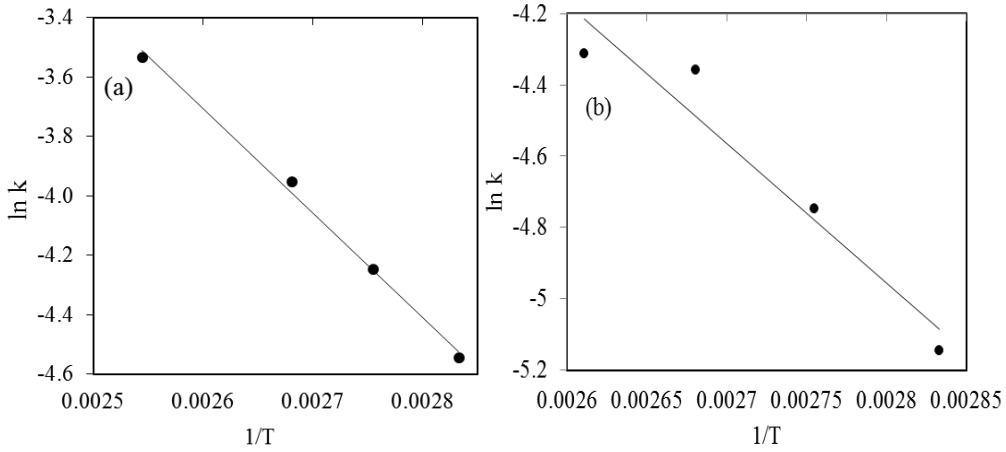

Figure 16. Arrhenius plot for determination of Ea over, (a) $(PW_{12})_3$/MCM-41 and (b) $(PW_{11})_3$/MCM-41.

The Ea value for $(PW_{12})_3$/MCM-41 was found to be low as compared to $(PW_{11})_3$/MCM-41, and hence the order is,

- $(PW_{12})_3$/MCM-48 > $(PW_{11})_3$/MCM-48.

Control experiments and Heterogeneity tests

The control experiment of Gly and BA was carried (Table 2) and it was observed, that the support MCM-41 was not much active towards esterification and catalytic activity of active species PW_{12}/PW_{11} has been retained in the catalysts. Thus, we were successful in synthesizing heterogeneous catalysts.

Table 2. Control experiments for esterification of Gly[a] and BA[b] with AA.

Catalyst	% Conversion [a/b]	% Selectivity		TON [a/b]
		DAG	TAG	
No catalyst	8/5	-	-	-
MCM-41	20/15	30	-	-
PW_{12}	89/90	45	5	742/750
$(PW_{12})_3$/MCM-41	87/96	60	15	725/800
PW_{11}	80/88	40	10	629/694
$(PW_{11})_3$/MCM-41	89/90	49	13	700/710

% Conversion based on substrate: [a] mole ratio- 1:6, amount of PW_{12}/PW_{11}- 34.6 mg, catalyst- 150 mg, time- 6 h; [b] mole ratio- 1:2, amount of PW_{12}/PW_{11}- 34.6 mg, catalyst- 150 mg, time- 2 h for $(PW_{12})_3$/MCM-41 and 3 h for $(PW_{11})_3$/MCM-41.

Heterogeneity test [53] was carried out for esterification of Gly and BA. The catalysts were filtered from the reaction mixture after 4 h and allowed the filtrate to react up to 7 - 8 h (Gly reaction) Figure 17. The reaction mixture of 4 h and filtrate was analysed by GC. No change in % conversion or % selectivity was found indicating the present catalyst falls into category C. Similar observation was obtained for BA esterification (Figure 18). There was no leaching of PW_{12}/PW_{11} from the support and present catalysts are truly heterogeneous in nature.

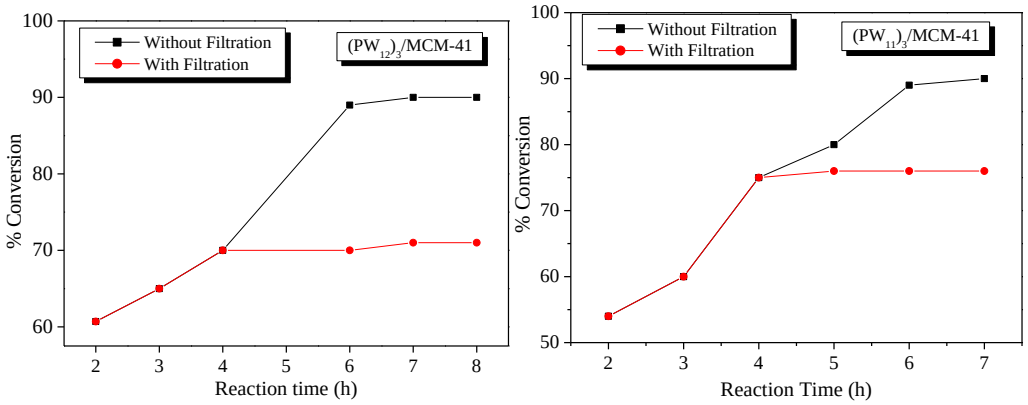

Figure 17. Heterogeneity test for esterification of Gly over (a) $(PW_{12})_3$/MCM-41 and (b) $(PW_{11})_3$/MCM-41; mole ratio Gly/AA- 1:6, catalyst amount- 150 mg, time- 6 h, temperature- 100 ^oC.

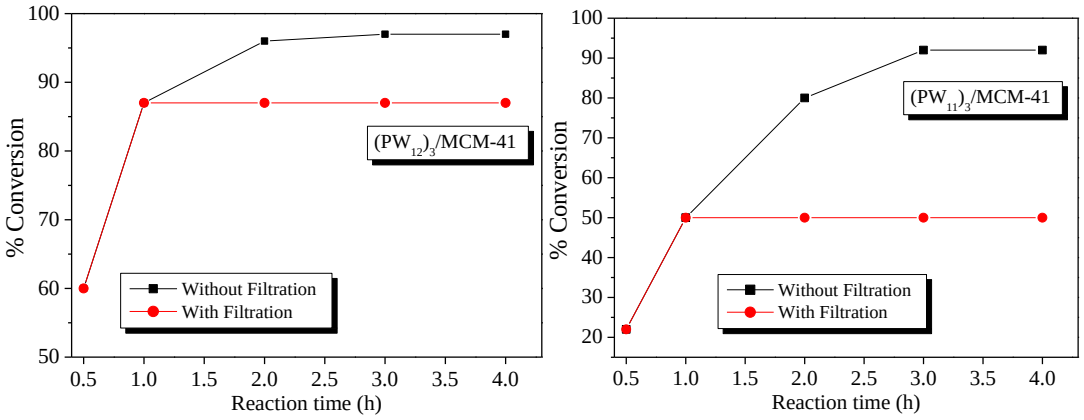

Figure 18. Heterogeneity test for esterification of BA over (a) $(PW_{12})_3$/MCM-41 and (b) $(PW_{11})_3$/MCM-41; mole ratio BA/AA- 1:2, catalyst amount- 150 mg, time- 2 h for $(PW_{12})_3$/MCM-41 and 3 h for $(PW_{11})_3$/MCM-41, temperature- 100 ^oC.

Recycling and regeneration of catalysts

The catalysts were recycled up to four times in order to test their activity in successive runs for esterification of Gly (Figure 19) and BA (Figure 20). The catalysts were separated from the reaction mixture by simple centrifugation, washed with 5 mL methanol and then with 5 mL distilled water, dried at 100 ^oC in an oven for 10 h and the recovered catalysts were charged for the further runs. Thus, the catalysts can be reused up to four cycles with minimal loss in the activity.

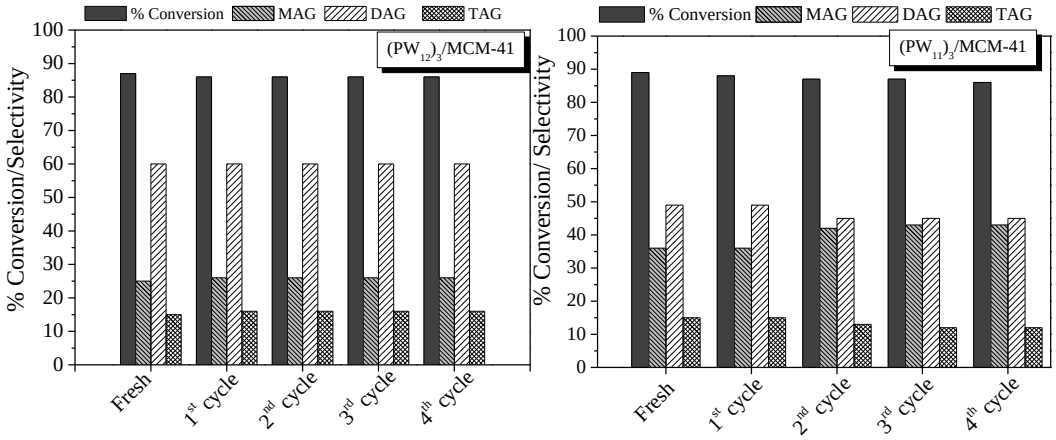

Figure 19. Recycling study for esterification of Gly: molar ratio of Gly: AA- 1:6, catalyst amount- 150 mg, time- 6 h, and temperature- 100 °C.

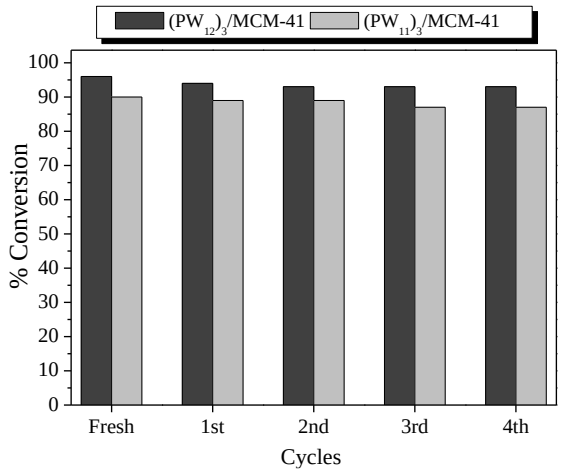

Figure 20. Recycling study for esterification of BA: molar ratio of BA: AA- 1:2, catalyst amount- 150 mg, time- 2 h for $(PW_{12})_3$/MCM-41 and 3 h for $(PW_{11})_3$/MCM-41, and temperature- 100 °C.

Characterisation of regenerated catalysts

Further, recycled catalysts were characterized for acidic strength, FT-IR, Raman and XRD analysis in order to see any structural change. The results are previously presented in *Chapter 2a,* hence they are not included here again.

2B (II) Esterification of Gly and BA over PW_{12}/MCM-48 and PW_{11}/MCM-48.

- ***Esterification of Gly***

Optimisation studies for maximum conversion was carried out similar to the *previous section (I).*

Effect of % loading of PW_{12}/PW_{11}

The effect of % loading of PW_{12}/PW_{11}, on esterification reaction was carried out with 10 to 40% loadings (Figure 21). It was observed that with increase in the % loading of PW_{12}/PW_{11}, % conversion also increases. From acidity measurements it was observed that the acidity increases with increase in PW_{12}/PW_{11} loading (Table 8, Chapter 1). The value of total acidity is directly related to the concentration of active species, PW_{12}/PW_{11}. Hence, increase in total acidity with increase in % loading of PW_{12}/PW_{11} was obvious.

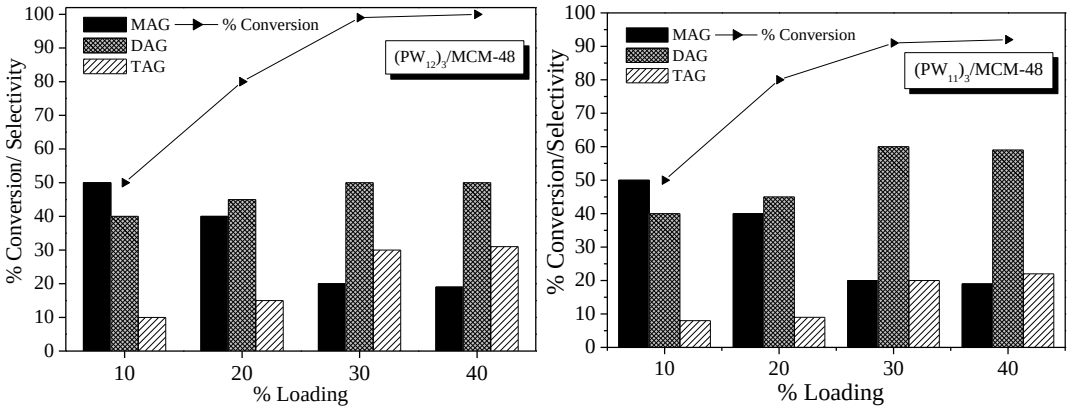

Figure 21. Effect of % loading of PW_{12}/PW_{11}: mole ratio of Gly: AA- 1:6, catalyst amount - 150 mg, temperature- 100 ^{o}C, time- 6 h.

On increasing the loading from 30 to 40%, there was no significant difference in % conversion. In this work, the target products were both DAG and TAG due to their industrial importance and maximum selectivity for DAG and TAG was observed for 30% PW_{12}/PW_{11} loaded catalyst. Hence, the catalyst containing 30% loading of PW_{12}/PW_{11} was selected for further detail studies.

Effect of mole ratio of Gly: AA

The influence of molar ratio was examined- 1:1, 1:3, 1:5, 1:6 and 1:9, at fixed temperature- 100 ^{o}C and keeping the catalyst amount to 150 mg (Figure 22). It was observed from Figure 22, that Gly conversion increases with increase in Gly/AA molar ratio and reaches a maximum at 1:6. Presence of excess AA can promote the formation of DAG and TAG rather than MAG which can be explained by the excess esterification agent that drives the reaction towards formation of higher glycerol acetates. Similar trend in catalytic activity was observed for $(PW_{11})_3$/MCM-48.

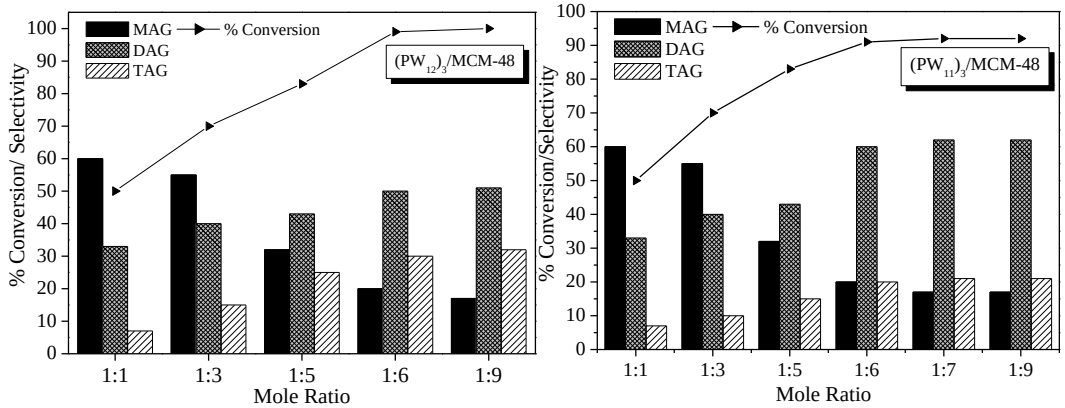

Figure 22. Effect of mole ratio: catalyst amount- 150 mg, temperature- 100 ^{o}C, time- 6 h.

Effect of catalyst amount

Effect of catalyst amount was investigated by varying the amount within a range of 50-200 mg (Figure 23).

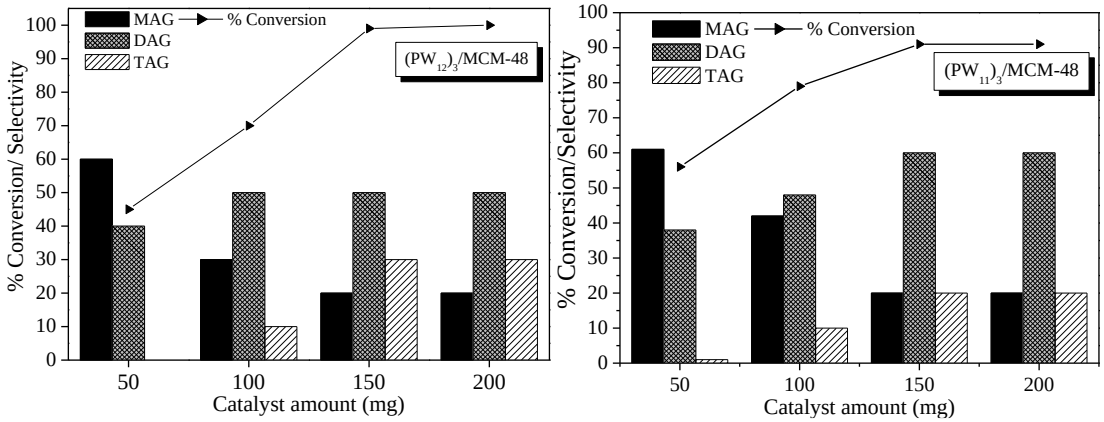

Figure 23. Effect of catalyst amount: mole ratio of Gly: AA- 1:6, temperature- 100 ^{o}C, time- 6 h.

Increasing the catalyst amount resulted in promoting Gly conversion. This is due to increase in total number of accessible active sites, which could effectively drive esterification to completion. Increasing the catalyst amount up to 150 mg resulted in 99% Gly conversion and high selectivity for DAG and TAG. However, on increasing catalyst amount from 150-200 mg for both the catalysts, there was no significant increase in conversion as well as selectivity. The maximum conversion 99% for $(PW_{12})_3$/MCM-48 and 91% for $(PW_{11})_3$/MCM-48 was obtained with 150 mg catalyst.

Effect of reaction time

Effect of reaction time on Gly conversion was studied (Figure 24). Conversion increases with increase in reaction time. It was observed that initially no TAG was observed but as the reaction time was prolonged selectivity for TAG improved. This is due to the fact that with increase in time, esterification of MAG to DAG and TAG was enhanced due to nucleophilic attack of the remaining hydroxyl groups of MAG moiety on the acid site-acetic acid complex. Gly conversion was 99% in 5 h over $(PW_{12})_3$/MCM-48 and combined selectivity for DAG+TAG observed was 80% with 30% selectivity towards TAG. Similarly, Gly conversion was 91% in 6 h over $(PW_{11})_3$/MCM-48 and combined selectivity for DAG+TAG observed was 80% with 20% selectivity towards TAG.

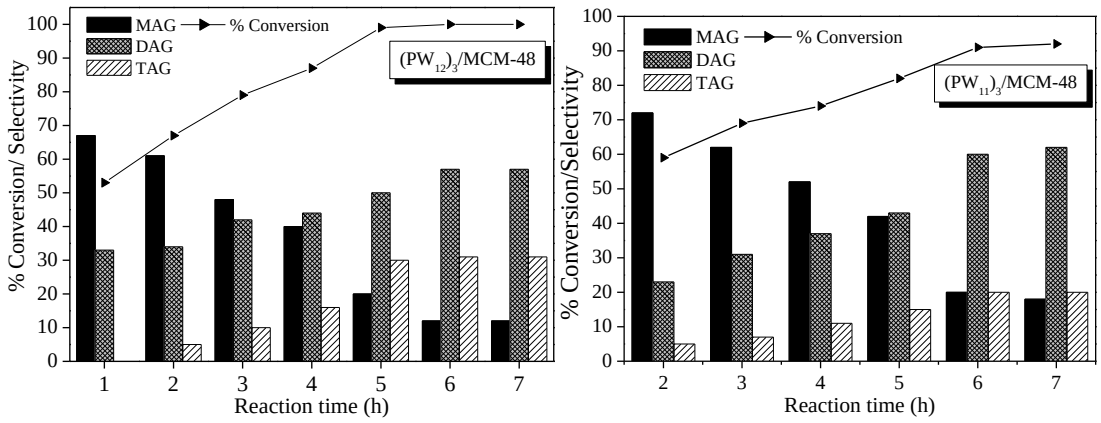

Figure 24. Effect of reaction time: mole ratio of Gly: AA- 1:6, catalyst amount- 150 mg, temperature- 100 ^{o}C.

Effect of reaction temperature

Influence of temperature (Figure 25) was studied in the range 70 - 110 ^{o}C. It is very well known that Gly esterification takes place at endothermic conditions. The primary advantage of higher temperatures is a shorter reaction time. Hence, with temperature higher than 90 ^{o}C, there was observed increase in the conversion.

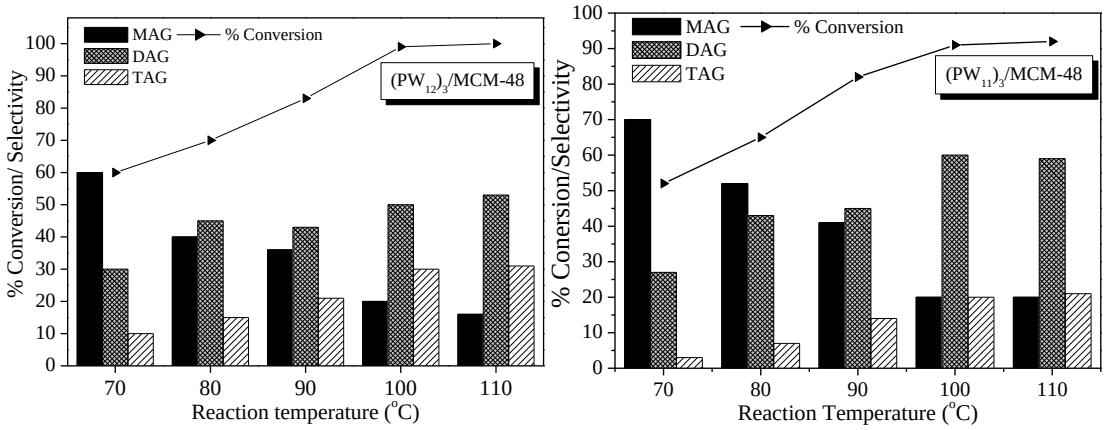

Figure 25. Effect of reaction temperature: mole ratio of Gly: AA- 1:6, catalyst amount- 150 mg, time- 5 h for $(PW_{12})_3$/MCM-48 and 6 h for $(PW_{11})_3$/MCM-48.

At higher reaction temperature, higher selectivity towards the desired DAG and TAG products were observed for both the catalysts. This can be explained due to the enhanced subsequent (from MAG → DAG → TAG) endothermic esterification at elevated temperatures. At 100 ^{o}C, maximum conversion of glycerol was observed along with highest selectivity for DAG and TAG for both the catalysts.

Optimized conditions: [99% conversion $(PW_{12})_3$/MCM-48 and 91% conversion $(PW_{11})_3$/MCM-48] mole ratio of Gly/AA- 1:6, catalyst amount- 150 mg, time- 5 h for $(PW_{12})_3$/MCM-48 and 6 h for $(PW_{11})_3$/MCM-48 and temperature- 100 ^{o}C.

Kinetic study

The plot of log C_o/C versus time (Figure 26) shows a linear relationship of Gly consumption with respect to time. With increase in reaction time there is a gradual and linear decrease in the Gly concentration over both the catalysts. These observations indicate that esterification of Gly follows first order dependence with respect to time.

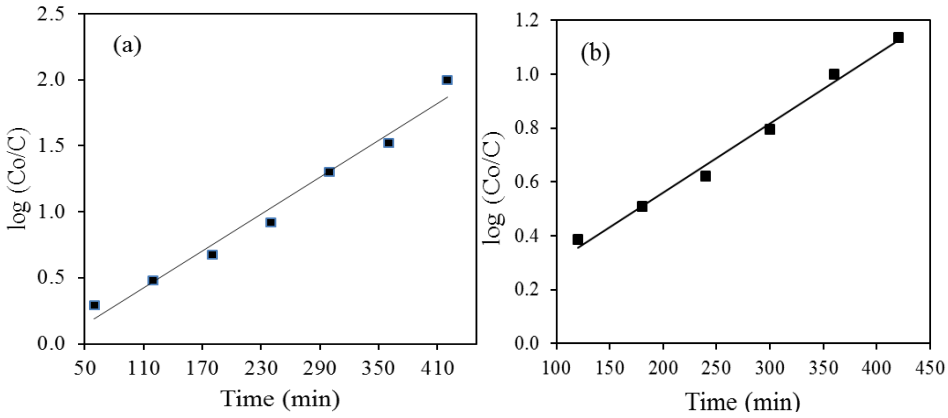

Figure 26. First-order plot for esterification of Gly over, (a) $(PW_{12})_3$/MCM-48 and (b) $(PW_{11})_3$/MCM-48.

The catalyst concentration was varied at fixed substrate concentration of 10 mmol and at temperature 100 °C. It can be observed from the Figure 27 that rate of reaction increases with increase in the catalyst concentration. The plot of reaction rate versus catalyst concentration (Figure 27) also show a linear relationship.

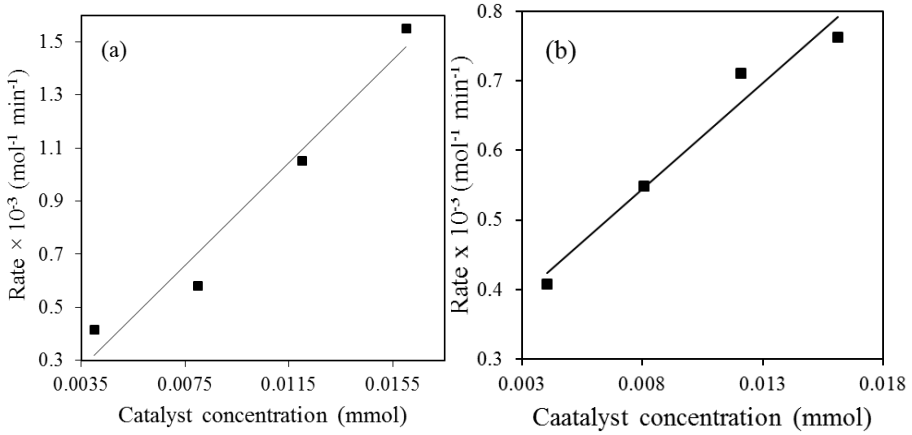

Figure 27. Rate of reaction versus catalyst concentration over, (a) $(PW_{12})_3$/MCM-48 and (b) $(PW_{11})_3$/MCM-48.

The graph of ln k versus. 1/T was plotted (Figure 28) and the value of activation energy (E_a) was determined from the plot. In the present case, Ea was 36.8 kJ/mol for $(PW_{12})_3$/MCM-48 and 42.3 kJ/mol for $(PW_{11})_3$/MCM-48 and hence the rate was truly governed by chemical step where the catalyst was used to its maximum and there was no diffusion limitation/mass transfer limitation.

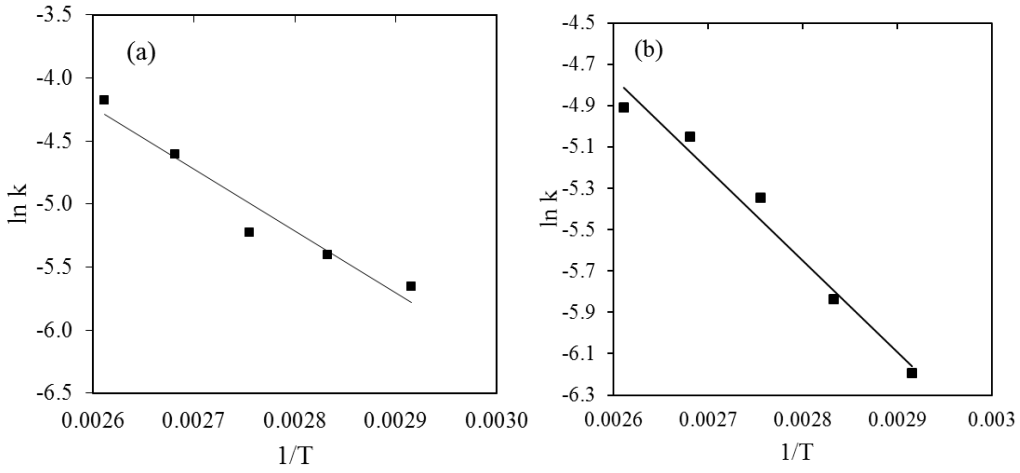

Figure 28. Arrhenius plots for determination of Ea, (a) $(PW_{12})_3$/MCM-48 and (b) $(PW_{11})_3$/MCM-48.

From the values of Ea the order of catalyst was concluded as, $(PW_{12})_3$/MCM-48 > $(PW_{11})_3$/MCM-48.

- ***Esterification of BA***

Esterification of BA with AA was carried out over $(PW_{12})_3$/MCM-48 and $(PW_{11})_3$/MCM-48. Optimisation studies for maximum conversion was carried out similar to the *previous section (I)*.

Effect of % loading of PW_{12}/PW_{11}

Catalytic activity over different loadings of PW_{12}/PW_{11} was carried out and from Figure 29, it was observed that conversion increases on increasing PW_{12}/PW_{11} loading. The enhanced catalytic activity could be directly correlated with the increase in PW_{12}/PW_{11} active species and the surface acidity of the catalysts (which increases for 30% loading as compared to MCM-

48). 40% loaded catalysts showed no significant increase in the conversion of BA. For most active catalyst (30% loading), 98% conversion and 100% benzyl acetate selectivity was obtained for $(PW_{12})_3$/MCM-48. Similar trend in catalytic activity was observed for $(PW_{11})_3$/MCM-48.

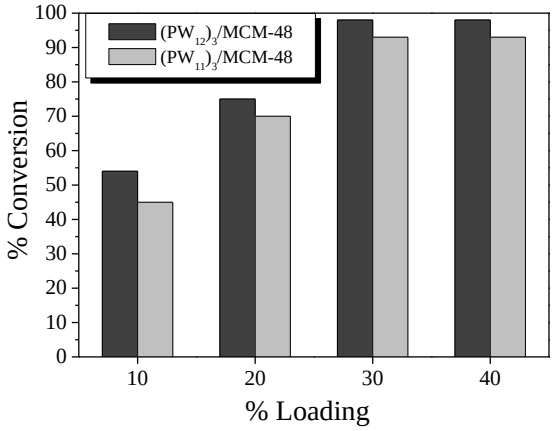

Figure 29. Effect of % loading of PW_{12}/PW_{11}: mole ratio of BA: AA- 1:2, catalyst amount - 150 mg, temperature- 100 ^oC, time- 2 h.

Effect of mole ratio of BA:AA

Experiments were carried out to see the effect of mole ratio of BA: AA (Figure 30). It was observed that on increasing the concentration of acid to 2 times, higher conversion was obtained, which further becomes almost constant after 1:2 molar ratio in 2 h. So, considering the economic aspects, 1:2 molar ratio was optimized for further studies. Under these conditions 98% conversion was obtained for $(PW_{12})_3$/MCM-48 and 93% for $(PW_{11})_3$/MCM-48.

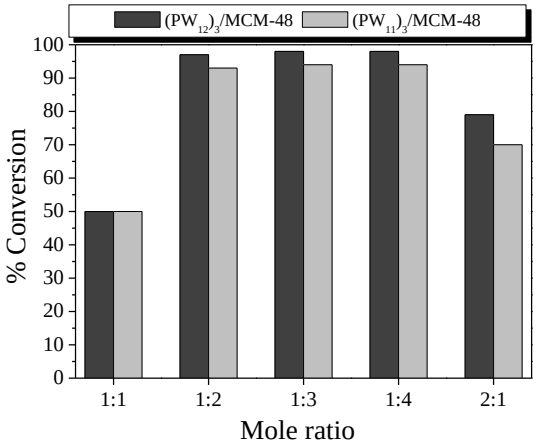

Figure 30. Effect of mole ratio: catalyst amount - 150 mg, temperature- 100 ^oC, time- 2 h.

Effect of catalyst amount

The effect of catalyst amount (50-200 mg) on conversion was studied (Figure 31). On increasing the catalyst amount, conversion also increases and reaches a saturation at 150 mg. Increase in conversion can be accredited to an increase in the number of available catalytically active sites. Hence, 150 mg catalyst amount was considered optimum for maximum conversion.

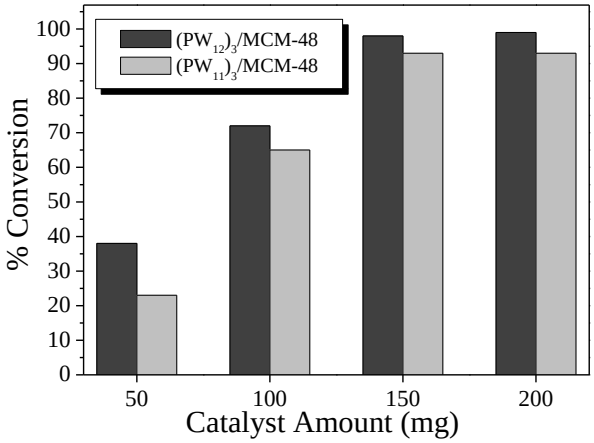

Figure 31. Effect of catalyst amount: mole ratio of BA: AA- 1:2, time- 2 h, temperature- 100 ^{o}C.

Effect of reaction time

The effect of reaction time on conversion was studied and it was observed (Figure 32) that there was an increase in conversion with an increase in reaction time.

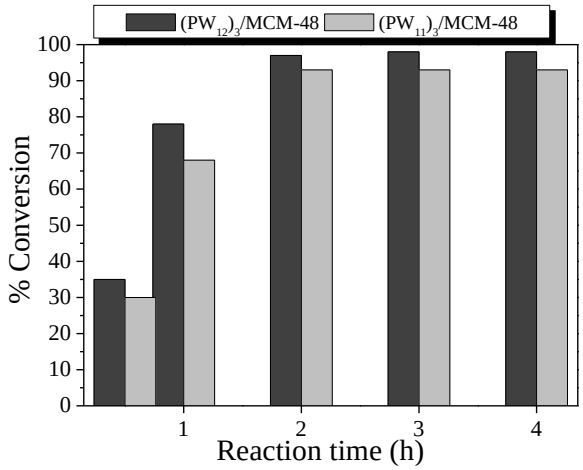

Figure 32. Effect of reaction time: mole ratio BA: AA- 1:2, catalyst amount - 150 mg, temperature- 100 °C.

As the reaction time was prolonged, further esterification of BA was enhanced. Therefore, long reaction time has become one of the vital factors to drive the reaction to completion. The conversion increases with increase in reaction time from 1 h up to 2 h for both the catalysts. However, on further increasing reaction time, conversion does not increase. Hence, reaction time of 2 h was considered to be optimum for maximum conversion.

Effect of reaction temperature

The effect of temperature on BA conversion was studied and it was seen that temperature evidently affects both the reaction rate and conversion of BA (Figure 33). With subsequent increase in the temperature, conversion was also increases. It can be seen that at 100 ^{o}C optimum conversions were obtained for both the catalysts.

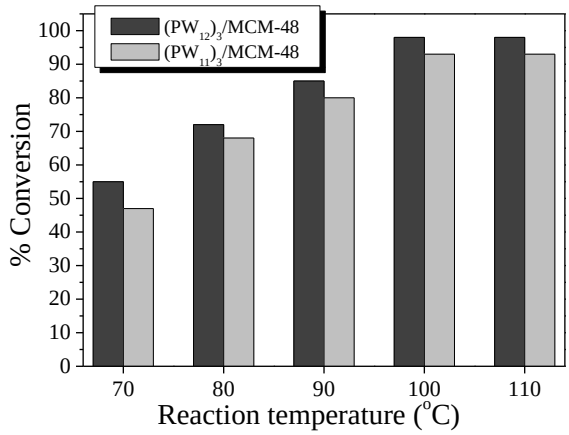

Figure 33. Effect of reaction temperature: mole ratio BA: AA- 1:2, catalyst amount - 150 mg, temperature- 100 °C.

Optimized conditions: [98% conversion $(PW_{12})_3$/MCM-48 and 93% conversion $(PW_{11})_3$/MCM-48] mole ratio BA to AA- 1:2, catalyst amount- 150 mg, temperature- 100 °C, time- 2 h.

Kinetic study

A detailed study on the kinetic behaviour was tested for esterification of BA over both the catalysts. The plot of log (Co/C) versus time (Figure 34) shows a linear association of BA consumption with respect to time for both the catalysts. Since AA was taken in large excess, the rate law follows first-order dependence.

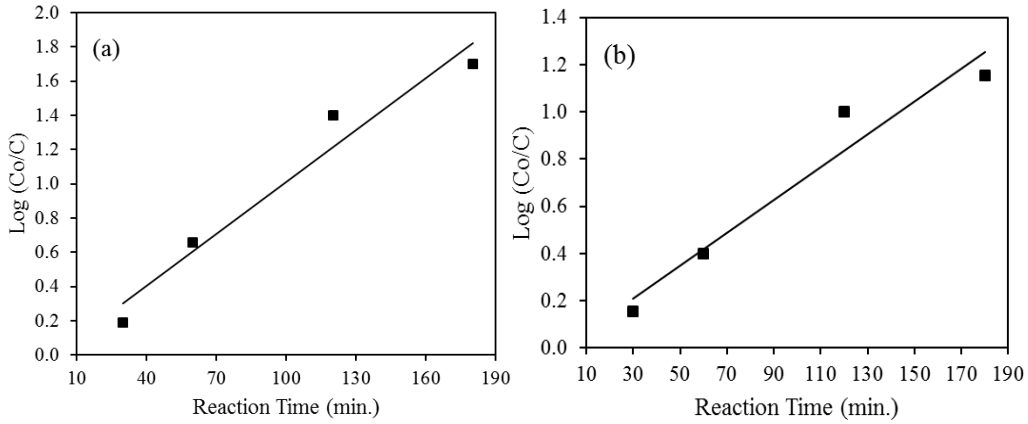

Figure 34. First-order plot for esterification of BA with AA over (a) $(PW_{12})_3$/MCM-48 and (b) $(PW_{11})_3$/MCM-48.

The catalyst concentration (Figure 35) was varied in different time interval at a fixed substrate concentration of 10 mmol and at 100 °C temperature. The plot of reaction rate versus catalyst concentration shows linear relationship.

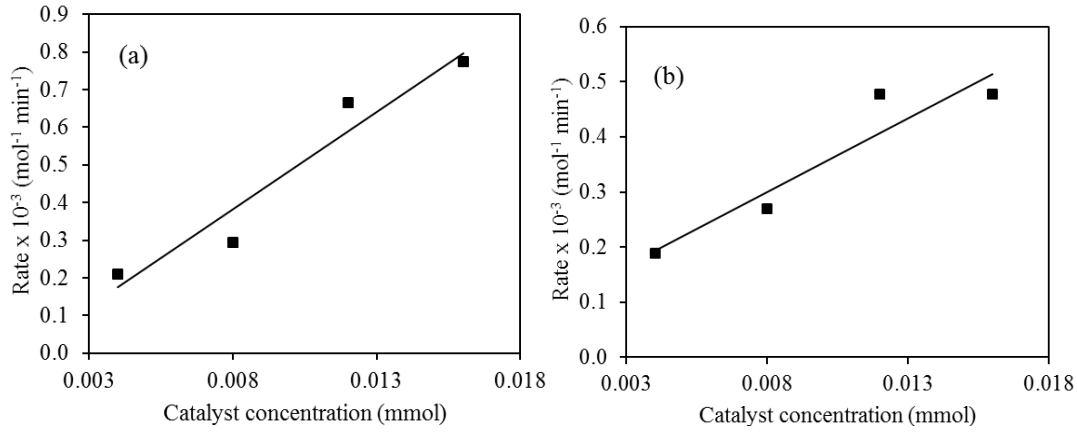

Figure 35. Plot of reaction rate versus catalyst concentrations over (a) $(PW_{12})_3$/MCM-48 and (b) $(PW_{11})_3$/MCM-48.

The graph of ln k versus 1/T was plotted (Figure 36) and value of activation energy (Ea) was calculated from the plot. Ea for $(PW_{12})_3$/MCM-48 was 29.7 kJ mol^{-1} and 31.2 kJ mol^{-1} for $(PW_{11})_3$/MCM-48 and hence, it was concluded that reaction rate was truly governed by chemical step without any diffusion/mass transport limitations.

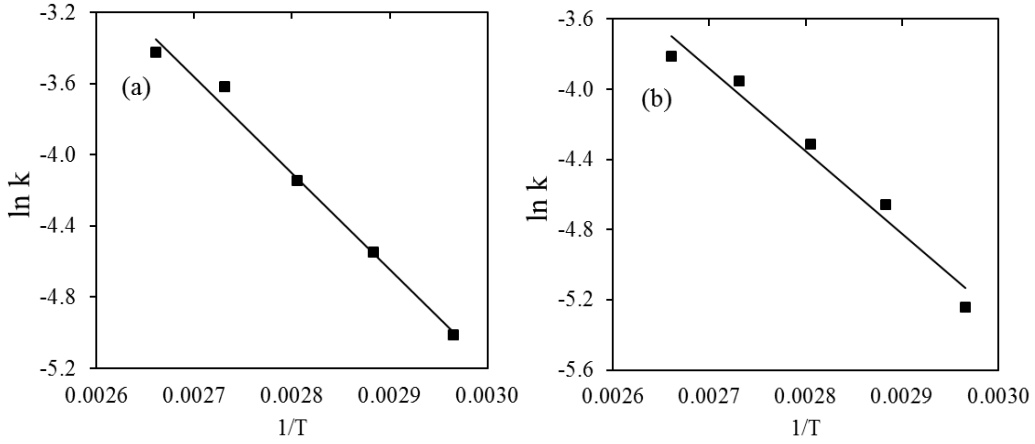

Figure 36. Arrhenius plots for determination of Ea over (a) $(PW_{12})_3$/MCM-48 and (b) $(PW_{11})_3$/MCM-48.

Based on the values of Ea the order is found to be, $(PW_{12})_3$/MCM-48 > $(PW_{11})_3$/MCM-48.

Control experiments and Heterogeneity tests

The control experiments with MCM-48 and PW_{12}/PW_{11} were carried out under optimized conditions (Table 3). Reaction was carried out with active amount of PW_{12}/PW_{11} and it was observed that catalytic activities of PW_{12}/PW_{11} have been retained in the respective catalysts indicating that PW_{12}/PW_{11} behaves as real active species. Thus, we were successful in anchoring PW_{12}/PW_{11} to MCM-48 and hence in overcoming traditional problems of homogeneous catalysis.

Table 3. Control experiments for esterification of Gly[a] and BA[b] with AA.

Catalyst	% Conversion [a/b]	% Selectivity [a]		TON [a/b]
		DAG	TAG	
No catalyst	8/5	-	-	-
MCM-48	35/15	30	-	-
PW_{12}	89/90	45	5	742/750
$(PW_{12})_3$/MCM-48	99/98	50	30	825/816
PW_{11}	80/88	40	10	629/694
$(PW_{11})_3$/MCM-48	91/93	60	20	715/733

% Conversion based on substrate: [a] mole ratio 1:6, amount of PW_{12}/PW_{11}- 34.6 mg, Catalyst- 150 mg, time- 5 h for $(PW_{12})_3$/MCM-48 and 6 h for $(PW_{11})_3$/MCM-48, [b] mole ratio- 1:2, amount of PW_{12}/PW_{11}- 34.6 mg, catalyst- 150 mg, time- 2 h.

Heterogeneity test (Figure 37) was carried out for Gly by filtering catalyst from the reaction mixture at 100 ^oC after 3 h and 4 h for $(PW_{12})_3$/MCM-48 and $(PW_{11})_3$/MCM-48 respectively, and filtrate was allowed to react up to 7 h. The reaction mixture without filtration and filtrate after filtration were analyzed by GC. No change in % conversion and % selectivity was found indicating that active species does not leach and the catalysts are truly heterogeneous in nature. Similar heterogeneity test was carried out for BA (Figure 38).

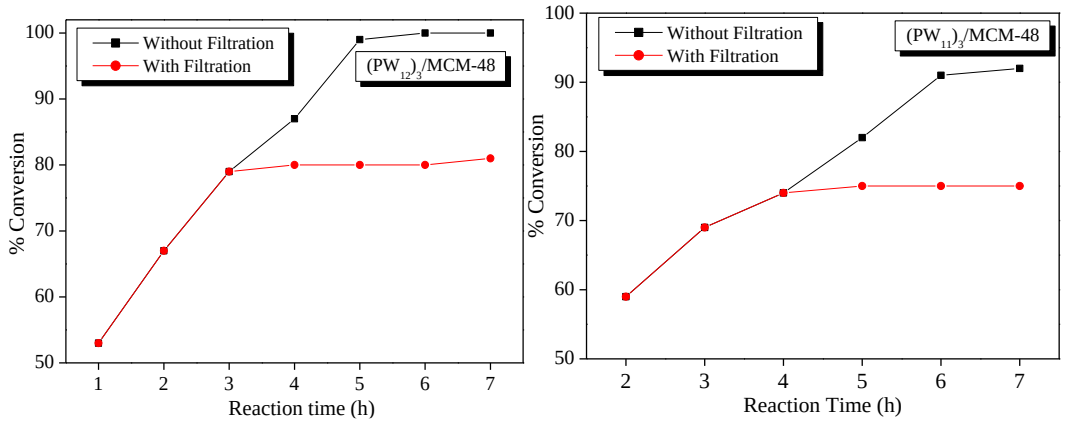

Figure 37. Heterogeneity test for esterification of Gly: mole ratio Gly/AA- 1:6, catalyst amount- 150 mg, temperature- 100 ^{o}C.

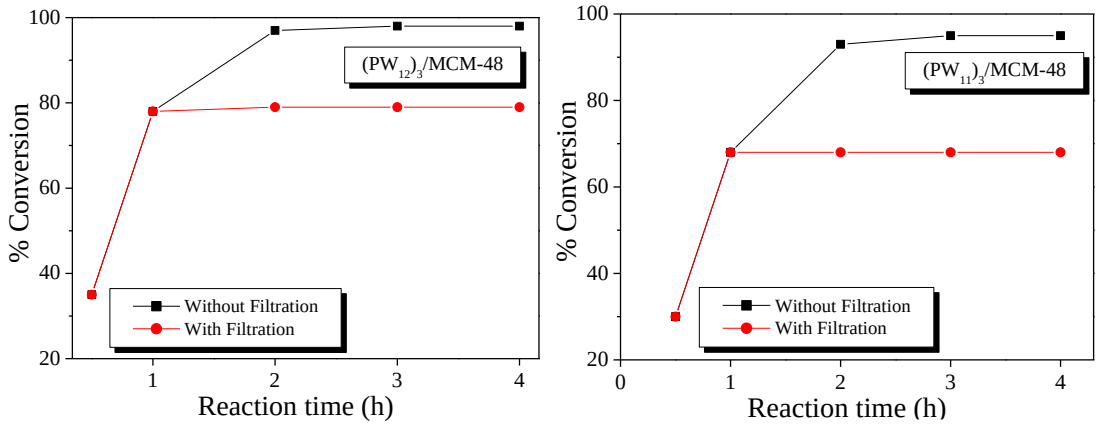

Figure 38. Heterogeneity test for esterification of BA: mole ratio BA/AA- 1:2, catalyst amount- 150 mg, temperature- 100 ^{o}C.

Recycling and regeneration of catalysts

The catalysts were recycled up to four times in order to test their activity in successive runs for Gly esterification (Figure 39). The catalysts were separated from reaction mixture by simple centrifugation, washed with 5 mL methanol and then with 5 mL distilled water, dried at 100 ^{o}C in an oven for 10 h and recovered catalysts were charged for the further runs. Similar recycling study was also carried out for BA esterification over both the catalysts (Figure 40). Thus, the catalysts can be reused up to four cycles with minimal loss in the activity.

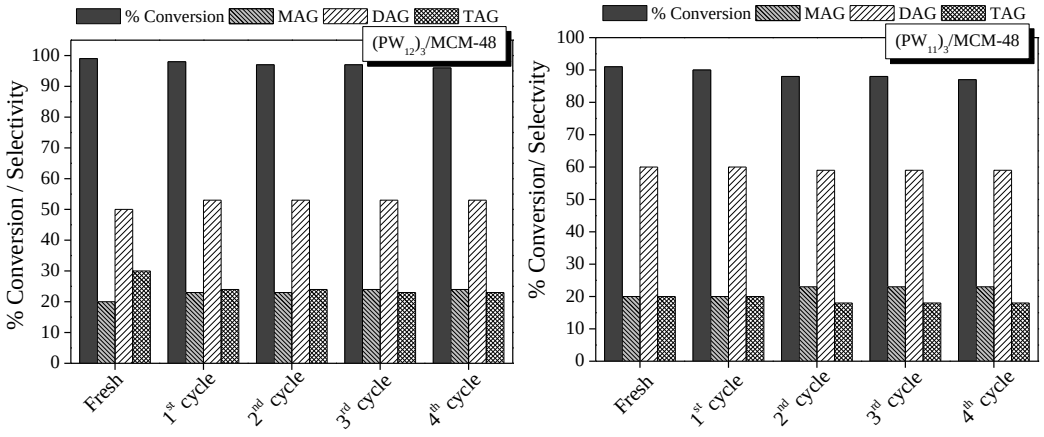

Figure 39. Recycling study for esterification of Gly: molar ratio of Gly: AA- 1:6, catalyst amount- 150 mg, time- 5 h for $(PW_{12})_3$/MCM-48, 6 h for $(PW_{11})_3$/MCM-48 and temperature- 100 °C.

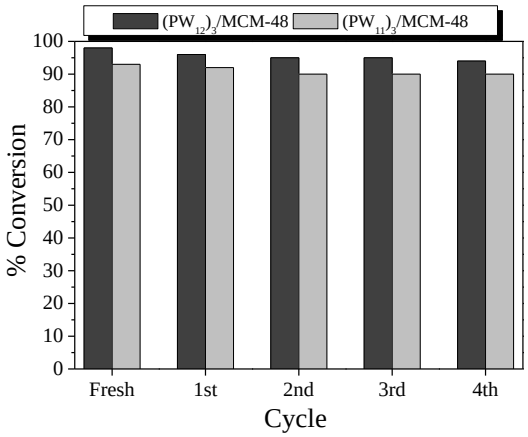

Figure 40. Recycling study for esterification of BA: mole ratio of BA: AA- 1:2, catalyst amount- 150 mg, time- 2 h and temperature- 100 °C.

Substrate scope for different alcohols

For esterification reaction, set of primary and secondary alcohols were selected (Table 4). Under the optimized reaction conditions linear alcohols such as n-butanol and benzyl alcohol led to >90% conversion, whereas cyclic alcohols led to <55% conversion. Aliphatic primary alcohols give good conversion as compared to aliphatic secondary alcohol. Lower conversion in the case of cyclic alcohols may be due to ring strain.

Table 4. Esterification reaction of different alcohol substrates.

Alcohols	Esters	%Yield [a/b/c/d]	TON [a/b/c/d]
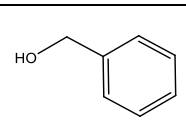	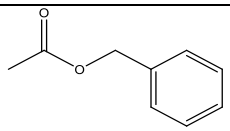	96/90/98/93	891/816/910/843
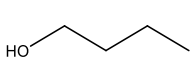	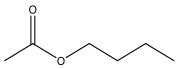	92/85/95/87	854/770/882/789
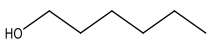	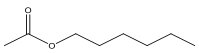	70/53/72/59	650/480/668/535
	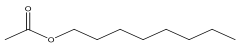	60/44/68/45	557/398/631/408
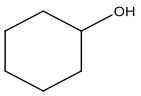	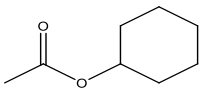	60/50/62/50	557/452/572/453
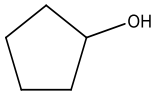	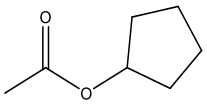	49/40/52/40	454/361/479/362

Reaction conditions: mole ratio BA/AA- 1:2, catalyst amount- 150 mg, time- 2 h for [a] *$(PW_{12})_3$/MCM-41,* [c] *$(PW_{12})_3$/MCM-48,* [d] *$(PW_{11})_3$/MCM-48 and 3 h for* [b] *$(PW_{11})_3$/MCM-41, temperature- 100* ^{o}*C.*

Probable mechanism for esterification reactions

The probable mechanism for esterification of Gly with AA is presented in Scheme 3 (a). The interaction of acidic sites with acetic acid results in formation of a higher positive charge on the carbonyl group. Accordingly, the hydroxyl group of glycerol attacks the carbon atom of the carbonyl, which results in formation of new C-O bond between oxygen atom of hydroxyl group of glycerol and the carbon atom of carbonyl. New MAG molecule is formed with the elimination of water. The formation of MAG at initial stages of reaction is evident from gas chromatography results. Subsequent formation of DAG and TAG was evidence to the fact that acidity plays role in the conversion and agrees well with the above mechanistic investigation.

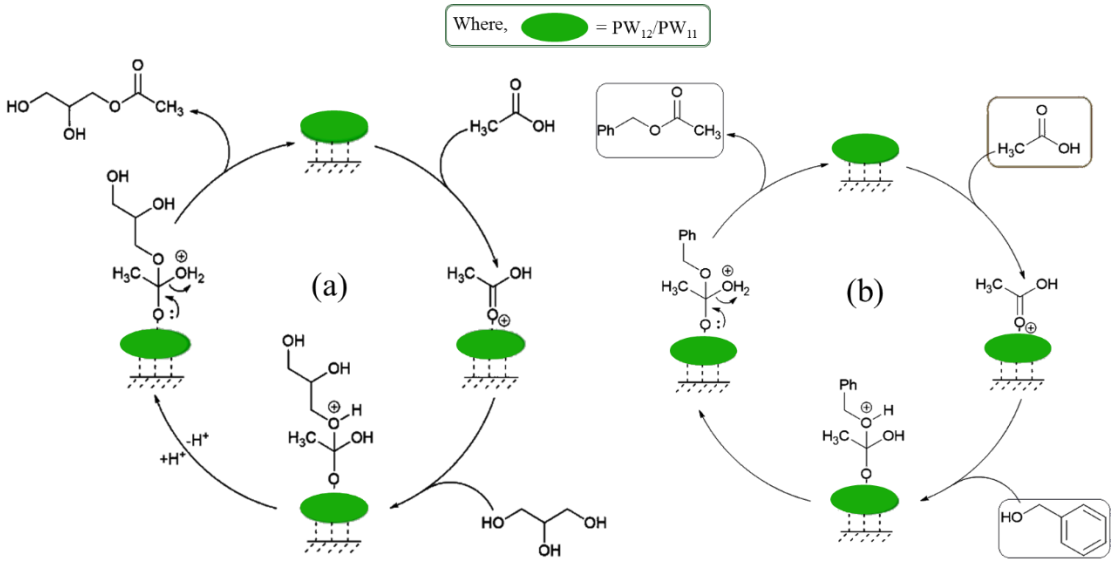

Scheme 3. Probable reaction mechanism for acid catalysed esterification of (a) Gly with AA and (b) BA with AA.

Due to steric constraints, the primary hydroxyl group preferentially proceeds with a nucleophilic attack on acetic acid, thus leading to formation of 1-MAG than 2-MAG. Subsequently, the MAG undergoes further esterification with acetic acid and leads to formation of DAG and TAG. It is known that the Lewis acid sites can also act as active catalytic sites involved in the formation of reactive nucleophilic intermediate [26]. Hence, on the basis of above

explanation it was reported that both Bronsted and Lewis acidic sites play a role in the conversion which can be rate determining step.

The proposed reaction mechanism for esterification of BA has been presented in Scheme 3b. The interaction of the carbonyl oxygen of AA with the active species (PW_{12}/PW_{11}) of the catalyst generates a carbocation. The nucleophilic attack of BA to the carbocation yields a tetrahedral intermediate. The tetrahedral intermediate eliminates H_2O to form one mole of BA [54].

Comparison of active species and supports for acid catalysed reactions

Effect of active species PW_{12}/PW_{11}

Comparison of effect of active species (PW_{12}/PW_{11}) anchored to the supports, MCM-41 and MCM-48 for various acid catalysed reactions were carried out under similar reaction conditions. Table 5 describes the activity of MCM-41 anchored PW_{12}/PW_{11} for different acid catalysed reaction. It is clear that activity of $(PW_{12})_3$/MCM-41 is higher than that of $(PW_{11})_3$/MCM-41 for both transesterification as well as esterification reactions of OA, Gly and BA. This can be explained as follows: The activity of catalysts were found to be consistent with the acidic strength of both the catalysts. The acidic character of polyoxometalates is mainly due to the acidic addenda atoms i.e. tungsten in the present case and removal of one tungsten-oxygen unit from the parent PW_{12} is expected to decrease the acidity and as a result activity of the PW_{11}. This can be seen by the decrease in the values of acidic strength of $(PW_{11})_3$/MCM-41 as compared to $(PW_{12})_3$/MCM-41 (Table 5).

Table 5. Comparison of activity over PW_{12}/MCM-41 and PW_{11}/MCM-41.

Reaction	Catalyst	Surface area (m^2/g)	Acidic strength (mV)	Total acidity (m.equiv./g)	% Conv.	TON	Ea (kJ/mol)
Esterification of OA [a]	$(PW_{12})_3$/MCM-41	360	410	3.6	98	1227	50.4
	$(PW_{11})_3$/MCM-41	252	250	3.0	89	950	54.3
Transesterification of SO [b]	$(PW_{12})_3$/MCM-41	360	410	3.6	93	247	-
	$(PW_{11})_3$/MCM-41	252	250	3.0	85	239	-
Esterification of BA [c]	$(PW_{12})_3$/MCM-41	360	410	3.6	96	798	30.0
	$(PW_{11})_3$/MCM-41	252	250	3.0	90	710	32.5
Esterification of Gly [d]	$(PW_{12})_3$/MCM-41	360	410	3.6	88	725	42.3
	$(PW_{11})_3$/MCM-41	252	250	3.0	89	700	43.0

[a b] Mole ratio (OA: MeOH)= 1 : 40, catalyst amount = 100 mg, temperature = 60 °C, time = 14 h; [b] Weight ratio (SO: MeOH) = 1 :4, catalyst amount = 250 mg, temperature = 65 °C, time = 8 h; [c] Mole ratio (BA: AA)= 1 : 2, catalyst amount = 150 mg, temperature = 100 °C, time = 2 h; [d] Mole ratio (Gly: AA) = 1 : 6, catalyst amount = 150 mg, temperature = 100 °C, time = 6 h.

Table 6. Comparison of activity over PW_{12}/MCM-48 and PW_{11}/MCM-48.

Reaction	Catalyst	Surface area (m^2/g)	Acidic strength (mV)	Total acidity (mequiv./g)	% Conv.	TON	Ea (kJ/mol)
Esterification of OA [a]	$(PW_{12})_3$/MCM-48	286	450	3.9	95	1189	40.3
	$(PW_{11})_3$/MCM-48	319	290	3.4	90	960	52.3
Transesterification of SO [b]	$(PW_{12})_3$/MCM-48	286	450	3.9	97	266	-
	$(PW_{11})_3$/MCM-48	319	290	3.4	91	267	-
Esterification of BA [c]	$(PW_{12})_3$/MCM-48	286	450	3.9	98	860	29.7
	$(PW_{11})_3$/MCM-48	319	290	3.4	93	845	31.2
Esterification of Gly [d]	$(PW_{12})_3$/MCM-48	286	450	3.9	99	816	36.8
	$(PW_{11})_3$/MCM-48	319	290	3.4	91	715	42.3

[a] Mole ratio (OA: MeOH)= 1 : 20, catalyst amount = 100 mg, temperature = 60 °C, time = 8 h, 14 for $(PW_{11})_3$/MCM-48; *[b] Weight ratio (SO: MeOH) = 1 : 4, catalyst amount = 250 mg, temperature = 65 °C, time= 8 h; [c] Mole ratio (BA: AA)= 1 : 2, catalyst amount= 150 mg, temperature= 100 °C, time= 2 h; [d] Mole ratio (Gly: AA)= 1 : 6, catalyst amount= 150 mg, temperature = 100 °C, time= 5 h.*

The surface area of $(PW_{11})_3$/MCM-41 (252 m^2/g) was lower than $(PW_{12})_3$/MCM-41 (360 m^2/g). This suggests that the catalytic activity of both the catalysts is not directly proportional to the surface area confirming that the present catalytic systems are not surface type heterogeneous in which the catalytic activity is directly proportional to surface area. Hence, it can be concluded that the present catalytic system is pseudo-liquid type (I) heterogeneous catalyst where activity is directly proportional to the acidic strength of the catalyst. The order of the catalytic activity was $(PW_{12})_3$/MCM-41 > $(PW_{11})_3$/MCM-41 for all the acid catalysed reactions. Similar trend was found in the case of catalysts comprising PW_{12}/PW_{11} and MCM-48 support. The catalytic activity was found to be depending on the acidic strength of the catalysts (Table 6). The order of activity was $(PW_{12})_3$/MCM-48 > $(PW_{11})_3$/MCM-48 for all the acid catalysed reactions.

Effect of Supports

It is known that, 'Support' does not play always merely a mechanical role but it can also modify the catalytic properties of the POMs. In order to see the effect of supports, the catalytic activities of PW_{12}/PW_{11} anchored to different supports MCM-41 and MCM-48 have been compared under identical reaction conditions for various acid catalysed esterification reactions (Table 7). In almost all the reactions, $(PW_{12})_3$/MCM-48 exhibited excellent activity as compared to that of $(PW_{12})_3$/MCM-41. Similarly activity of $(PW_{11})_3$/MCM-48 was better than that of $(PW_{11})_3$/MCM-41.

The acidity of support is responsible for the catalytic activity, as it is well known that MCM-41 as well as MCM-48 both exhibit acidic character. MCM-48 (2.2 mequiv./g) is more acidic than MCM-41 (2.0 mequiv./g). Therefore, the higher value of total acidity for $(PW_{12})_3$/MCM-48 as well as for $(PW_{11})_3$/MCM-48 was observed collectively from PW_{12}/PW_{11} as well as support MCM-48. The trend in the activity of all the catalysts was in good agreement with their acidic

strength. The catalyst $(PW_{12})_3$/MCM-48 having highest acidic strength and produced better conversions.

Table 7. Effect of supports on different esterification reactions.

Catalyst	Surface area (m^2/g)	Pore width (Å)	Acidic strength (mV)	Total acidity (mequiv./g)	% Conv. BA	% Conv. Gly	% Conv. OA
$(PW_{12})_3$/MCM-41	360	30.1	410	3.6	96	88	98
$(PW_{12})_3$/MCM-48	286	20.2	450	3.9	98	99	95
$(PW_{11})_3$/MCM-41	252	30.0	250	3.0	90	89	89
$(PW_{11})_3$/MCM-48	318	27.5	290	3.4	93	91	90

Among all the catalysts (Table 7), MCM-48 based catalysts proved to be best catalyst for in terms of conversion, high TON as well as lower Ea value. It is known that MCM-48 has well-ordered 3D pore network which allows better dispersion of the active species. This high dispersion leads to better mass transfer which allows the product and reactant molecules to move in the channels of support. The selection of MCM-48 as best support was thus performed, taking into account the acidity, pore geometry and Kinetic studies.

Conclusions

- The present catalyts exhibit excellent conversion for *esterficiation of glycerol* with acetic acid under mild conditions.
- High selectivity towards *DAG and TAG* products were obtained and selectivity of the products found to be depend on the acidity of the catalysts.
- Present catalysts also displays outstanding activities for *esterification of benzyl alcohol* to synthesize benzyl acetate.
- Kinetic studies for both the reactions indicated absence of mass transfer/ diffusion limitation and it follows *first order rate law*.
- Control experiments and heterogeneity test proved catalysts to be truly *heterogeneous in nature*.
- The catalysts were regenerated and reused successfully up to four cycles without significant loss in the activity.
- Overall *economic* and *environmatal benefits* were accomplished as glycerol, a byproduct of biodiesel, has been utilized to give value added products.
- The order of catalytic activity for acid catalysed esterification and tranesterification was:
  - In terms of support **MCM-48 > MCM-41.**
  - In terms of catalysts **$(PW_{12})_3$/MCM-48 > $(PW_{12})_3$/MCM-41 > $(PW_{11})_3$/MCM-48 > $(PW_{11})_3$/MCM-41.**

References

1. M. A. Dasari, P. P. Kiatsimkul, W. R. Sutterlin, G. J. Suppes, Appl. Catal. A: Gen., 281, 225, (2005).
2. M. Pagliaro, M. Rossi, *The Future of Glycerol: New uses of a versatile raw material*, RSC publications, Cambridge, UK, (2008).
3. R. R. Soares, D. A. Simonetti, J. A. Dumesic, Angew. Chem. Int. Ed., 45, 3982, (2006).
4. M. Pagliaro, R. Ciriminna, H. Kimura, M. Rossi, C. Della Pina, Angew. Chem., 119, 4516, (2007).
5. C. -H. Zhou, J. N. Beltrami, Y.-X. Fan, G. Q. Lu, Chem. Soc. Rev., 37, 527, (2008).
6. C. H. Zhou, H. Zhao, D. S. Tong, L. M. Wu, W. H. Yu, Catal. Rev., 55, (2013).
7. N. Rahmat, A. Z. Abdullah, A. R. Mohamed, Renew. Sus. Energy Rev. 14, 987, (2010).
8. T. J. Jalinski, US Patent WO2006084048-A1, (2006).
9. P. J. Delgado, EP Patent 1,331,260 A2, (2003).
10. J. A. Melero, R. van Grieken, G. Morales, M. Paniagua, Energy Fuel, 21, 1782, (2007).
11. R. Luque, V. Budarin, J. H. Clark, D. J. Macquarrie, Appl. Catal. B: Env., 82, 157, (2008).
12. M. Gupta, N. Kumar, Renew. Sust. Energy Rev. 16, 4551, (2012).
13. S. Kesling, L. J. Karas, F. J. Liotta, Diesel fuel. US Patent 5 308 365, (1994).
14. D. Margolese, J. A. Melero, S. C. Christiansen, B. F. Chmelka, G. D. Stucky, Chem. Mater., 12, 2448, (2000).
15. R. Wessendorf, Petrochemie, 48, 138, (1995),
16. V. L. C. Gonçalves, B. P. Pinto, J. C. Silva, C. J. A. Mota, Catal. Today, 133, 673, (2008).
17. L. Zhou, T. H. Nguyen, A. A. Adesin, Fuel Process. Technol., 104, 310, (2012).
18. H. Rastegari, H. S. Ghaziaskar, M. Yalpani, Ind. Eng. Chem. Res., 54, 3279, (2015).

19. I. D. Rodriguez, E. M. Gaigneaux, Catal. Today 195, 14, (2012).
20. P. Sudarsanam, B. Mallesham, P. S. Reddy, B. M. Reddy, J. Chem. Sci. Technol., 2, 161, (2013).
21. M. Popova, Á. Szegedi, A. Ristić and N. N. Tušar, Catal. Sci. Technol., 4, 3993, (2014).
22. M. H. M. Yusof, A. Z. Abdullah, J. Taiwan Inst. Chem. Eng., 60, 199, (2016).
23. Arun P, S. M. Pudi, P. Biswas, Energy Fuel, 30, 584, (2015).
24. M. Trej, K. Stawick, A. Dubinsk, M. Ziolek, Catal. Today 187, 129, (2012).
25. P. S. Reddy, P. Sudarsanam, G. Raju, B. M. Reddy, Catal Commun., 11, 1224 (2010).
26. S. B. Troncea, S. Wuttke, E. Kemnitz, S. M. Comana, V. I. Parvulescu, Appl. Catal. B: Env., 107, 260, (2011).
27. M. Rezayat, H. S. Ghaziaskar, Green Chem., 11, 710, (2009).
28. J. A. Sánchez, D. L. Hernández, J. A. Moreno, F. Mondragón, J. J. Fernández, Appl. Catal. A: Gen., 405, 55, (2011).
29. I. Kim, J. Kim, D. Lee, Appl. Catal. A: Gen., 482, 31, (2014).
30. X. Gao, S. Zhu, Y. Li, Catal. Commun., 62, 48, (2015).
31. P. Ferreira, I. M. Fonseca, A. M. Ramos, J. Vital, J. E. Castanheiro, Appl. Catal. B: Env., 91, 416, (2009).
32. P. Ferreira, I. M. Fonseca, A. M. Ramos, J. Vital, J. E. Castanheiro, Catal. Commun., 10, 481, (2009).
33. P. Ferreira, I. M. Fonseca, A. M. Ramos, J. Vital, J. E. Castanheiro, Catal. Commun., 12, 573, (2011).
34. M. Balaraju, P. Nikhitha, K. Jagadeeswaraiah, K. Srilatha, P. S. Sai Prasad, N. Lingaiah, Fuel Process. Technol., 91, 249, (2010).
35. K. Jagadeeswaraiah, M. Balaraju, P. S. Sai Prasad, N. Lingaiah, Appl. Catal. A: Gen., 386, 166, (2010).
36. M. S. Khayoon, B. H. Hameed, Appl. Catal. A: Gen., 433, 152, (2012).
37. S. Zhu, Y. Zhu, X. Gao, T. Moa, Y. Zhu, Y. Li, Bioresour. Technol., 130, 45, (2013).

38. I. Kim, J. Kim, D. Lee, Appl. Catal. B: Env., 148-149, 295, (2014).
39. P. Y. Hoo, A. Z. Abdullah, Chem. Eng. J., 250, 274, (2014).
40. P. Y. Hoo, A. Z. Abdullah, Ind. Eng. Chem. Res., 54, 7852, (2015).
41. M. A. Betiha, H. M. A. Hassan, E. A. E. Sharkawy, A. M. A. Sabagh, M. F. Menoufy, H. E. M. Abdelmoniem, Appl. Catal. B: Env., 182, 15, (2016).
42. S. Shanmugam, B. Vishwanathan, T. K Vardarajan, J. Mol. Catal. A: Chem., 223, 143, (2004).
43. M. Schmitt, C. Scala, P. Moritz, H. Hasse, Chem. Eng. Process., 44, 677, (2005),
44. R. L. Augustine, S. K. Tanielyan, J. Mol. Catal. A: Chem., 87, 311, (1994).
45. A. Benhmid, K.V. Narayana, A. Martin, B. Lucke, Chem. Commun., 2118, (2004).
46. S. R. Kirumakki, N. Nagaraju, S. Narayanan, Appl. Catal. A: Gen., 273, 1, (2004).
47. S. H. Ali, S. Q. Merchant, Ind. Eng. Chem. Res., 48, 2519, (2009).
48. T. Joseph, S. Sahoo, S. B. Halligudi, J. Mol. Catal. A: Chem., 234, 107, (2005).
49. H. Zhou, J. Yang, L. Ye, H. Lin, Y. Yuan, Green Chem., 12, 661, (2010).
50. S. L. Barbosa, G. R. Hurtado, S. I. Klein, V. L. Junior, M. J. Dabdoub, C. F. Guimaraes, Appl. Catal. A: Gen., 338, 9, (2008).
51. A. Ghosh, F. Stellacci, R. Kumar, Catal. Today, 198, 77, (2012).
52. D. P. Sawant, A. Vinu, J. Justus, P. Srinivasu, S. B. Halligudi, J. Mol. Catal., 276, 150, (2007).
53. R. A. Sheldon, M. Walau, I. W. E. C. Arends, U. Schuchurdt, Acc. Chem. Res., 31, 485, (1998).
54. L. Xu, Y. Wang, X. Yang, X. Yu, Y. Guo, J. H. Clark, Green Chem., 10, 746, (2008).